Vertebrate Polysialyltransferases:
A Study on Structure-Function Relationships

Von der Naturwissenschaftlichen Fakultät der

Gottfried Wilhelm Leibniz Universität Hannover

zur Erlangung des Grades

Doktorin der Naturwissenschaften

*D*r. *rer. nat*.

genehmigte Dissertation

von

Dipl.-Biochem. Almut Christine Günzel

geboren am 30. November 1979 in Gifhorn

2008

Referentin: Prof. Dr. Rita Gerardy-Schahn

Korreferent: Prof. Dr. Walter Müller

Tag der Promotion: Montag, 08.12.2008

Schlagworte: Polysialyltransferasen, Polysialinsäure, Glykosyltransferase

Key words: polysialyltransferases, polysialic acid, glycosyltransferase

Erklärung zur Dissertation

Hierdurch erkläre ich, dass die Dissertation „Vertebrate Polysialyltransferases: A Study of Structure-Function Relationships" selbstständig verfasst und alle benutzten Hilfsmittel sowie evtl. zur Hilfeleistung herangezogene Institutionen vollständig angegeben wurden.

Die Dissertation wurde nicht schon als Diplom- oder ähnliche Prüfungsarbeit verwendet.

Table of Contents

Zusammenfassung

Polysialinsäure (PolySia) ist ein lineares Homopolysachcharid aus a2,8-verknüpften Sialinsäureeinheiten. Als dynamisch regulierte posttranslationale Modifikation des Neuralen Zelladhäsionsmoleküls NCAM übernimmt die PolySia eine wichtige Rolle in der Regulation interzellulärer Erkennungs- und Adhäsionsvorgänge. Durch eine hohe negative Oberflächenladungsdichte hat PolySia eine hohe Wasserbindungskapazität. Die daraus resultierende Größe des NCAMs wird als wichtigster Regulator zellulärer Interaktionen betrachtet. PolySia unterstützt motile Prozesse wie z.B. Migration, axonales Wachstum aber auch axonale Wegfindung, Neurogenese und Regeneration. PolySia wird in einigen hoch malignen Tumoren exprimiert. Es wird angenommen, dass die Motilität-unterstützenden Eigenschaften des Zuckers für das hohe Metastasierungspotential dieser Tumore verantwortlich sind.

Die Schlüsselenzyme der PolySia Biosynthese sind die Polysialyltransferasen (PolySTs), ST8SiaII und ST8SiaIV. PolySTs sind Golgi residente Typ-II-Transmembranproteine und besitzen eine kurze N-terminale cytoplasmatische Domäne sowie eine katalytische Domäne, die im Golgilumen positioniert ist. PolySTs sind Glykoproteine mit sechs bzw. fünf *N*-Glykanen. Beide Enzyme sind in der Lage die eigenen *N*-Glykane durch die Addition von PolySia zu modifizieren, was als Autopolysialylierung bezeichnet wird. Eine frühere Arbeit unserer Gruppe hat gezeigt, dass nur solche Enzymformen aktiv sind, die die Fähigkeit zur Autopolysialylierung besitzen. Die Tatsache, dass sowohl *N*-Glykane als auch Disulfidbrücken für die Herstellung aktiver eukaryontischer PolySTs notwendig sind, stellt eine bedeutende Barriere für die Expression des rekombinanten Proteins dar und beschränkt die Expression auf eukaryontischen Expressionssysteme. In diesen konnten allerdings bislang keine ausreichenden PolyST-Mengen hergestellt werden, um deren Struktur-Funktionszusammenhänge näher zu analysieren.

Ziel meiner Doktorarbeit war es, Wege zu finden, die die Herstellung funktionell aktiver rekombinanter polySTs verbessern. Eine bioinformatischen Analyse ergab, dass in ST8SiaII aus Zebrafisch (zST8SiaII) eine der hoch konservierten und für die Funktion der homologen Enzyme essentiellen *N*-Glykosylierungsstellen fehlt. Dieses Protein wurde deshalb als Modell verwendet, um in iterativen Schritten alle *N*-Glykosylierungsstellen zu inaktivieren und über N-terminale Verkürzungen das minimal aktive Protein darzustellen. Auf diesem Weg konnte eine lösliche und aktive Variante des Enzyms hergestellt werden. Die N-terminal verkürzte Enzymvariante zST8SiaII?N86 konnte in Insektenzellen als hoch reines Protein im

Milligrammbereich hergestellt und für erste Struktur-Funktions-Analysen über NMR-Spektroskopie eingesetzt werden.

In einem weiteren Ansatz wurde die ST8SiaII aus der Maus als Modellenzym eingesetzt und der Versuch unternommen, vorhandene *N*-Glykane durch Motive auszutauschen, die in Knochenfischen als „Ersatz" für *N*-Glykane identifiziert worden waren. Dadurch gelang die Herstellung einer *N*-Glykan-freien Variante. Erste Versuche, dieses Protein in Bakterienzellen zu exprimieren, ergaben zwar sehr gute Proteinausbeuten, allerdings zeigte das rekombinant hergestellte Protein nur eine geringe Stabilität und keine Aktivität. Einen wesentlichen Anteil am Fehlen von Stabilität und Funktion in diesem Enzym könnte die unvollständige Ausbildung der Disulfidbrücken haben. In weiteren Untersuchungen soll nun die Optimierung des Proteins vorangetrieben werden.

Abstract

Polysialic acid (polySia) is a linear homopolymer consisting of α-2,8 linked sialic acid building blocks. The polymer predominately occurs as dynamically regulated posttranslational modification of the neural cell adhesion molecule NCAM. Thus, it plays a major role in regulating NCAM-mediated interactions involved in cellular plasticity. The negative charge of polySia causes in a large hydrodynamic volume of NCAM and subsequently attenuates NCAM-mediated cell-cell contacts. In line with this, polySia enables numerous neuronal processes such as migration, axonal outgrowth and orientation as well as neurogenesis up to the point of nerve regeneration. PolySia is also expressed in a number of highly malignant tumors, where it is supposed to increase the metastatic potential by enhancing the motility of tumor cells.

PolySia is synthesized by two polysialyltransferases (polySTs): ST8SiaII and ST8SiaIV. Both enzymes reside in the Golgi apparatus and represent type-II-transmembrane proteins with a short N-terminal cytoplasmic domain and a catalytic domain extending into the Golgi lumen.

PolySTs are glycoproteins with six or five putative N-glycosylation sites, respectively. Both enzymes, ST8SiaII and ST8SiaIV, are capable of polysialylating their own N-glycans – a process referred to as "autopolysialylation".

Results from earlier studies in our laboratory show, that only enzymes capable of autopolysialylation are able to polysialylate NCAM. Since neither N-Glycans nor disulfide bonds occur in prokaryotes, but N-glycosylation and disulfide bonds are essential for the formation of active polySTs, expression systems had been limited to eukaryotic cells so far. However, eukaryotic systems provide only very small protein yields of recombinant mammalian polySTs that are not sufficient to intensively analyze structure-function relationships. My Ph.D. thesis, therefore, is concentrated on the large-scale expression of functional ST8SiaII to be used to characterize polySTs in detail by applying biochemical and biophysical analyses.

Former bioinformatic analyses had shown that ST8SiaII from zebrafish (zST8SiaII) is lacking one out of two N-glycosylation sites, identified as important for the ST8SiaII activity in homologues enzymes. Therefore, this enzyme was used as a model to determine the minimal length of the active enzyme and the impact of N-glycans on activity. As a result, a soluble and active variant of the enzyme was generated and purified in milligram quantities

from insect cells. Consequently, the analysis of structure-function relationship by NMR-spectroscopy has been commenced.

The second goal of my PhD study was the generation of a murine ST8SiaII variant with no-or a minimal number of *N*-glycans. This was achieved by substituting the *N*-glycan functions by motifs found instead of *N*-glycans in the bony-fish family. *N*-glycan free mST8SiaII variants were generated that allowed soluble expression using a bacterial system. Unfortunately, the recombinant protein produced in bacteria was - probably due to the lack of disulfide bonds - inactive and quickly degraded. Further studies will be focused on the optimization of murine ST8SiaII for a subsequent expression in bacteria.

General Introduction

Polysialic acid

In vertebrates the term polysialic acid (polySia) describes a linear homopolymer of a2,8-linked sialic acid (Sia) residues. The monomeric building block Sia is a nine-carbon sugar with a carboxylic acid function at position C1. So far, more than 50 naturally occurring Sia derivatives have been identified in various kingdoms of life (including vertebrates, invertebrates and bacteria). All sialic acids are derived from the monosaccharide 2-keto-3-deoxy-5-acetamido-D-glycero-D-galacto-nonulosonic acid (acetylneuraminic acid, Neu5Ac) (Angata and Varki, 2002; Varki and Varki, 2007). Remarkably, only three monomers have been identified in polySia: N-acetylneuraminic acid (Neu5Ac), N-glycolylneuraminic acid (Neu5Gc) and 2-keto-3-deoxy-D-glycero-D-galacto-nonulosonic acid (Kdn) (Troy, 1992). The linear homopolysaccharide as well as the three Sia derivatives present in polySia are shown in figure 1.
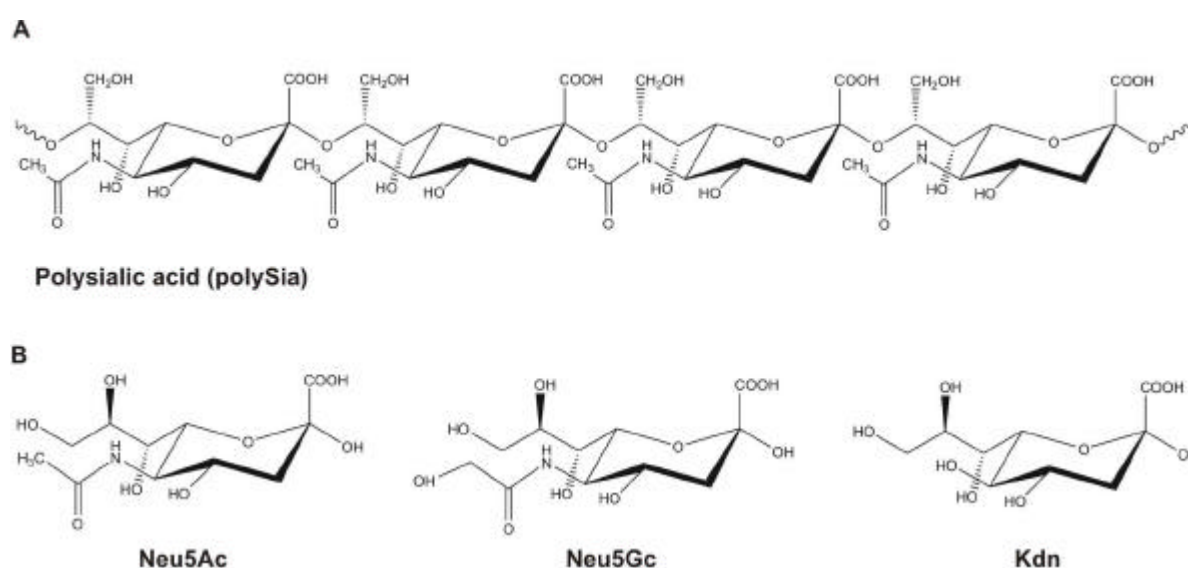
Figure 1: Chemical structures. *A*. Structure of a2,8-linked polysialic acid (polySia). *B*. Structures of N-acetylneuraminc acid (Neu5Ac), N-glycolylneuramininic acid (Neu5Gc) und deamino-neuraminic acid (2-Keto-3-deoxy-D-glycero-D-galacto-nonulosonsäure, Kdn).

Under physiological conditions polySia is negatively charged due to the carboxylate function at position C1 of each monomer. The polyanionic nature of polySia involves high water binding capacity resulting in a large hydrodynamic volume (Yang, Yin, and Rutishauser, 1992). Based on NMR-studies, polySia in solution is assumed to exhibit a helical

conformation, with approximately nine residues per turn (Brisson *et al.*, 1992). PolySia chains with a polymerization degree (Dp) higher than above eleven were shown to form filamentous networks (Toikka *et al.*, 1998).

Several neuroinvasive bacteria such as *E. coli* K1 and *N. meningitidis* serogroup B are protected by an extracellular polysaccharide capsule composed of polySia (Troy, 1992). In vertebrates, polySia forms a posttranslational modification of the neural cell adhesion molecule (NCAM) (Rothbard *et al.*, 1982). For many years NCAM was assumed to be the only polySia carrier in the mammalian system. However, more recent studies have provided evidence that other polySia carriers exist. Additional polySia carrying proteins include the a subunit of the voltage dependent sodium channel (Zuber *et al.*, 1992), the scavenger receptor CD36, identified as soluble protein in human breast milk (Yabe *et al.*, 2003) and, as shown in a most recent study, neuropilin-2 expressed on matured dendritic cells (Curreli *et al.*, 2007).

Function of polySia in vertebrates

As mentioned above, NCAM, a membrane bound glycoprotein belonging to the family of immunoglobuline-like proteins, is the major polySia carrier in vertebrates. The three major isoforms NCAM-180, NCAM-140 and NCAM-120 (fig. 2) are characterized by their respective molecular mass arising from alternative splicing of a single gene (Cunningham *et al.*, 1987; Kolkova, 2008).

NCAM contains five immunoglobuline (Ig)-like domains and two fibronectin type-III (FNIII)-like repeats in the extracellular domain. NCAM-180 and NCAM-140 are transmembrane proteins varying in the length of their intracellular domain (fig. 2) whereas NCAM-120 is a glycosyl-phosphatidylinositol (GPI)-anchored protein (Cunningham *et al.*, 1987). Six *N*-glycosylation sites are located within the extracellular Ig-like domains 3-5. Interestingly, polysialylation occurs exclusively at *N*-glycosylation site 5 and 6 located in the fifth Ig-like domain (Nelson, Bates, and Rutishauser, 1995; Liedtke *et al.*, 2001). Further modifications of NCAM such as *O*-glycosylation were reported for an isoform found in skeletal muscle myotubes (Walsh *et al.*, 1989) and for NCAM variations co-expressed with the polySia-synthesizing enzyme in cell culture (Close *et al.*, 2003; Colley, 2008).
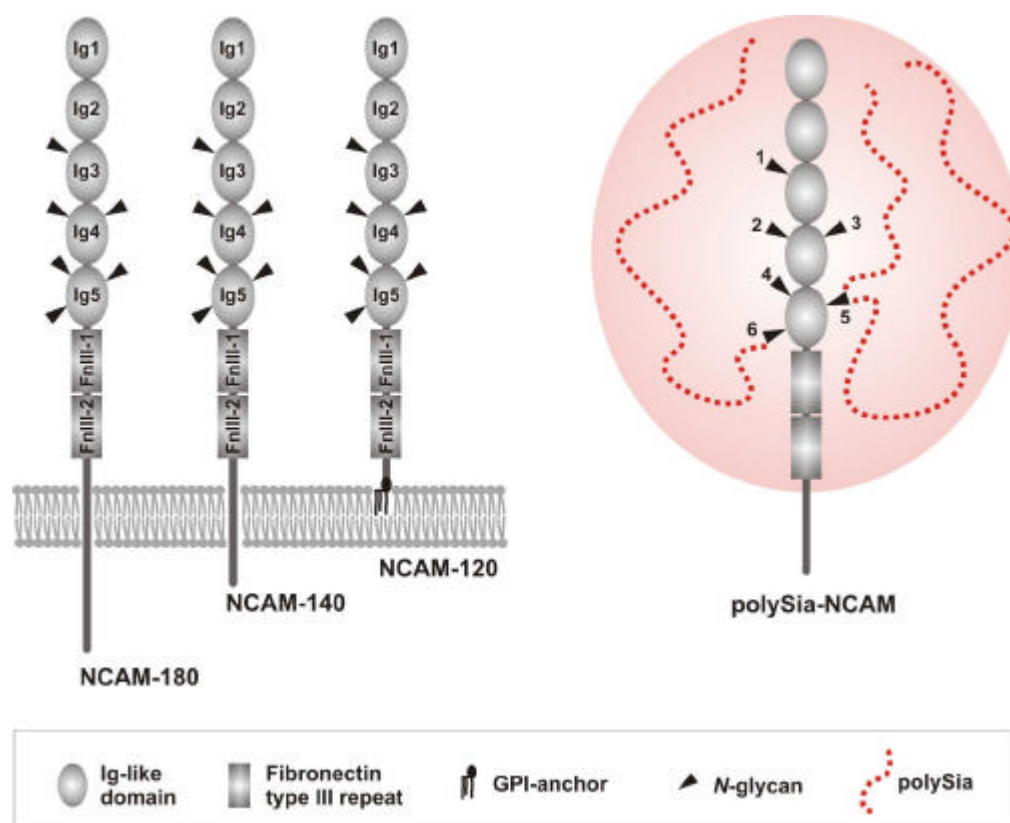
Figure 2: Scheme of the three major NCAM isoforms and the polysialylated from of NCAM (reprint Hildebrandt, Mühlenhoff, and Gerardy-Schahn, 2008). *A*. The extracellular part of NCAM is composed of five immunoglobulin (Ig)-like domains and two fibronectin type III (FNIII) like repeats. NCAM is a glycoprotein with in total six *N*-glycosylation sites. *B*. Transfer of polySia to NCAM involves two *N*-glycan sites (no. 5 and 6) in the 5th Ig-domain. The presence of polySia increases the hydrodynamic radius of NCAM as illustrated by the shaded sphere.

NCAM was first reported as calcium independent homophilic adhesion molecule abundantly expressed in the nervous system (Rutishauser, Hoffman, and Edelman, 1982; Hinsby, Berezin, and Bock, 2004). Like other cell adhesion molecules, NCAM participates in signaling pathways by homo- or heterophilic interactions of the extracellular domain. For instance, heterophilic interaction of NCAM and the fibroblast growth factor receptor (FGFR) activates a signal cascade to promote axonal outgrowth (Saffell *et al.*, 1997). Down-regulation of NCAM-mediated cell adhesion by association of NCAM with the glial-derived neurotrophic factor family receptor a (GFRa) results in Schwann cell migration and axonal growth in hippocampal and cortical neurons (Paratcha, Ledda, and Ibanez, 2003).

Another possibility of NCAM to modulate signaling pathways is mediated by polySia. In the presence of the negatively charged sugar polymer, hippocampal and hypothalamic neurons are more sensitive to the brain-derived neurotrophic factor (BDNF) (Muller *et al.*, 2000; Vutskits *et al.*, 2001). Accordingly, *in vivo* experiments demonstrated that enzymatic removal of polySia from NCAM or application of soluble polySia from exogenous sources affect physiological functions as e.g. long-term potentiation (LTP) in the hippocampus and that

these effects could be rescued by external addition of BDNF (Muller *et al.*, 2000). To explain this so-called "positive" regulatory effect of polySia, two models are currently discussed:

(1) NCAM bound polySia may raise the concentration of BDNF at the receptor site or

(2) NCAM bound polySia could decrease inhibitory effects established by NCAM/BDNF-receptor interactions (Hildebrandt *et al.*, 2007).

Several findings substantiate the assumption that polySia acts as a "negative" regulator of cell adhesion and differentiation. The presence of bulky and highly hydrated polySia increases inter-membrane repulsion (Yang, Major, and Rutishauser, 1994; Rutishauser, 1998; Johnson *et al.*, 2005). Based on this sterical effect, polySia is believed to weaken adhesive properties of cells and simultaneously facilitates cell motility. The migration-supportive effect of polySia seems to enable rostral migration of progenitor cells from their birthplace in the subventricular zone (SVZ) along a given pathway to the olfactory bulb (for review Rutishauser, 2008). Enzymatic removal of polySia from these progenitor cells was shown to inhibit their ability to migrate, accompanied by a premature differentiation of the cells. The induction of the differentiation process is most likely mediated by the presence of polySia free NCAM (Hu *et al.*, 1996; Petridis, El Maarouf, and Rutishauser, 2004; Rockle *et al.*, 2008; Rutishauser, 2008). An impressive illustration for the regular functions of polySia during mouse development has been obtained in a mouse model with depleted polySia synthesis. This model demonstrates that the absence of polySia goes along with a gain of function for NCAM resulting in a lethal phenotype (Weinhold *et al.*, 2005).

This finding clearly argues for an essential role of polySia in the control and coordination of NCAM interactions during mouse development (Weinhold *et al.*, 2005). *In vivo* analysis of mouse brain revealed that polySia biosynthesis starts on embryonic day 8-8.5 and the maximum level is reached in the perinatal phase. Thereafter a rapid decrease by approximately 70 % within only one week was observed (Probstmeier, Bilz, and Schneider-Schaulies, 1994; Kurosawa *et al.*, 1997; Oltmann-Norden *et al.*, 2008; Hildebrandt, Mühlenhoff, and Gerardy-Schahn, 2008). In accordance with its function, polySia remains expressed in the adult brain in areas of persistent neural plasticity such as the subventricular zone and the rostral migratory stream (Miragall *et al.*, 1990; Theodosis, Rougon, and Poulain, 1991; Seki and Arai, 1993; Hu *et al.*, 1996).

In addition to its essential role in neural development, polySia represents a tumor marker (Roth *et al.*, 1988; Fukuda, 1996). PolySia is re-expressed on several malignant neuroectodermal and neuroendocrine tumors, including Wilm`s tumor (Roth *et al.*, 1988; Zuber *et al.*, 2005), lung carcinoma (Scheidegger *et al.*, 1994; Tanaka *et al.*, 2001),

rhabdomyosacroma (Glüer *et al.*, 1998b) and neuroblastoma (Glüer *et al.*, 1998a; Hildebrandt *et al.*, 1998; Seidenfaden *et al.*, 2003). By destabilisation of cell-cell contacts polySia might facilitate detachment of cells during metastasis. In addition, the life span of tumor cells in circulation might be increased, because polySia can mask tumor specific antigens (Bitter-Suermann and Roth, 1987) that are otherwise recognised by the immune system. In accordance with this hypothesis the polySia levels of two clonal sublines of a small cell lung carcinoma line (polySia$^+$ and polySia$^-$) were correlated to metastasis in xenografted nude mice (Scheidegger *et al.*, 1994). Another mouse model revealed that metastasis and invasion of a polySia expressing rhabdomyosacroma cell line was drastically reduced after enzymatic removal of polySia (Daniel *et al.*, 2001). This correlation between polySia and the tumor potential for metastasis was also monitored in a retrospective study of non-small cell lung cancer patients resulting in a worse prognosis for polySia positive patients (Tanaka *et al.*, 2001).

While tumor biology provided evidence for the cell motility promoting function of polySia, more recent nerve regeneration studies proved these findings (El Maarouf and Rutishauser, 2008). In general, the adult central nervous system (CNS) is unable to reverse damage produced by injury or disease and severed CNS axons are unable to re-grow and re-innervate their targets. Usually, this deficiency is not caused by an intrinsic incapacity to resume elongation, but reflects a non-permissiveness of the CNS environment and of scar tissue at lesion sites in particular (David and Aguayo, 1981; Fawcett and Asher, 1999; Batchelor and Howells, 2003). Therefore, the introduction of polySia into lesion sites by a viral vector, containing the polySia synthesizing enzyme, may create an environment that on the one hand supports cell motility and on the other hand reduces inhibitory effects of the CNS environment. Studies carried out in this field demonstrated that re-expression of polySia in astrocytes promotes re-growth of axons through the lesion site in spinal cord. Moreover, the retrieval of a polySia expressing path between the subventricular zone (SVZ) and a brain lesion site was demonstrated to facilitate the recruitment of progenitor cells of the SVZ to the damaged area (El Maarouf, Petridis, and Rutishauser, 2006; El Maarouf and Rutishauser, 2008).

Aiming at exploiting the axon growth promoting functions of polySia for regeneration in the peripheral nervous system, studies have been initiated to use the purified polymer as an external growth support. Experiments carried out so far demonstrate that polySia represents a suitable matrix for the cultivation of primary neural cells that are candidates for therapeutic strategies in peripheral nerve tissue reconstruction approaches. Compared to classical culture

conditions, significantly improved survival and proliferation rates were obtained with primary neuronal and glial cells (Haile *et al.*, 2008).

Biosynthesis of polySia

As schematically shown in fig. 3, the biosynthesis of sialylated and polysialylated glycoconjugates involves virtually all cellular compartments. While the biosynthetic steps delivering sialic acid are localized in the cytosol, the metabolic activation of Sia to cytidine monophosphate-sialic acid (CMP-Sia) by the CMP-Sia-synthetase takes place in the cell nucleus (Kean, Munster-Kuhnel, and Gerardy-Schahn, 2004). A specific CMP-Sia transporter transfers the activated sugar into the Golgi (Eckhardt, Gotza, and Gerardy-Schahn, 1998), where CMP-Sia serves as a substrate for sialyl- and polysialyltransferases (Harduin-Lepers *et al.*, 2001).
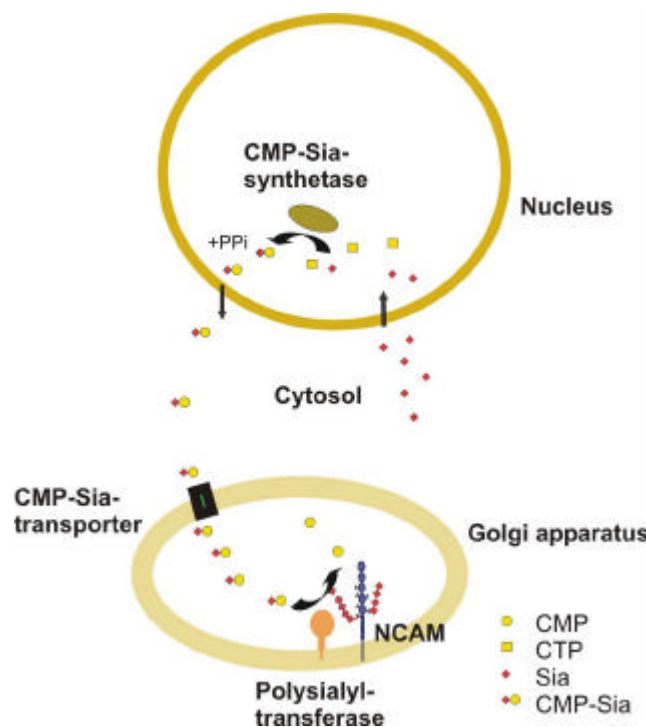
Figure 3: Schematic representation of the polysialylation process in the eukaryotic vertebrate cell.

The polySia biosynthesis is performed by two polysialyltransferases (polyST), ST8SiaII and ST8SiaIV. In early development and in the perinatal phase ST8SiaII is the predominant polyST whereas ST8SiaIV prevails in adult mice (Oltmann-Norden *et al.*, 2008). Both polySTs are able to synthesize polySia independently of NCAM *in vitro* and *in vivo* (Angata

et al., 2000; Oltmann-Norden *et al.*, 2008). In a comparative *in vitro* study carried out with recombinant soluble polysialyltransferases, ST8SiaIV was found to be more efficient in terms of NCAM polysialylation. Moreover, ST8SiaIV synthesized longer polySia chains than ST8SiaII. Using *N*-glycosylation site mutants of NCAM, ST8SiaIV strongly preferred the 6th over the 5th *N*-glycosylation site, whereas this preference was only moderate for ST8SiaII. A synergistic effect, resulting in higher numbers of added polySia chains as well as in a higher degree of polymerization, was observed, if the two polySTs were acting together (Angata, Suzuki, and Fukuda, 1998; Angata, Suzuki, and Fukuda, 2002).

Different from the *in vitro* observations, the analysis of mouse brain samples isolated from animals expressing only one functional polyST (ST8SiaII- and ST8SiaIV-knockout mice) revealed that both polySTs favor the 6th over the 5th *N*-glycosylation site. Synergy in this study could be limited to the transfer of polySia onto the 5th *N*-glycosylation site, where longer polySia chains were found in wild type than in single polyST knockout mice (Galuska *et al.*, 2008).

The *in vivo* analysis confirmed that each enzyme individually is able to synthesize long polySia chains (up to Dp 90). However, compared to wild-type, the percentage of long polySia chains was decreased to 50 % in mice expressing only ST8SiaII and to 25-33 % in mice expressing only ST8SiaIV (Galuska *et al.*, 2008). Consequently, ST8SiaII knockout mice exhibit a different phenotype compared to ST8SiaIV knockout mice. ST8SiaII deficiency caused morphological changes in brain structures and altered fear conditioning, whereas loss of ST8SiaIV resulted in reduced learning and memory in adult mice (Angata *et al.*, 2004; Eckhardt *et al.*, 2000). Double-knockout mice of ST8SiaII and ST8SiaIV are characterized by a complete lack of polySia. These animals are drastically retarded in growth and more than 80 % die within four weeks after birth (Weinhold *et al.*, 2005; Angata *et al.*, 2007).

Polysialyltransferases

The two polysialyltransferases, ST8SiaII and ST8SiaIV, were cloned and functionally expressed from mouse and other species (Eckhardt *et al.*, 1995; Nakayama *et al.*, 1995; Scheidegger *et al.*, 1995; Kojima *et al.*, 1995; Kudo *et al.*, 1998). Both mammalian polySTs belong to the a2,8-sialyltransferase protein family and share 59 % identity at the amino acid level (Eckhardt *et al.*, 1995; Nakayama *et al.*, 1995; Harduin-Lepers *et al.*, 2005).

PolySTs contain the three sialyl sequence motifs, found in all a2,8-sialyltransferases (fig. 4 *A*). The L-motif (large motif) is involved in binding of the activated sugar CMP-Sia, whereas the S-motif (short motif) binds to CMP-Sia as well as to the acceptor substrate (Datta and Paulson, 1995; Datta, Sinha, and Paulson, 1998). Mutation of the VS-motif (very short motif) resulted in an inactive enzyme (Kitazume-Kawaguchi, Kabata, and Arita, 2001). For polySTs, an additional motif, the so-called polyST domain (PSTD) could be identified. This motif consists of 32 amino acids and is essential to establish polysialylation capacity. It is postulated that electrostatic interaction between the polybasic PSTD and the polyanionic polySia chain tether nascent polySia chains to the enzyme and thus facilitate the processive addition of new Sia residues to the non-reducing end of the growing chain (Nakata, Zhang, and Troy, 2006).

The polySTs contain highly conserved cysteine residues. The first cysteine (C) located in the L-motif and the cysteine of the S-motif form a disulfide bridge, whereas the second cysteine in the sialyl-motif L and the cysteine located at the very C-terminus of the enzymes form a second disulfide bond (fig. 4) (Angata *et al.*, 2001). The catalytic domain of the type-II-transmembrane polyST is located in the lumen of the Golgi-apparatus (Close and Colley, 1998; Mühlenhoff *et al.*, 2001).
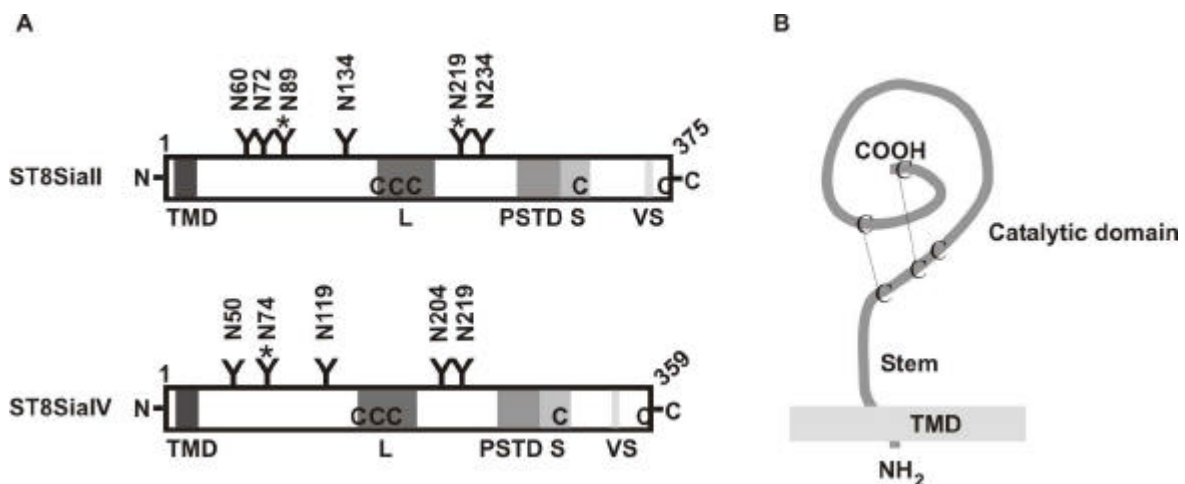
Figure 4: Schematic representation of polySTs. *A*. Schematic representation of ST8SiaII and ST8SiaIV. The large (L), small (S) and very short (SV) sialylmotifs and the polyST domain (PSTD) are indicated as shaded boxes. Conserved cysteines and *N*-glycosylation sites are marked. *N*-glycosylation sites important for polyST activity are indicated by asterisk. *B*. Type II membrane topology of polySTs. Transmembrane domain (TMD), stem region (stem) and catalytic domain are indicated. Conserved cysteine residues and disulfide bridges are charted in.

Both polySTs are glycoproteins with six and five putative *N*-glycan attachment sites, respectively. *N*-glycosylation occurs on all acceptor sites mentioned above, as shown by Dr. Mühlenhoff in our laboratory (Mühlenhoff *et al.*, 2001). Interestingly, the *N*-glycans N89, N219, and N234 of ST8SiaII and N50, N74, and N119 of ST8SiaIV are additionally modified

by polysialylation, although it remains unclear whether this modification is added intra- or intermolecularly. This self-modification is referred to as autopolysialylation (Close *et al.*, 2001; Close, Tao, and Colley, 2000; Mühlenhoff *et al.*, 2001).

For the murine ST8SiaII, depletion of the *N*-glycan-attachment sites N89 and N219 by site-directed mutagenesis of the asparagine-residue (N) in the respective consensus sequences (**N-X-S/T**) resulted in a loss of autopolysialylation and in decreased NCAM-polysialylation activity. The same results were obtained for the deletion of N74 in ST8SiaIV (Close, Tao, and Colley, 2000; Close *et al.*, 2001; Mühlenhoff *et al.*, 2001). A complete loss of polyST activity was reported for the murine ST8SiaII and ST8SiaIV when all *N*-glycan attachment sites were deleted (Mühlenhoff *et al.*, 2001).

The transfer of polySia onto NCAM needs priming of the acceptor sites by terminal 2,3- or 2,6-linked sialic-acid residues. Moreover, the mammalian polySTs seem to be strictly dependent on the way the polySia acceptor sites on NCAM are presented to the enzymes. Attempts to transfer polySia onto artificial non-protein acceptors dramatically reduced the potential of these enzymes to synthesize polySia (Angata *et al.*, 2000; Angata, Suzuki, and Fukuda, 2002).

To ascertain which parts of NCAM serve as recognition sites for polySTs, a detailed study has been carried out in Prof. Colley's laboratory. In this study, deletion mutants prepared from NCAM showed that a construct harboring the entire FNIII-1 domain together with the adjacent Ig5 domain is sufficient for polySia transfer. Moreover, this group demonstrated that replacement of acidic patches in the NCAM FNIII-1 domain alters polysialylation. An a-helix identified in this domain is critical for contact formation between polyST and NCAM and the correct presentation of the *N*-glycans localized in the Ig5 domain to the polySTs (Mendiratta *et al.*, 2005; Mendiratta *et al.*, 2006; Colley, 2008). However, no corresponding protein-recognition site could be identified in the polySTs so far.

Evolution of polysialyltransferases

The a2,8-sialyltransferase (ST8Sia) family consists of six subfamilies that all transfer Sia residues in an a2,8-linkage on terminally sialylated acceptors. Members of the ST8Sia-family can act on glycoproteins and glycolipids. The six subfamilies split into two branches, containing three enzymes each: ST8SiaI, V and VI in the first branch and ST8SiaII, III, and IV in the second branch, respectively. Members of the subfamilies localized in the first branch transfer only one sialic acid residue to form disialyl structures, whereas the second

branch contains the polysialyltransferases ST8SiaII and -IV as well as the oligosialyltransferase ST8SiaIII (Harduin-Lepers *et al.*, 2005). Remarkably, an ancestor gene of all members of the ST8Sia family has been identified in the cephalochordate amphioxus (Harduin-Lepers *et al.*, 2005). Therefore, the variety of sialyltransferases is likely to have evolved as a result of massive gene duplications that took place early in vertebrate evolution and early after fish radiation (Amores *et al.*, 1998).
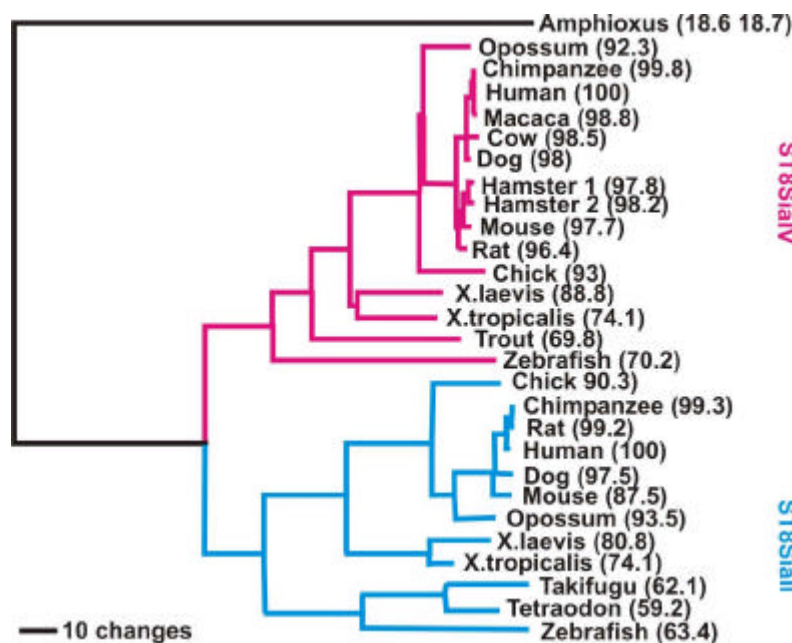
Figure 5: Evolutionary relationships between vertebrate polysialyltransferases as recovered from Minimum-Evolution and Neighbor-Joining analysis (reprint Marx *et al.*, 2007). The consensus tree is based on amino acid sequence alignment. Bootstrap support is shown for relevant nodes. The sequence identity scores (regarding their human homologue) are given in brackets beside the taxis label. ST8SiaII and ST8SiaIV proteins are recovered as monophyletic groups with comparable evolutionary dynamics, as observed in their branching pattern. The clustering of fish ST8SiaII differs from the one observed for fish ST8SiaIV. As fish ST8SiaIV genes differ in their overall dN/dS ratio, they do not cluster as a sister clade basal to tetrapods.

In zebrafish, a member of the bony-fish family, expression analysis, gene-target knockdown experiments, and *in vitro* catalytic assays indicate that ST8SiaII is the predominant polyST (Marx *et al.*, 2007). Unexpectedly, the ST8SiaIV gene seems to be completely lost in some members of the bony-fish family like takifugu and tetraodon. These findings might support the assumption that early after the evolutionary appearance of polySTs in lower vertebrates, ST8SiaIV had no significant function. The high frequency of chromosomal rearrangements detected in the region containing ST8SiaIV genes in fish and mammals, may explain the divergent evolution of ST8SiaIV compared to the conserved evolution of ST8SiaII in lower and higher vertebrates.

Objectives

PolySia is a linear and negatively charged homopolymer of a2,8-linked sialic acid residues and mainly attached to the neural cell adhesion molecule (NCAM). Due to the large hydrodynamic radius of polySia, adhesive properties of NCAM in homo- and heterophilic interactions are attenuated. In accordance with these features, polySia has been demonstrated to be involved in conferring plasticity to e.g. neuronal tissue. PolySia expression is high during embryonic development and reaches a maximum in the perinatal brain. In the adult organism polySia expression is highly restricted, but polySia is re-expressed in a number of malignant tumors. ST8SiaII is the predominant polyST in developing tissue as well as in tumors. Therefore, tumor specific inhibition of ST8SiaII might provide an attractive means in cancer therapy.

Depending on the enzyme (ST8SiaII and IV) and species, polysialyltransferases contain five to six *N*-glycan attachment sites, which, as shown in an earlier study, are all modified with core structures. Moreover, two out of the six *N*-glycans in the murine ST8SiaII are involved in the formation of an active enzyme.

To further explore structure-function relationships in the polysialyltransferases, my work was focused on the production of minimally glycosylated and soluble recombinant polysialyltransferases. Including ST8SiaII from murine and fish origin, the first goal was to determine the minimal active enzyme at linear sequence level. As a second goal the influence of individual *N*-glycans for solubility, activity, and stability of recombinant proteins was addressed. For this purpose, recombinant proteins were planed to be comparatively expressed in mammalian and insect cells. Ultimately, this study aimed at identifying a way to express ST8SiaII in a bacterial system in the absence of *N*-glycans to generate yields sufficient to initiate protein crystallization trials.

Chapter 1:

Characterization of the eukaryotic polysialyltransferase ST8SiaII from zebrafish

1.1. Introduction

Carbohydrates that are components of glyco-lipids and –proteins are well known cellular communication structures and the passed decade has demonstrated that biosynthetic deficiencies in conjunction with the formation of cellular glycoconjugates (summary term for glycolipids and glycoproteins) cause severe human diseases (Endo, 2007). Glycosylation starts in the endoplasmatic reticulum (ER) and follows the secretory pathway of the vertebrate cells (Trombetta, 2003). In particular, the *N*-glycans of molecules involved in the transport of cellular signals like receptors, adhesion molecules and also soluble ligands, have been intensively studied (Zhao *et al.*, 2008).

N-glycosylation of glycoproteins starts in the ER and follows the secretory pathway of the cells. In the rough ER, an oligosaccharide precursor (Glc3Man9GlcNAc2) preassembled on dolichol-pyrophosphate is transferred onto the asparagine (N) residues located in **N-**X-S/T consensus motifs of nascent polypeptide chains, X thereby is any amino acid except proline. Remodelling processes of the precursor glycan, which occur during the transport of the glycoconjugate along the secretory pathway generate a diverse set of *N*-glycans. In the ER the protein has to reach the "native conformation" to be allowed to exit and reach the subsequent compartment. A chaperon assisted quality control system exists in the ER and supports the folding process. Proteins involved in this quality control system are lectins that recognize the oligosaccharide precursor after the ER-resistent glucosidases I and II have removed two glucose residues (Glc1Man9GlcNAc2). Only properly folded proteins are further transported along the secretory pathway (Trombetta, 2003).

Properties of proteins can be altered by *N*-glycan addition. A prominent example in this field is the neural cell adhesion molecule NCAM, which, due to the addition of polysialic acid (polySia) can switch its adhesive into anti-adhesive properties. NCAM is a member of the immunoglobuline superfamily (Cunningham *et al.*, 1987; Colley, 2008). The molecule contains five immunoglobuline(Ig)-like and two fibronectin type-III(FNIII)-like domains in the extracellular part. PolySia, a linear homopolymer of a2,8- linked sialic acid (Sia) residues, can be added to *N*-glycan attachment sites in the fifth Ig-like domain. Due to the

high water binding capacity of the negatively charged polymer, a large hydrate shell covers the entire NCAM protein surface and by stereochemical means (hindrances and electrostatic repulsion) interferes with homophilic and heterophilic interactions of NCAM. Polysialylation of NCAM results in an enlarged intermembrane space that leads to a decrease of cell-cell interactions (Yang, Yin, and Rutishauser, 1992; Johnson *et al.*, 2005).

Two enzymes are capable to synthesize polySia in eukaryotes – the polysialyltransferases (polySTs) ST8SiaII and ST8SiaIV. Both enzymes have been cloned, sequenced and shown to be involved in the polysialylation of NCAM (Eckhardt *et al.*, 1995; Nakayama *et al.*, 1995; Scheidegger *et al.*, 1995; Kojima *et al.*, 1995). Both mammalian polySTs belong to the a2,8-sialyltransferase family. Members of this protein family share three highly conserved amino acid motifs: L-motif (large motif), S-motif (short motif) and VS-motif (very short motif). In addition, the PSTD-motif (polysialyltransferase domain) has been identified to mark polySTs in this family (Harduin-Lepers *et al.*, 2005; Nakata, Zhang, and Troy, 2006).

Studies carried out to identify the function of conserved motifs showed that the L-motif is involved in binding of the donor substrate CMP-Neu5Ac (shown for a2,6-sialyltransferase; ST6Gal I), whereas the S-motif participates in binding both CMP-Neu5Ac as well as the acceptor protein (Datta and Paulson, 1995; Datta, Sinha, and Paulson, 1998). Mutation of a conserved histidine residue in the VS-motifs (very short motif) of ST8SiaII and ST8SiaIV resulted in inactive enzymes (Kitazume-Kawaguchi, Kabata, and Arita, 2001). The PSTD-motif is essential to establish polysialylation capacity as demonstrated by recombinant expression of ST8SiaIV variants lacking the PST domain or harboring a truncated PSTD (Nakata, Zhang, and Troy, 2006).

In addition, studies using the thiol-directed alkylating reagents, N-ethylmaleimide and iodoacetamide with fractions containing embryonic chick brain polySTs revealed that at least one out of six conserved cysteine residues is critical for polysialylation activity (Drickamer, 1993; Sevigny *et al.*, 1998). Further studies demonstrated that the first cysteine residue (C) located in the L-motif and the cysteine of the S-motif form a disulfide bridge, whereas the second cysteine in the sialyl-motif L and the cysteine located at the very C-terminus of the enzymes form a second disulfide bond (Angata *et al.*, 2001).

Beside the integrity of the conserved functions described above, *N*-glycosylation is a prerequisite for polyST activity. Previous studies revealed that ST8SiaII and ST8SiaIV comprise six and five *N*-glycosylation attachment sites, respectively. Comprehensive mutagenesis studies were applied to determine the influence of each *N*-glycan on polyST activity. These characterizations indicated that ST8SiaII activity depends on the presence of

N-glycosylation sites N89 and N219, whereas ST8SiaIV requires an *N*-glycan at position N74. Remarkably, the *N*-glycans at positions N89, N219, and N234 in ST8SiaII as well as N50, N74, and N119 in ST8SiaIV are additionally modified by polySia. This modification of polySTs by polySia has been referred to as autopolysialylation, although it is not clear yet, whether the modification represents an intra- or intermolecular process (Close, Tao, and Colley, 2000; Close *et al.*, 2001; Mühlenhoff *et al.*, 2001).

Interestingly, only a few protein acceptors carrying polySia have been identified until now, whereupon NCAM is by far the most prevalent (Rothbard *et al.*, 1982). Additional polySia carriers are the a subunit of the voltage dependent sodium channel (Zuber *et al.*, 1992), the scavenger receptor CD36, identified as soluble protein in human breast milk (Yabe *et al.*, 2003) and, as shown in a most recent study, neuropilin-2 expressed on matured dendritic cells (Curreli *et al.*, 2007). The selectivity of the polysialylation reaction has recently been rationalized by the identification of a polyST recognition site on NCAM. Within the first FNIII-like domain of NCAM two structural motifs - an acidic patch and an α-helix - were identified as critical for polysialylation efficiency and precise contact formation between polyST and NCAM, respectively. The precision of protein-protein interaction between NCAM and polyST has been suggested to be needed also for the correct presentation of the *N*-glycans localized in the Ig5 domain (Mendiratta *et al.*, 2005; Mendiratta *et al.*, 2006; Colley, 2008).

These latter results may also explain the observed drop in activity if polySTs were tested with free sugar acceptors (Angata *et al.*, 2000). Nonetheless, initiation of polysialylation on protein free monosialyl (Neu5Aca(2,3)-Galß(1,4)-R) and disialyl acceptors (Neu5Aca(2,8)-Neu5Aca(2,3)-Galß(1,4)-R) was observed (Angata *et al.*, 2000; Angata, Suzuki, and Fukuda, 2002).

Since the cloning in 1995 significant effort has been made to gain insight into the catalytic mechanism of polySTs, however, all these studies were drastically hampered by the availability of recombinant enzymes. Logically, information on the 3D-structure of polySTs is completely missing. Since *N*-glycosylation and disulfide bonds are important for the formation of active polySTs, expression systems have so far been limited to eukaryotic cells (CHO, COS, and insect cells), resulting in only very small protein yields for the recombinant mammalian polySTs (Mühlenhoff *et al.*, 2001; Angata *et al.*, 2001).

Interestingly, the homologous enzyme from the lower vertebrate zebrafish (zST8SiaII) lacks one out of six *N*-glycosylation sites, whereupon a functional enzyme is maintained (Marx *et*

al., 2007). Therefore, we speculated that zST8SiaII is a suitable candidate for a purification approach.

The first goal of my study was to optimize the conditions for recombinant expression of zST8SiaII, by identifying the minimally active enzyme at the linear sequence level with respect to the number of functionally important *N*-glycosylation sites. Furthermore large scale production using a baculoviral expression system was established and finally enabled the preparation of an active eukaryotic polyST in good yield and high purity. Using saturation-transfer-difference (STD)-NMR spectroscopy we gained first insight into substrate binding properties of eukaryotic polySTs.

1.2. Experimental Procedures

1.2.1. Materials

Endoneuraminidase NF (endoNF) was purified from *Escherichia coli K1* bacteriophage as described previously (Gerardy-Schahn *et al.*, 1995). Recombinant soluble proteinA-NCAM was expressed in CHO-2A10 cells and purified as described in Mühlenhoff *et al*. (1996). The eukaryotic expression vector pPROTA (Sanchez-Lopez *et al.*, 1988) was kindly provided by Dr. R. Beathnach (INSERM, Nantes, France). Oligosaccharide acceptors and CMP-Neu5Ac were purchased from Nakalai. Neu5Acß2Me and Neu5Aca2Me were generously provided by Prof. Dr. Mark von Itzstein (Griffith University, Gold Coast, Australia).

1.2.2. Expression Plasmids

To construct N-terminally truncated zST8SiaII variants for expression in (CHO)-cells, ST8SiaII from zebrafish (genbank accession number NP_705948) was amplified from the plasmid of full length, N-terminally Flag-HA tagged zST8SiaII (pFlagHA-ST8SiaII; Marx *et al.*, 2007) using the following primer pairs:

N?26: GCATGAATTCGGAAGTGGAGGAAGAA / reverse primer: CGTAGAATTCATG TAGGAGGTTTGCA

N?54: GCATGAATTCGGATCTGAATGCTGCCCC / reverse primer: CGTAGAATTCAT GTAGGAGGTTTGCA

N?86: GCATGAATTCGGCTTCATCCTCATCTGAATGG / reverse primer: CGTAGAAT TCATGTAGGAGGTTTGCA

N?95: GCATGAATTCGAGAACCTTGTCTAACCTC / reverse primer: CGTAGAATTCA
TGTAGGAGGTTTGCA

PCR products were digested with *Eco*RI and after gel purification (Qiagen) ligated into the corresponding restriction site of pProtA, a cell culture vector containing a transin secretion signal sequence and the sequence encoding IgG binding domain of *Staphylococcus aureus* proteinA. The resulting plasmids drive the expression of N-terminally proteinA-fusion proteins. The identity of all constructs was confirmed by sequencing.

To construct N-terminally truncated zST8SiaII variants for expression in insect cells, ST8SiaII from zebrafish was amplified from the plasmid pFlagHA-ST8SiaII using the primer pairs:

N?26: CGGCTCATGACGGAAGTGGAGGAAGAAATCGC / reverse primer: CGGAAGC
TTTTATGTAGGAGGTTTGCATGGTC

N?86: CGGCTCATGACGTCATCCTCATCTGAATGGAC / reverse primer CGGAAGCTT
TTATGTAGGAGGTTTGCATGGTC

PCR products were digested with *Bsp*HI and *Hind*III, gel purified (Qiagen) and ligated into the restriction sites *Nco*I and *Hind*III of a modified pFastbac1 vector (Invitrogen) containing a honeybee melittin (HBM) secretion signal and a N-terminal His-tag. The resulting plasmids express an N-terminal His-tagged protein. The identity of all constructs was confirmed by sequencing.

1.2.3. Site-directed mutagenesis of ST8SiaII cDNA

N-glycosylation site deficient zST8SiaII variants were generated by PCR using the QuikChange site-directed mutagenesis kit (Stratagene) following the manufactures guidelines. *N*-glycosylation sites were destroyed by substituting the asparagine (N) in the N-X-S/T motifs by glutamine (Q). For site directed mutagenesis the plasmid pFlagHA-ST8SiaII was used as template. The primer pairs used are listed below (point mutations are in bold):

N95Qs:CTCATCTGAATGGACTTTC**C**AA**A**GAACCTTGTCTAACCTC

N95Qas:GAGGTTAGACAAGGTTCTTTGGAAAGTCCATTCAGATGAG

N140Qs:GACCGTCAGAGCACCACA**C**AA**A**TCTCAGAGAATCTGTAC

N140Qas:GTACAGATTCTCTGAGATTTGTGTGGTGCTCTGACGG

N174Qs:GAACTCTGGCATACTACTG**C**A**G**AGCAGCTGCGGCAGAGAG

N174Qas:CTCTCTGCCGCAGCTGCTCTGCAGTAGTATGCCAGAGTTC

PCR products were subcloned into *Eco*RI and *Bst*XI sites of pFlagHA-ST8SiaII and the identity of all constructs was confirmed by sequencing. To generate double or triple variants

in terms of *N*-glycosylation sites, the corresponding mono or double variants were used as templates in an additional site-directed mutagenesis approach.

To obtain the corresponding ProtA-fusion proteins, the Flag-HA-ST8SiaII variants were used as template using the primer pairs described above.

1.2.4. Cultivation of CHO cells

PolySia negative *Chinese hamster ovary* (CHO)-2A10 cells, defective in the ST8SiaIV gene (Eckhardt *et al.*, 1995), were kept in a humidified incubator at 37°C and 5 % CO_2. Cells were cultured in DMEM/HAM's F12 medium (Biochrom) supplemented with 5 % fetal calf serum (biochrom) and 1 mM sodium pyruvate (Gibco BRL). Confluent cell layers were treated with PBS/EDTA to detach the cells from culture vessel and diluted 1:20 in fresh medium.

For long term storage in liquid nitrogen, cells were pelleted by centrifugation (5 min, 200xg, RT) and resuspended in culture medium containing 20 % fetal calf serum and 10 % DMSO at a concentration of $1x10^7$ cells/ml. Aliquots of 1 ml were filled in cryo vials, stored overnight at -80°C and then transferred to liquid nitrogen.

To recover frozen cell pellets, they were kept on dry ice for 5 min, thawed in a water bath at 37°C and diluted by drop wise addition of culture medium containing 10 % fetal calf serum. After centrifugation (5 min, 200xg, RT) the cell pellet was again resuspended in culture medium containing 10 % fetal calf serum and transferred to culture vessels.

1.2.5. Transfection of CHO cells

For transient transfection of CHO cells $1.9x10^6$ cells were seeded in 100 mm culture vessels and cultivated over night as described in 1.2.4. A transfection mix was prepared by diluting 4 µg plasmid DNA and 24 µl Lipofectamine (Invitrogen) in 400 µl OptiMEM (Gibco BRL) each. Both dilutions were combined and incubated for 30 min at RT.

The CHO cell layer (70-80 % confluent) was washed twice in PBS and incubated with freshly prepared transfection mix diluted in 3.2 ml OptiMEM for 5-6 h. The transfection was stopped by replacement of the transfection mix with 8 ml culture medium. Cells were cultivated for additional 72 h.

For immunofluorescence staining $0.9x10^5$ cells were seeded per well of a six well tissue culture plate, containing coverslips. The transfection procedure was performed as described above, using 1 µg DNA and 6 µl Lipofectamin diluted in 100 µl OptiMEM each. The total volume of the prepared transfection mix was 1 ml per well of a six well tissue culture plate. After 5-6 h, transfection mix was replaced by 2.5 ml fresh culture medium and cells were incubated for another 48 h as described in 1.2.4.

1.2.6. Cultivation of *Sf9* cells

Suspension cultures of *Spodoptera frugiperda (SF9)* cells were cultivated at 27°C and 90 rpm in protein free Insect XPress-medium (BioWhittaker). Cell density was maintained between 0.5×10^6 and 5×10^6 cells per millilitre by diluting dense cultures in fresh medium.

For long term storage in liquid nitrogen, cells were pelleted by centrifugation (5 min, 200xg, RT) and resuspended in the conditioned culture medium containing 10 % DMSO at a concentration of 2×10^7 cells/ml. Aliquots of 1 ml were filled in cyro vials and cooled down by subsequent incubations at 4°C and -20°C for 1 h each. Cells were stored overnight at -80°C and then transferred to liquid nitrogen.

To recover frozen cell pellets, they were kept on dry ice for 5 min, thawed in a water bath at 37°C and directly added to 30 ml culture medium in a culture vessel.

1.2.7. In vitro assay for Auto- and NCAM polysialylation

PolySia negative CHO-2A10 cells, defective in the ST8SiaIV gene (Eckhardt *et al.*, 1995), were transfected as described in 1.2.5. To standardize the concentration of ProtA-zST8SiaII variants for the polysialylation assay, an enzyme-linked immunosorbent assay (ELISA) was used as described in Mühlenhoff *et al.* (2001).

Round-bottom microtiter plates (Greiner) were coated overnight with 0.2 µg murine IgG (Pierce) at 4°C and blocked with bovine serum albumin (1 % in PBS) (Sigma) for 2 h at RT. Plates were washed with PBS prior to addition of 20 µl/well of cell supernatant that contained ProtA-zST8SiaII variants. Plates were incubated for 1 h at RT to allow binding of ProtA– polyST fusion variants to IgG. In parallel, serial dilutions (1 - 0.05 ng/ml) of the recombinant IgG-binding fragment of ProteinA (Sigma) were included to generate a standard curve. After the adsorption step, plates were washed three times with PBS, before adding 20 µl/well of biotinylated anti-ProteinA antibody in a 1:80,000 dilution (Sigma). The plates were incubated for 1 h at 37°C and washed three times with PBS. The bound biotinylated antibody was detected with streptavidin-horseradish peroxidase conjugate (Roche) using 20 µl/well of an 1:20,000 dilution. After 30 min at 37°C plates were washed three times with PBS and developed with 50 µl/well of substrate solution containing 5 µg 3,3',5,5'-tetramethylbenzidine (TMB), 100 mM sodium acetate, 100 mM citric acid, and 0.0045 % H_2O_2. The staining reaction was stopped after 20 min by adding 25 µl/well 2 N H_2SO_4, and the optical density at 450 nm was determined using a PowerWave 340 microtiter plate spectrophotometer (BioTek). All samples were measured in serial dilutions, and triple values were analyzed for each dilution.

Subsequently, polyST activity was assayed by incorporation of [^{14}C]-labeled sialic acid residues into a growing polySia chain and monitored by SDS-PAGE followed by autoradiography. 1 µg of each enzyme variant was incubated with 20 µl IgG-coated sepharose beads (Pierce) for 1 h at 4 °C in a head-over-head shaker, to allow adsorption of the proteinA-tagged polyST variants to the beads. Afterwards the beads were washed three times with 1 ml PBS and two times with 1 ml reaction buffer (10 mM sodium cacodylate buffer or MES pH 6.7; 10 mM MnCl$_2$) before resuspended in 40 µl reaction buffer containing 0.12 mM (21 Bq/µl) [^{14}C]-CMP-Neu5Ac (GE Healthcare). Samples were incubated at 27°C and 1300 rpm to allow enzyme reaction. After 4 h reactions were terminated by washing the beads two times with 1 ml PBS. As an assay control, one out of two parallel samples was treated with 20 µg/ml of the polySia-degrading enzyme EndoNF in a final volume of 50 µl PBS for 30 min at 37°C. After two additional washing steps with 1 ml PBS each, residual buffer was removed and 20 µl of 2xLaemmli loading buffer containing 2 % ß-mercaptoethanol were added. Samples were heated for 10 min at 60°C and analyzed by SDS-PAGE followed by autoradiography (Mühlenhoff *et al.*, 2001). To investigate NCAM-polysialylation, cell culture supernatant containing 30 ng of recombinant polySia-free ProtA-NCAM was additionally adsorbed to IgG-coated sepharose beads and the assay was performed as described above.

1.2.8. Immunofluorescence of zST8SiaII variants in CHO 2A10 cells

48 h after transfection (1.2.5), cells were washed with PBS, fixed in 4 % paraformaldehyde for 20 min, and washed two times with PBS. Coverslips were blocked in 20 % horse serum in PBS for 30 min. Subsequently, polySia staining was performed with 5 µg/ml of primary monoclonal antibody 735 (Behring Werke Marburg) in 20 % horse serum. After washing three times with PBS, the cells were incubated for 30 min at RT with sheep anti-mouse IgG-Cy3 (1:300; Sigma) in 20 % horse serum. For intracelullar Flag-staining, cells were permeabilized in 0.2 % triton X100 in PBS for 9 min and stained with anti-Flag M5 (Sigma). After washing three times with PBS, the cells were incubated for 30 min with sheep anti-mouse IgG-Cy3 in 20 % horse serum.

The cells were washed three times with PBS, and coverslips were mounted in vectashield (Vectashield) and analyzed under an Axiovert 200 M fluorescence microscope (Zeiss).

1.2.9. zST8SiaII expression and purification from insect cells

Recombinant baculoviruses were generated based on transposon-mediated recombination in *E. coli* DH10Bac cells using the Bac-to-Bac Baculovirus Expression System (Invitrogen).

Preparation of recombinant bacmid DNA:

100 µl of competent *E. coli* DH10Bac were thawed on ice and incubated for 30 min with 20 ng of the respective pFastBac vector construct. The transformation mix was subjected to a heat shock at 42°C for 45 sec and incubated on ice for 2 min. 900 µl of SOC-medium were added, the cell suspension was incubated at 37°C for 4 h before plated on selective LB-agar plates containing 50 µg/ml kanamycin, 7 µg/ml gentamicin, 10 µg/ml tetracycline and 40 µg/ml IPTG. For blue-white screening 30 µl of X-Gal solution (20 mg/ml in DMSO) were spread on the plates prior to plating. Positive transformants were identified after 48 h incubation at 37°C as pure white colonies and re-streaked on fresh plates to confirm the phenotype. 5 ml LB-medium containing 50 µg/ml kanamycin, 7 µg/ml gentamicin and 10 µg/ml tetracycline were inoculated with a positive colony and incubated overnight at 37°C and 300 rpm. Bacmid DNA was isolated using the "Concert High Purity Plasmid Purification System" (GibcoBRL) according to the manufactures instructions. 3 ml of bacterial culture were pelleted (1 min, 12,000xg, RT), resuspended in 400 µl buffer E1 and lysed for 5 min at RT after addition of 400 µl buffer E2. 400 µl neutralization buffer E3 was added, the samples were centrifuged (10 min, 12,000xg, RT) and the supernatant was applied to the concert HP columns, equilibrated in buffer E4. After washing two times with 2.5 ml buffer E5, bound bacmid DNA was eluted in 900 µl buffer E6. 630 µl of 2-propanol were added to the eluent and the DNA was pelleted (30 min, 20,000xg, 4°C). The pellet was washed with 1 ml of 70% ethanol and centrifugated (15 min, 20000xg, 4°C). The bacmid DNA was air-dried for 30 min and resolved in 50 µl of 5 mM Tris/HCl pH 8 for 2 h at RT and stored at 4°C.

Production of recombinant baculoviruses and high-titer stocks:

Baculoviruses were produced by transfecting the prepared recombinant bacmid DNA into *Sf9* cells. For transient transfection $1x10^6$ cells were seeded per well of a six well tissue culture plate. Transfection mix was prepared from 5 µl of bacmid DNA and 6 µl Cellfectin (Invitrogen) in 100 µl of culture media each. Both dilutions were combined and incubated for 30 min at RT. The medium was aspirated from adherend *Sf9* cells and replaced with transfection mix diluted in 1 ml culture medium. The transfection mix was removed after 14 h and replaced with 2 ml culture medium. The transfected cells were incubated at 27°C for 4-7 days until signs of viral infection like enlarged cell diameters and a granular appearance of the cells were clearly visible.

The supernatant (low-titer P1-stock) was harvested and stored at -80°C. For virus amplification 40 µl P1-stock were added to 4 ml *Sf9* cells ($2x10^6$ cells) in a 25 cm^2 cell culture bottle (Sarsted) and incubated for 3-4 days (P2-stock). Further amplification of the

baculovirus stock was performed by infecting 50 ml suspension culture ($2x10^6$ cells/ml) with 50 µl of P2-stock. After three days, the cells were pelleted by centrifugation (5 min, 300xg, RT) and the supernatant was sterile filtered (0.2 µm cellulose acetate filter; Sartorius) and stored at 4°C (P3-stock).

Baculoviral expression of ST8SiaII variants in *Sf9* cells:

For baculoviral expression of recombinant zST8SiaII variants log-phase *Sf9* cells at a density of $1.5-2x10^6$ cells/ml were infected with different concentrations of P3-stock and cultivated for time response at 27 °C and 90 rpm. Culture supernatants were assayed for protein expression by SDS-PAGE followed by western blot analysis (1.2.11).

The dose of baculovirus required for optimal expression of recombinant protein was used for subsequent large scale expressions cultures.

Purification of baculoviral expressed zST8SiaII variants from *Sf9* cells:

4 L-expression cultures were infected with the optimal baculovirus concentration and harvested at the time point determined previously. To harvest the recombinantly expressed protein, cells were pelleted (10 min, 300xg, 4°C) and the supernatant was adjusted with NaOH to pH 7.5 and re-centrifugated (20 min, 7,000xg, 4°C). Subsequently, the supernatant was filtered (0.22 µM Millipore-1L-device) and concentrated to 100 ml (Ultrasette 10,000 MWCO) at 4°C. To remove low molecular weight inhibitors the concentrate was diluted 1:5 with buffer DT (50 mM Tris/HCl; 100 mM NaCl; pH 7.5) and concentrated to 80 ml. Protein containing solution was filtered (0.22 µM) and 10 % glycerol was added. Coupling to Ni^{2+}chelating matrix (Probond-resin; Invitrogen) was performed overnight at 4°C. For all following steps Äkta FPLC (GE Healthcare) was used with a flow rate of 1 ml/min. The protein was eluted stepwise starting with 10 mM imidazole in precooled buffer A (50 mM Tris/HCl pH 7.5; 100 mM NaCl; 10 % glycerol) followed by 100 mM imidazole and 400 mM imidazole in buffer A, respectively. 1 ml fractions were collected and protein containing fractions were analyzed with SDS-PAGE followed by western blot analysis and silver staining (1.2.11/12). Polysialyltransferase containing fractions were concentrated in a vivaspin concentrator (10,000 MVCO PES; Vivascience), quick-frozen in liquid nitrogen and stored at –80°C or further analyzed by size-exclusion chromatography.

1.2.10. Size-exclusion chromatography

A Superdex 200 HR 10/30 column (Amersham Biosciences) was equilibrated in degassed and 0.22 µm sterile filtrated buffer *DT2 (*10 mM Tris/HCl pH 7.5*;*150 mM NaCl) using the Äkta FPLC system (GE Healthcare). Purified protein was applied and eluted in 0.5 ml fractions at a flow rate of 0.5 ml/min. Protein standards were applied under the same

conditions to generate a molecular weight standard curve. Polysialyltransferase containing fractions were concentrated in a vivaspin concentrator (10,000 MVCO PES; Vivascience) and stored at -80°C after quick-freezing in liquid nitrogen.

1.2.11. SDS-PAGE analysis and immunoblotting

For protein separation a SDS-PAGE was performed according to Laemmli (Laemmli, Beguin, and Gujer-Kellenberger, 1970). SDS-PAGE gels were composed of a 3 % stacking gel [125 mM Tris/HCl pH 6.8; 0.1 % SDS; 3 % polyacrylamide(40 % 4 K-Mix, AppliChem)] and a separating gel in a range of 7-14 % polyacrylamide [375 mM Tris/HCl pH 8.8; 0.1 % SDS; 7-14 % Acrylamide (40 % 4 K-Mix, AppliChem)]. After mixing all components polymerization was initiated by adding 0.1 % TEMED and 1 % ammonium persulphate.

For sample preparation, the samples were diluted 1:1 with Laemmli buffer containing 2 % ß-mercaptoethanol and boiled for 5 min or heated to 60°C for 10 min, if they contained heat-sensitive polySia.

Electrophoresis was performed in SDS-electrophoresis buffer (50 mM Tris; 350 mM glycine; 0.1 % SDS) at 60 V for the stacking gel and at 140 V for the separating gel.

After SDS-PAGE, separated proteins were transferred onto a nitrocellulose membrane (Schleicher & Schüll), using a semidry blotting chamber (Biometra) at 2 mA/cm^2 for 45 min. Gel and membrane were placed between two layers of filter paper (Whatman) soaked in blotting buffer (48 mM Tris, 39 mM glycine). Western blots were developed using the recommended primary antibody concentration, followed by anti-mouse alkaline phosphatase conjugate (Dianova). Nitro blue tetrazolium (NBT) and 5-bromo-4-chloro-3-inodyl phosphate (BCIP) were used as substrates for alkaline phosphatase staining reaction.

1.2.12. Silver staining

After SDS-PAGE, protein bands were visualized by silver staining. Initially, the SDS-gel was incubated in fixation solution (10 % acetic acid; 30 % ethanol; 1.85 % formaldehyde) for 20 min. After washing three times with 50 % ethanol for 20 min the gel was incubated for exactly 1 min in thiosulphate solution (20 mg thiosulphate in 20 ml H_2O) and washed in deionised water for 40 seconds. Subsequently the gel was incubated in silver staining solution (0.2 % $AgNO_3$; 2.8 % formaldehyde) for 20 min. After washing with deionised water the gel was incubated in developing solution (6 % $NaCO_3$; 2 % (v/v) thiosulphate solution; 1.85 % formaldehyde) until the bands appeared. Staining was stopped by washing with water and stop solution (10 % acetic acid; 30 % ethanol). Before drying, the gel was incubated in 30 %

ethanol for 30 min and subsequently in drying solution (10 % glycerol; 20 % ethanol) for 20 min. Gels were dried in cellophane foil overnight at 50 °C.

1.2.13. Soluble radioactive activity assay for polyST

To monitor the enzymatic activity of polyST in solution, purified zST8SiaII?N86 was incubated with a mixture of radiocarbon labeled CMP-Neu5Ac (860 Bq, Amersham Pharmacia Biotech), unlabeled CMP-Neu5Ac (0.25 mM) and purified NCAM in reaction buffer (10 mM sodium cacodylate buffer pH 6.7; 10 mM $MnCl_2$) for 3 h at 26 °C and 1300 rpm. Afterwards 2xLaemmli buffer containing 2 % ß-mercaptoethanol was added in a 1:1 ratio and half of the sample was incubated with 1 µl of 1 mg/ml EndoNF for 30 min and 1300 rpm at 37 °C. Samples were heated at 60 °C for 10 min and separated on a 7.5% SDS-gel followed by autoradiography.

1.2.14. Enzyme-linked immunosorbent assay for polysialyltransferase activity

To monitor polyST activity in a non radioactive test system an enzyme-linked immunosorbent assay (ELISA) was established by Dr. Stummeyer from our laboratory. A 96 well microtiter plate (Greiner) was coated with 25 µl/well of 10 µg/ml mouse IgG (Pierce) in PBS for 3 h at RT. After washing three times with PBS plastic surface was blocked with 1 % BSA in PBS (Sigma) overnight at 4°C. For NCAM-polysialylation 25 µl of 30 ng/ml polySia free proteinA-NCAM fusion protein was adsorbed for 1 h at RT. After washing three times with PBS and two times with reaction buffer (10 mM sodium cacodylate buffer pH 6.7; 10 mM $MnCl_2$, 3.3% human serum) 0.2 µg polyST were directly incubated in reaction buffer, containing 1 mM CMP-Neu5Ac for 3 h at 27°C or overnight at RT. The plates were washed two times with PBS and subsequently incubated with 25 µl/well of biotinylated fab-fragments of mAb 735 (Davids Biotechnologie) diluted 1:500 in 1 % BSA (Sigma) for 1 h at RT. Afterwards, plates were washed three times with PBS. The bound biotinylated antibody was detected with streptavidin-horseradish peroxidase conjugate (Roche) using 20 µl of a 1:20,000 dilution per well. After 30 min at 37°C plates were washed three times with PBS and developed with 50 µl of substrate solution containing 5 µg 3,3',5,5'-tetramethylbenzidine (TMB), 100 mM sodium acetate, 100 mM citric acid, and 0.0045 % H_2O_2. Reactions were stopped after 20 min by adding 25 µl 2N H_2SO_4, and the optical density at 450 nm was measured in PowerWave 340 microtiter plate spectrophotometer (BioTek).

1.2.15. Nuclear magnetic resonance (NMR) spectroscopy

All NMR spectroscopy experiments were performed on a Bruker Avance DRX 600 MHz spectrometer using a cryoprobe equipped with triple axis gradient at 283 K in deuterated buffer (10 mM Tris$_{d5}$/DCl, 1 mM MgCl$_2$, pH 6.8).

ST8SiaII?N86 samples were buffer exchanged using BioSpin 30 columns (BioRad) to deuterated 10 mM Tris$_{d5}$/DCl, 1 mM MgCl$_2$, pH 6.8.

1.2.16. Saturation-transfer-difference-(STD)-NMR spectroscopy

For STD-NMR spectroscopy (Mayer and Meyer, 2000) purified ST8SiaII was saturated on-resonance at 0.7 ppm. The off-resonance frequency was set to 40 ppm. A cascade of 40 selective Gaussian-shaped pulses of 50 ms duration with a 100 μs delay between each pulse were used in all STD-NMR experiments to saturate the protein for 2 s. For STD-NMR experiments, 13.5 μM recombinant ST8SiaII?N86 was used. All investigated ligands were added at a molecular ratio (protein:ligand) of 1:100. A total of 1024 transient experiments were acquired, and a WATERGATE sequence was used to suppress the residual HDO signal. A spin lock filter with a strength of 5 kHz and a duration of 10 ms was applied to suppress residual protein background signals.

1.2.17. ^{1}H-NMR spectroscopy based enzyme assay

All ^{1}H-NMR spectroscopy experiments were performed using 13.5 μM purified ST8SiaII?N86 and 1.35 mM CMP-Neu5Ac. All investigated substrates were added at a molecular ratio (protein:substrate) of 1:100. In a typical ^{1}H-NMR spectroscopy experiment, a spectrum containing the enzyme and the acceptor was acquired at t= 0 min. After addition of 1.35 mM CMP-Neu5Ac, ^{1}H-NMR spectroscopy spectra were recorded in 10 min time intervals over 2.5-5 h at 283 K or after overnight incubation at 293 K. A total of 8 transient experiments were acquired, and suppression of residual HDO signal was achieved by presaturation using a weak radio frequency field for 1.5 s during the relaxation delay. Data acquisition and processing were performed with Topspin software (Bruker). Fourier transformation, phase correction and base line correction were performed for all ^{1}H-NMR spectroscopy experiments.

1.2.18. Crystallization trials carried out with ST8SiaII

Crystallization trials were accomplished as sitting drop vapor diffusion experiments. Purified zST8SiaII?N86 was concentrated to 5.7 mg/ml in 10 mM Tris/HCl pH 7.5; 10 mM $MnCl_2$; 150 mM NaCl. Crystallization trials were performed in the presence or absence of the donor analogue CMP-Neu5Ac-3F (f.c. 2 mM) in our laboratory and at the HT-crystallization facility of EMBL; Hamburg (Mueller-Dieckmann, 2006).

1.3. Results

1.3.1. Comparison of zebrafish and murine ST8SiaII on primary sequence level

The polysialyltransferase (polyST) ST8SiaII from zebrafish (zST8SiaII) belongs to the a2,8-sialyltransferase protein family and therefore contains the L-,S- and VS-motif, respectively, that are highly conserved among family members. An alignment of murine and zebrafish enzymes revealed 61 % identity on the primary sequence level. Apart from the N-terminus these enzymes are highly conserved among the catalytic domain starting at amino acid 88 (71 % identity), as shown in figure 6 A. The positioning of predicted *N*-glycosylation sites of zebrafish and murine ST8SiaII is depicted in figure 6 B. Interestingly only five *N*-glycosylation attachment sites were predicted for the zST8SiaII whereas the murine homologue harbors six sites. Enzymatic activity of the murine enzyme crucially depends on the presence of the *N*-glycosylation attachment sites N89 (#3) and N219 (#5) (Mühlenhoff *et al.*, 2001; Close *et al.*, 2001).

As shown by the sequence alignment in figure 6 A the asparagine residue N95 (#3) of zST8SiaII corresponds to the important residue N89 (#3) of the murine enzyme. By contrast, no asparagine residue is located in a position equivalent to the *N*-glycosylation site N219 (#5) of the murine enzyme.

Further comparison revealed that zST8SiaII has a predicted *N*-glycosylation site in the conserved L-motif, which is unique among all polySTs characterized so far.
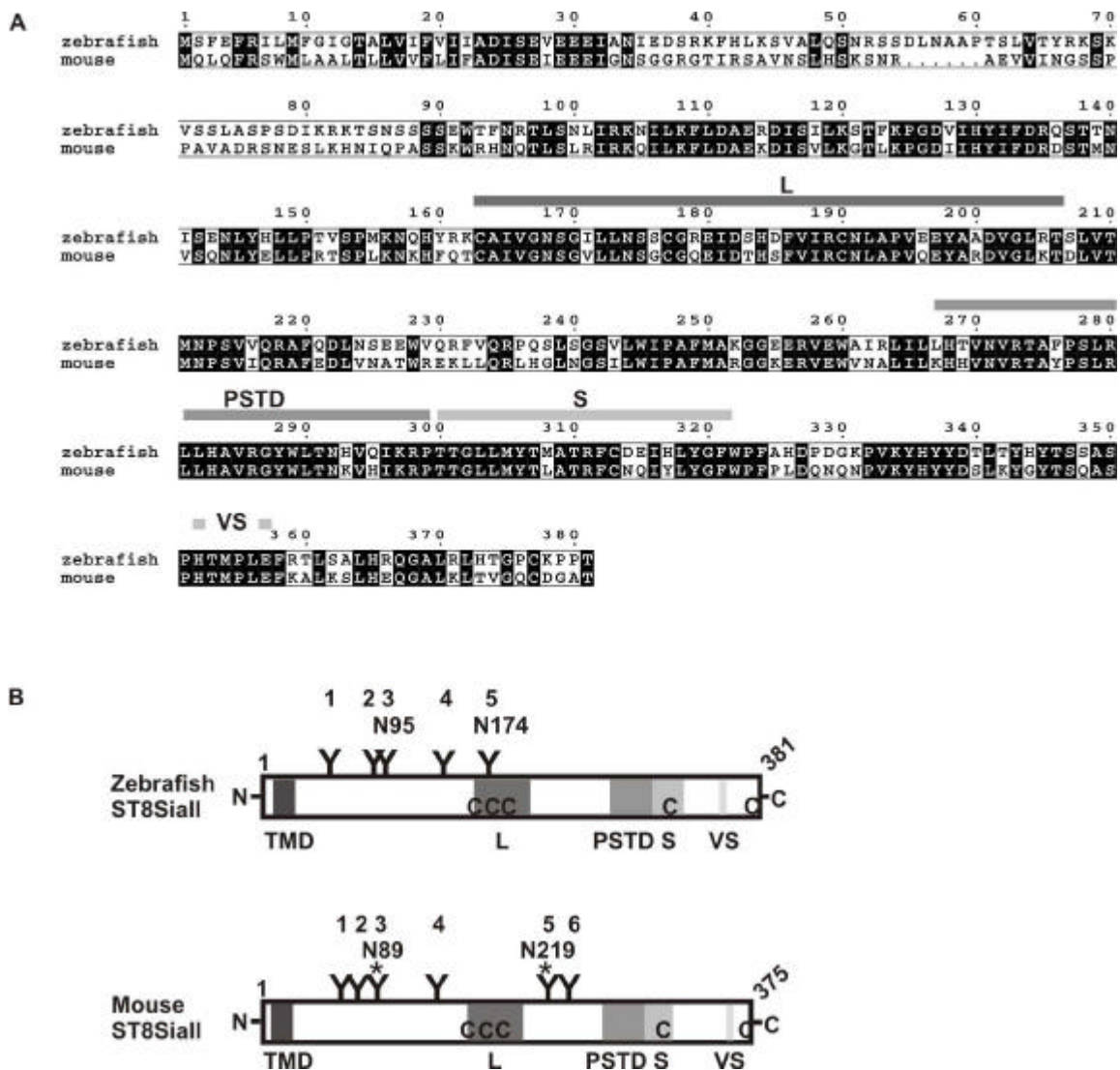
Figure 6: Comparison of eukaryotic ST8SiaII from zebrafish and mouse. *A*. Multiple sequence alignment of murine and bonefish ST8SiaII generated with *MultAlin* (Corpet, 1988). Sequence identity is highlighted in dark boxes and sialyl motifs (L, S and VS) as well as the polyST domain (PSTD), the transmembrane domain (TMD) and the stem region (stem) are indicated. *B*. Schematic representation of mouse and zebrafish polySTs. Positioning of *N*-glycosylation sites are given by the respective asparagine residues. Sialyl motifs (L, S and VS), polyST domain (PSTD) and conserved cysteine residues (C) are indicated. For the murine ST8SiaII *N*-glycosylation attachment sites required for polyST activity are marked by an asterisk.

1.3.2. N-terminal truncation of zebrafish ST8SiaII

In order to determine the minimal catalytic domain of zST8SiaII, a set of N-terminally truncated enzyme variants was generated. Enzymes lacking 26 (zST8SiaIIΔN26), 54 (zST8SiaIIΔN54), 86 (zST8SiaIIΔN86) and 95 (zST8SiaIIΔN95) amino acids from their N-terminus were transiently expressed as secreted proteinA fusion constructs in CHO-2A10 cells. Enzyme activity was assayed essentially as described by Mühlenhoff and coworkers (Mühlenhoff *et al.*, 2001). Briefly, enzyme contents of the culture supernatants were determined by ELISA directed against the proteinA fusion tag. 1 µg of each enzyme was immobilized on IgG-Sepharose beads and incubated with radiocarbon labeled CMP-[^{14}C]Neu5Ac in the presence or absence of proteinA-NCAM. Samples were separated by SDS-PAGE before and after treatment with the polySia-degrading enzyme endoneuraminidaseF (endoNF) and reaction products were visualized by autoradiography. Polysialylation activity is indicated by a broad radioactive smear removable by endoNF treatment. Due to the fact that endoNF does not degrade the last three sialic acid residues of a polySia chain, protein acceptors are visualized by the remaining [^{14}C]-labeled sialic acid residues. As depicted in figure 7, N-terminal truncation of up to 86 amino acids retained an autopolysialylation and NCAM-polysialylation competent enzyme. However, autopolysialylation activity of the Δ54 and Δ86 variants appears to be decreased when compared to the Δ26 truncation that lacks only the transmembrane domain. By contrast, N-terminal truncation of 95 amino acids resulted in a complete loss of activity (fig. 7). Loading control by western blot analysis revealed that all enzyme variants were bound to the sepharose beads in comparable levels (fig. 7 *C*).
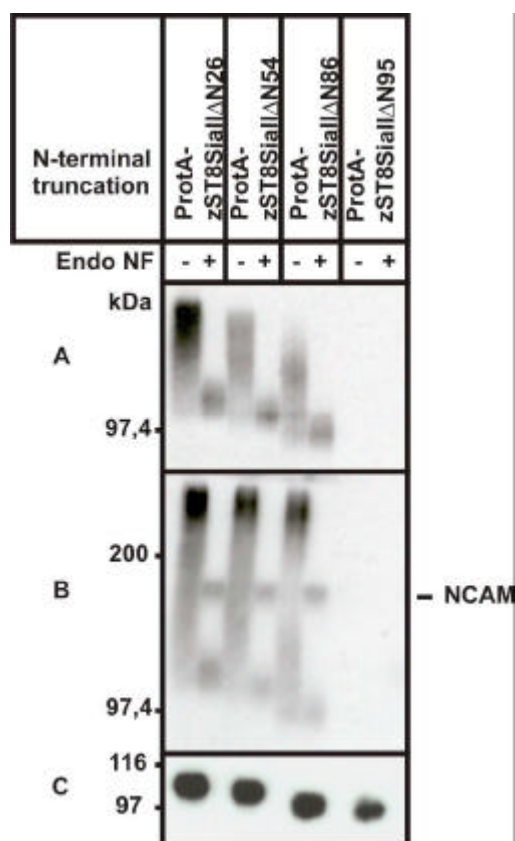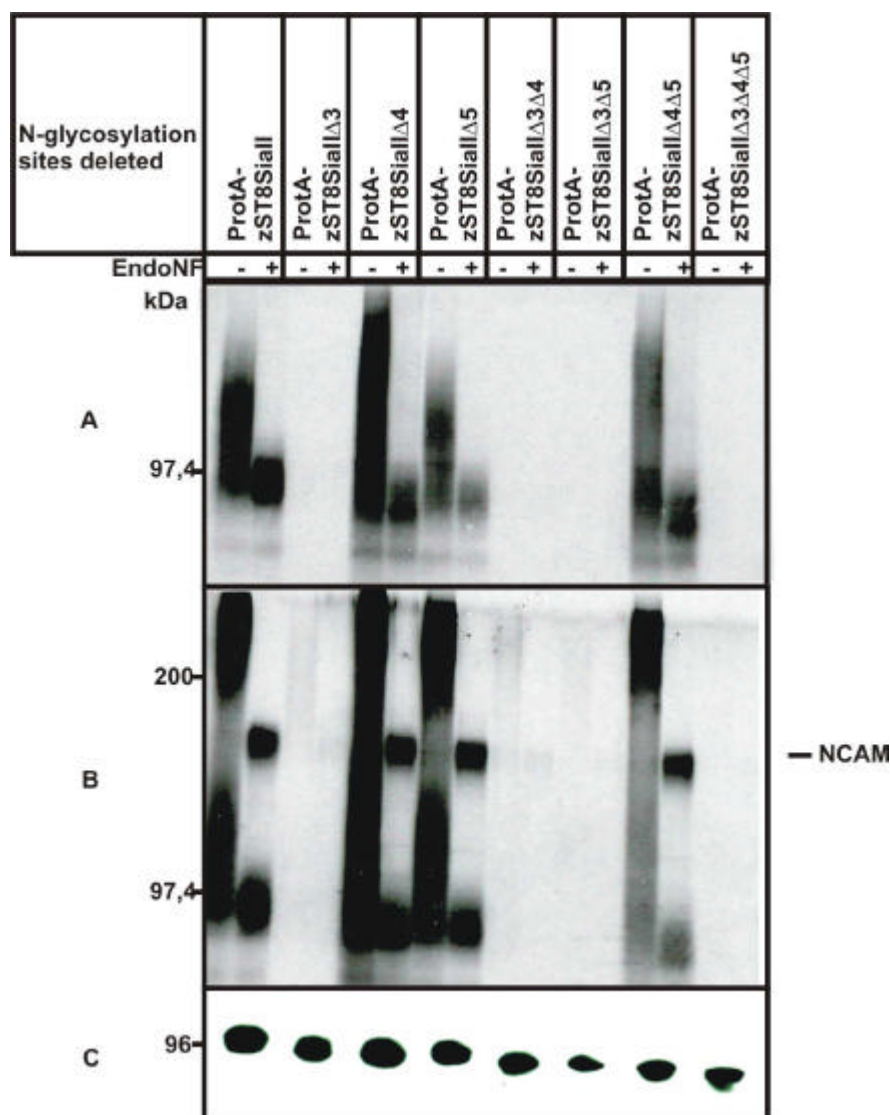
Figure 7: Polysialylation activity of N-terminal truncations of zebrafish ST8SiaII. Wild-type and N-terminally truncated variants of zST8SiaII were transiently expressed as secreted proteinA fusion constructs in CHO-2A10 cells. 72 h post transfection 1 µg of wild type or truncated zST8SiaII were adsorbed to IgG-Sepharose and used to analyze auto- and NCAM-polysialylation *in vitro*. *A*. For autopolysialylation proteinA-ST8SiaII variants bound to Sepharose-beads were incubated for 4 h at 37 °C in the presence of 0.12 mM CMP-[^{14}C]-Neu5Ac. Samples were separated by 10 % SDS-PAGE before (-) and after (+) treatment with EndoneuraminidaseF (EndoNF) and visualized by autoradiography. *B*. For NCAM-polysialylation samples were treated as described above, but additionally, 36 ng proteinA fused NCAM were adsorbed to the Sepharose-beads. The reaction mixture was analyzed by 7 % SDS-PAGE. *C*. Control of Sepharose-beads for comparable loading with proteinA (ProtA)-ST8SiaII variants by western blot analysis. Samples were analyzed by 10 % SDS-PAGE followed by western blotting using an antibody directed against the proteinA part.

1.3.3. *N*-glycosylation site N95 is important for polysialylation activity

Analysis of the N-terminally truncated enzyme variants described above revealed, that the first two *N*-glycosylation sites are of minor importance for zST8SiaII activity, because zST8SiaII?N86 lacking these sites was found to be active (fig. 7). To investigate the impact of the remaining three *N*-glycosylation sites of zST8SiaII?N86, a comprehensive site-directed mutagenesis approach was performed. Therefore, the respective asparagine residues (N) of the three **N**-X-S/T motifs were exchanged by glutamine in all possible combinations. The polysialylation ability of the resulting enzyme variants was analyzed as described in 1.3.2. All zST8SiaII?N86 glycosylation variants lacking the third *N*-glycosylation site N95 (?3) displayed drastically reduced activity in terms of NCAM-polysialylation as well as autopolysialylation (fig. 8 *A* and *B*). By contrast, the loss of *N*-glycosylation sites N140 (?4) and N174 (?5) revealed no significant effect with regard to polysialylation activity as all affected variants maintained activity. Remarkably, all identified potential *N*-glycosylation sites were found glycosylated, visible as a shift in molecular mass (fig. 7 *C*). Western blot analysis demonstrates that all analyzed zST8SiaII?N86 variants were secreted into the cell

culture supernatant. However, expression levels were analysed by proteinA-ELISA and found to be significantly reduced for all inactive enzyme variants lacking the third *N*-glycosylation site (up to fourfold for ProtA-zST8SiaII?3?4?5) as well as for the still active double mutant ProtA-zST8SiaII?4?5 (data not shown).

Figure 8: Polysialylation activity of *N*-glycosylation depletion variants of zebrafish ST8SiaII?N86. *N*-glycosylation variants of N-terminally truncated zST8SiaII?N86 were transiently expressed as proteinA fusion constructs in CHO-2A10 cells. 72 h after transfection 1µg of each enzyme were adsorbed to IgG-Sepharose and used to analyze auto- and NCAM-polysialylation *in vitro*. *A*. For autopolysialylation Sepharose-fixed proteinA-ST8SiaII variants were incubated for 4 h at 37 °C in the presence of 0.12 mM CMP-[^{14}C]-Neu5Ac. Samples were separated by 10 % SDS-PAGE before (-) and after (+) treatment with EndoneuraminidaseF (EndoNF) and visualized by autoradiography. *B*. For NCAM-polysialylation samples were treated as described above, but additionally, 36 ng proteinA fused NCAM were adsorbed to Sepharose-fixed proteinA-ST8SiaII variants. The reaction mixture was analyzed by 7% SDS-PAGE. *C*. Western blot analysis of 1 µg Sepharose immobilized proteinA-ST8SiaII variants. Samples were analyzed by 10 % SDS-PAGE followed by western blotting using an antibody directed against the proteinA part.

Taken together the mutagenesis study revealed that (i) all predicted *N*-glycosylation sites are glycosylated and that (ii) the presence of *N*-glycosylation site N95 is required and sufficient for zST8SiaII?N86 activity. This is an important difference to murine ST8SiaII, where two *N*-glycans were found to be required for *in vitro* activity (Mühlenhoff *et al.*, 2001).

1.3.4. Enzymatic activity of zST8SiaII variants *in vivo*

So far the crucial impact of *N*-glycosylation site N95 (#3) was analyzed exclusively using the N-terminally truncated enzyme variant zST8SiaII?N86. To exclude that the observed loss of activity in enzyme variants lacking this site is an artificial effect that results from depriving the transmembrane domain and parts of the stem region, the site-directed mutagenesis approach described in 1.3.3. was repeated using full length enzyme. N-terminally Flag-tagged *N*-glycosylation variants of full-length zST8SiaII were transiently expressed in CHO-2A10 cells. These cells show no surface expression of polySia due to a defect in their intrinsic polysialyltransferase (Eckhardt *et al.*, 1995). After 48 h, cells were fixed with paraformaldehyde and stained with polySia specific monoclonal antibody 735. Full-length zST8SiaII variants, lacking the third *N*-glycosylation site (?3), exhibited a dramatically reduced polySia surface staining compared to wild-type. Cells with weak polySia staining were only sporadically found for those variants and only seen when the exposure time was increased up to threefold (fig. 9 *A*). For all other variants no significant alterations were detectable (fig. 9 *A*). Comparable transfection efficiency and expression of all zST8SiaII variants was confirmed by additional immunofluorescence experiments using an antibody directed against the N-terminal Flag-tag (fig. 9 *B*). In summary this cellular assay proves the fundamental influence of *N*-glycosylation site N95 (#3) on zST8SiaII activity in the full-length enzyme and verifies the results obtained using the truncated enzyme *in vitro*.
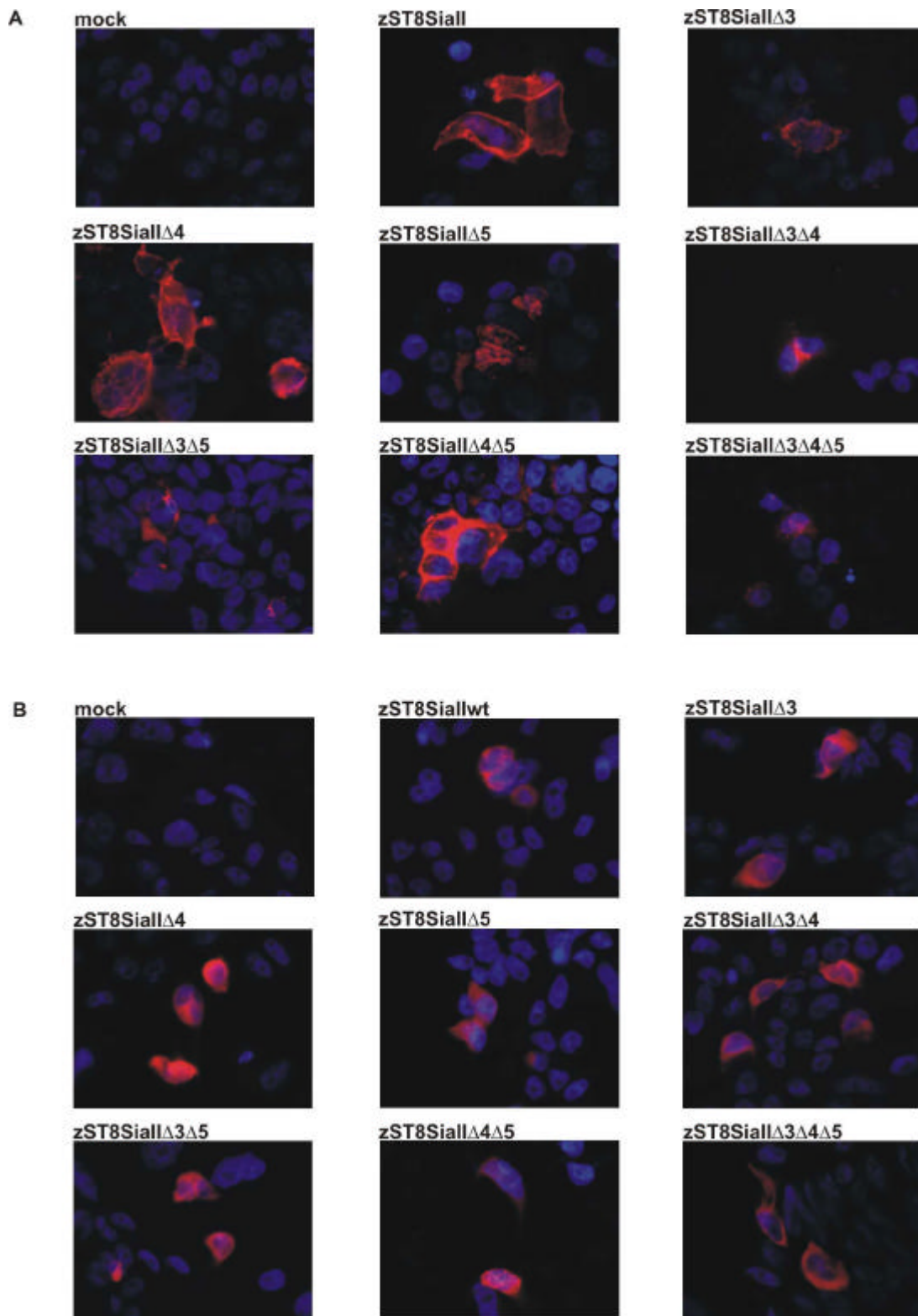
Figure 9: Polysialylation activity of *N*-glycosylation variants of full-length zebrafish ST8SiaII. N-terminally Flag-tagged wild-type and *N*-glycosylation variants of zST8SiaII were transiently expressed in polySia free CHO-2A10 cells. 48 h post transfection, cells were fixed with paraformaldehyde. *A*. PolySia surface staining using mAb 735 at 630-fold magnification. *B*. As expression control, cells were permeabilized and stained with an antibody directed against the N-terminal Flag-tag at 630-fold magnification.

1.3.5. Baculoviral expression of secreted zST8SiaII

Despite recent advances in the field of polysialyltransferases there is little known about the mechanism of polySia chain initiation, elongation and termination. To further investigate the catalytic mechanism, detailed biochemical studies using purified enzyme variants are indispensable. A complex expression system is required to obtain pure and active polySTs, due to the presence of essential disulfide bonds and *N*-glycosylation attachment sites. Although mammalian cell expression systems fulfill these requirements the yield of purified recombinant protein remains very low in comparison to the costs. To increase yields, a baculoviral based insect cell expression system (Invitrogen) was established and test-expressions of truncated and minimally glycosylated zST8SiaII variants were performed. To facilitate detection and purification an N-terminal Histidine tag was added to all constructs and secretion to the culture medium was enforced by addition of the honey bee melittin secretion sequence. Supernatants of infected *Sf*9 cells were collected at different time points post infection and analyzed by SDS-PAGE - directly or after trichloric acetic acid precipitation - followed by western blot analysis using an anti-penta-His antibody. The resulting time response data of secreted zST8SiaII variants are shown in figure 10. zST8SiaII?N26, truncated only by the transmembrane domain, is secreted in high yield compared to zST8SiaII?N86, lacking also parts of the stem region. The minimally glycosylated construct zST8SiaII?N86Δ4Δ5 that maintains only *N*-glycosylation site N95 was expressed and secreted in barely detectable amounts.
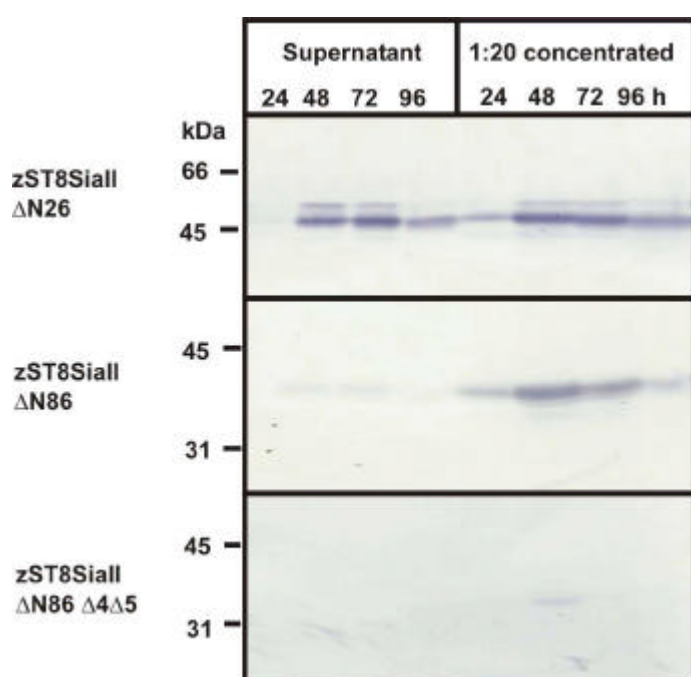
Figure 10: Baculoviral expression of secreted zST8SiaII variants in *Sf*9 cells. Time response of baculoviral expression in *Sf*9 cells analyzing three N-terminally truncated forms of zST8SiaII (ΔN26, ΔN86, ΔN86Δ4Δ5) at which the last-mentioned variant additionally lacks *N*-glycosylation sites 4 und 5. After 24, 48, 72 and 96 h cell culture supernatants of infected *Sf*9-cells were analyzed by 10 % SDS-PAGE - directly (supernatant) and after trichloric acetic acid precipitation (1:20 concentrated)- followed by western blot analysis using an anti-penta-His antibody.

Taken together the baculoviral expression study revealed that zST8SiaII can be produced in *Sf*9 insect cells in good quantities. However, parts of the stem region as well as the presence of *N*-glycosylation sites seem to have a major effect on protein yields.

1.3.6. Purification of Histidine-tagged zST8SiaII from insect cells

N-terminally His-tagged zST8SiaII?N26 and zST8SiaII?N86 constructs were expressed in *Sf*9 cells (fig. 11 *A*). 72 h post baculoviral infection, cell culture supernatants were concentrated to 80 ml and loaded on Ni^{2+}-NTA-beads. zST8SiaII was subsequently eluted with 100 mM imidazole and the quaternary structure was determined using size-exclusion chromatography. Samples of all purification steps were analyzed by 10 % SDS-PAGE followed by silver staining and western blot analysis (fig. 11 *B*). Both enzyme variants could be significantly enriched by affinity chromatography with only one contaminant left as visualized by silver staining (Ni^{2+}-NTA purified). Analysis of both enzymes after size-exclusion chromatography revealed that zST8SiaII?N86 could be purified to homogeneity by this additional purification step, whereas the main part of zST8SiaII?N26 decomposed into several degradation products. Those additional bands occurring in the silver staining of zST8SiaII?N26 are not detectable in the western blot and are therefore most likely N-terminal degradation products.
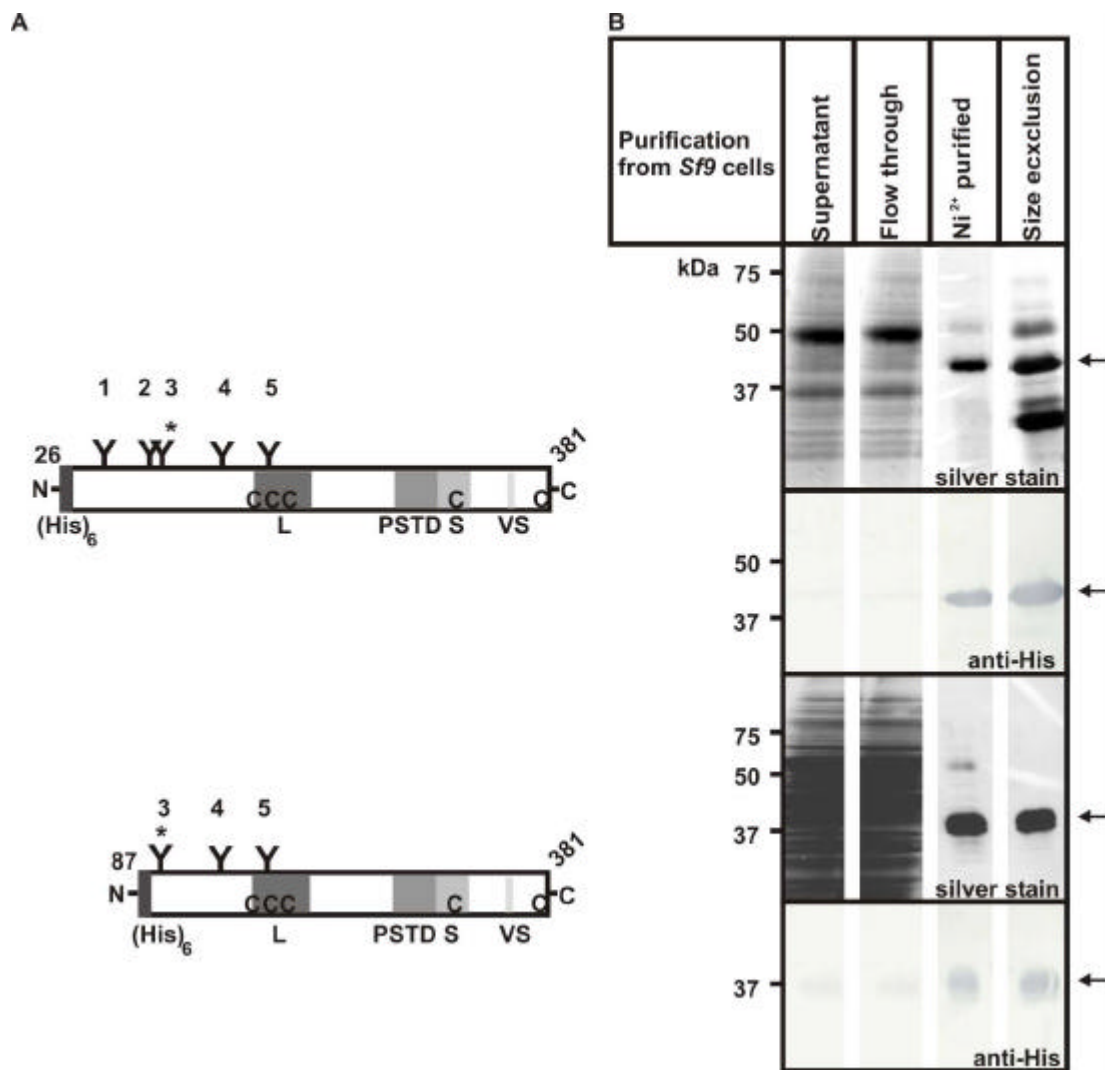
Figure 11: Purification of zST8SiaII?N26 and zST8SiaII?N86 from *Sf*9 cells. *A.* Schematic representation of the secreted N-terminally His-tagged zST8SiaII constructs, which were purified from insect cell culture supernatants. *B.* N-terminally His-tagged zST8SiaII variants were baculoviral expressed in *Sf*9 cells. 72 h post infection, secreted proteins were harvested by concentrating cell culture supernatant and incubated over night with Ni^{2+}-NTA-beads. Protein was eluted stepwise with imidazole and peak fractions were analyzed by 10 % SDS-PAGE followed by silver staining and western blot analysis using anti-penta-His antibody.

Further analyses were carried out with the stable zST8SiaII?N86 enzyme variant. A final yield of up to 2 mg/L pure enzyme was obtained using the purification procedure described above.

1.3.7. *Sf*9-cell expressed zST8SiaII?N86 is a monomeric protein displaying enzymatic activity

To analyze the oligomerization state of zST8SiaII?N86 an analytical size-exclusion chromatography of Ni^{2+}-NTA purified enzyme was performed using a Superdex 200 column that was calibrated with standard proteins. The elution profile is shown in figure 12 *A*. A single peak was obtained for zST8SiaII?N86 at a retention volume of 15.3 ml, which corresponds to a molecular mass of 37 kDa and is in perfect agreement with the calculated molecular mass of a monomer. All peak fractions were subsequently analyzed by SDS-PAGE followed by silver staining (upper panel) and western blot analysis using an anti-penta-His antibody (lower panel) to prove the presence of zST8SiaIIΔN86 (fig. 12 *B*). Enzymatic activity of the pooled peak fractions were investigated in a radioactive incorporation assay in solution. Therefore zST8SiaII?N86 was incubated with 0.25 mM CMP-[^{14}C]Neu5Ac in the presence of 1 µg NCAM, followed by SDS-PAGE and autoradiography (fig. 12 *C*).
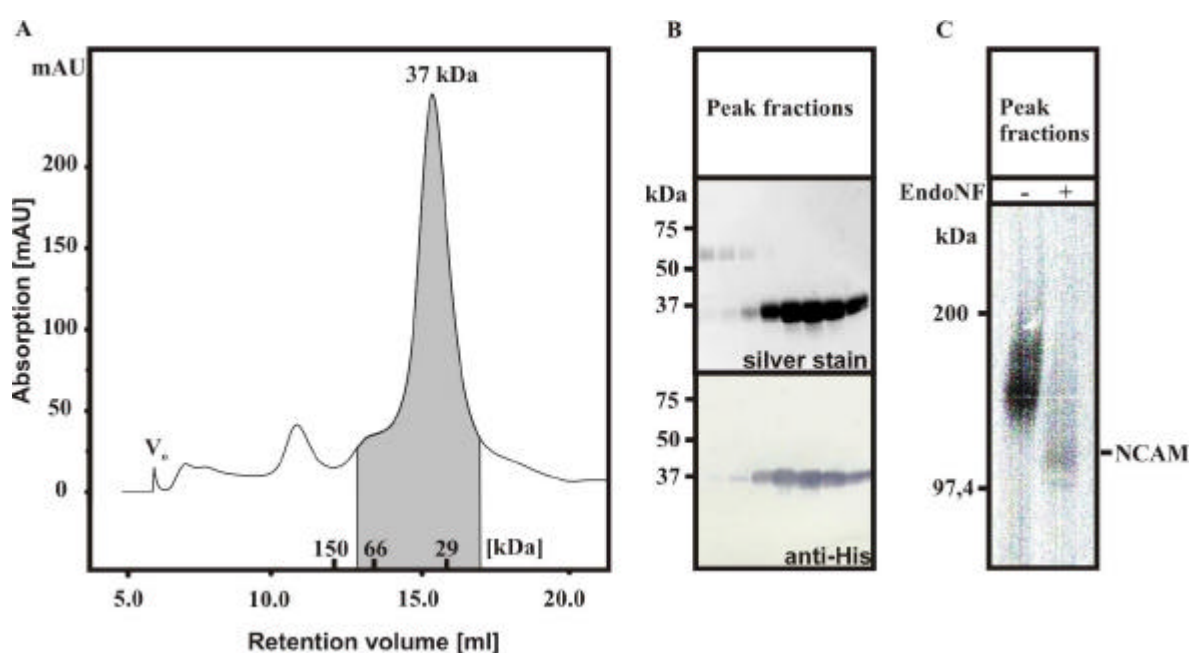
Figure 12: Size-exclusion chromatography of Histidine–tagged zST8SiaII?N86. The quaternary structure of Ni^{2+}-NTA purified zST8SiaII?N86 was determined by size-exclusion chromatography using a Superdex 200 column. *A*. Elution profile of zST8SiaII?N86. Void volume (V_0) and retention volumes of standard proteins are indicated. Peak fractions are shaded in grey. *B*. Peak fractions were analyzed by 10 % SDS-PAGE followed by silver staining (upper panel) or western blotting using an anti-penta-His antibody (lower panel). *C*. Enzymatic activity of pooled peak fractions was analyzed in a radioactive incorporation assay using 0.2 µg zST8SiaII?N86 in reaction buffer (10 mM sodium cacodylate buffer pH 6.7; 10 mM MnCl₂) containing 0.25 mM CMP-[^{14}C]-Neu5Ac, and 1 µg NCAM in a total volume of 20 µl. After 3 h incubation at 26°C samples were separated on 8 % SDS-PAGE before (-) and after (+) EndoneuraminidaseF (EndoNF) treatment and visualized by autoradiography.

Taken together, baculoviral expression of His-tagged zST8SiaIIΔN86 in insect cells and subsequent affinity purification followed by size-exclusion chromatography, revealed an efficient possibility to obtain stable, pure, active and apparently monodisperse enzyme in high yields. This enabled us for the first time to start protein demanding biophysical studies on a eukaryotic polysialyltransferase.

1.3.8. Adaptation of assay condition for NMR-spectroscopy studies

To gain first insight into the reaction mechanism of eukaryotic polySTs, the purified zST8SiaIIΔN86 described above was investigated by NMR spectroscopy. Binding properties of zST8SiaII?N86 towards different substrates were analyzed using Saturation-Transfer-Difference-(STD)-NMR spectroscopy. In addition the minimal acceptor length for zST8SiaII?N86 activity was determined by ^{1}H-NMR spectroscopy. Initially, the commonly used buffer system had to be adjusted to the requirements of NMR-spectroscopy to receive high resolution spectra. The Mn^{2+} cation, usually present in polyST activity assays had to be exchanged and a deuterated buffer system was needed. Therefore, polysialylation activity of zST8SiaIIΔN86 was tested under various conditions in an ELISA based assay system. To substitute Mn^{2+}, the influence of other divalent cations such as Mg^{2+} and Ca^{2+} was assayed. Furthermore, we analyzed whether the MES-buffer is exchangeable by the more convenient Tris-buffered system. The activity assays revealed that Mg^{2+} is most suitable to replace manganese cations as zST8SiaII?N86 maintained high levels of residual activity (fig. 13 *A*). Though using a Tris-buffered system affected enzyme activity, still sufficient residual activity was maintained. The Mg^{2+}/Tris-system was further improved by optimizing Mg^{2+} concentrations (fig. 13 *B*). The best assay condition suitable for NMR-spectroscopy was found to be 1 mM Mg^{2+} in 10 mM Tris-buffer pH 6.8. In the following, all NMR-spectroscopic analyses of zST8SiaII?N86 were carried out under these optimized conditions.
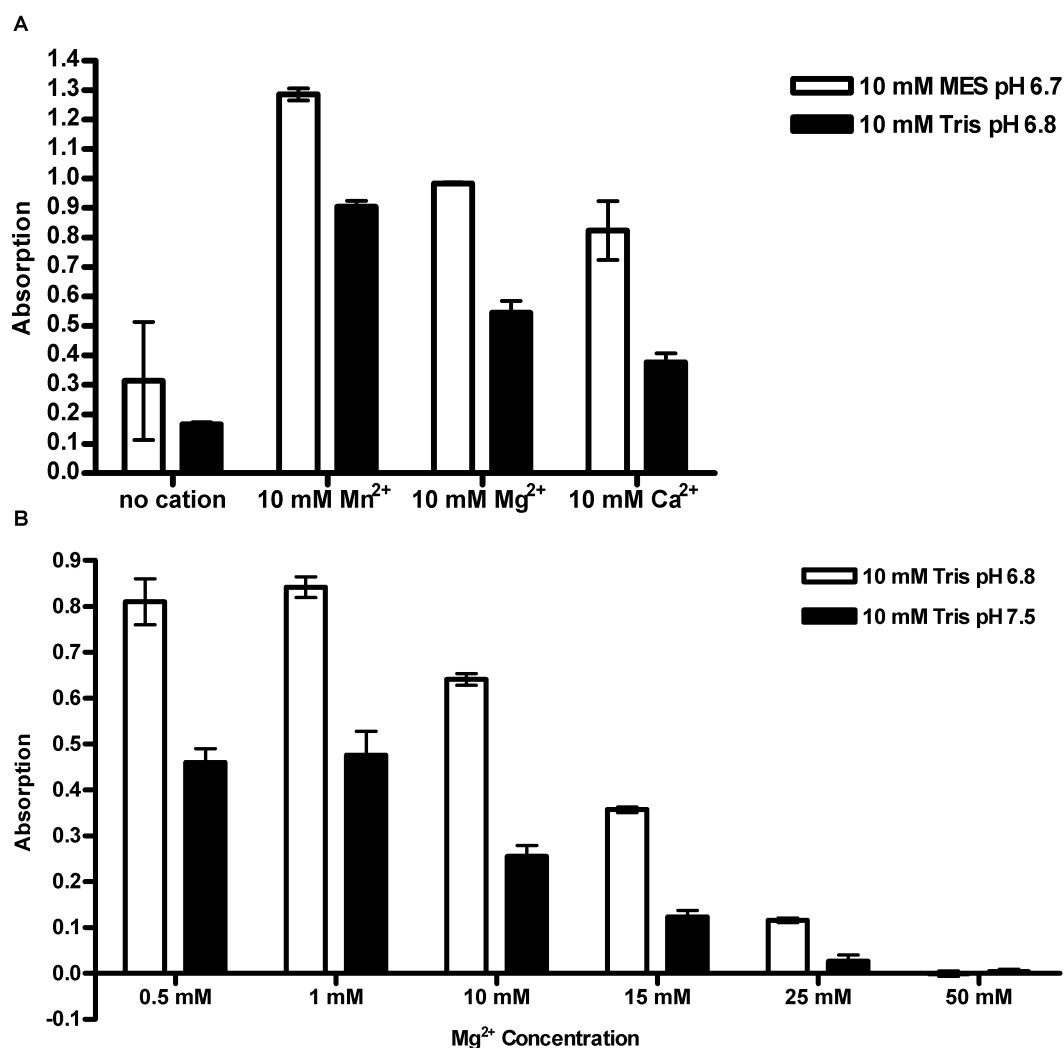
Figure 13: Adaption of assay conditions for NMR spectroscopy studies. For high resolution NMR-spectra, the standard assay conditions (2-(N-Morpholino) ethanesulphonic acid (MES)-buffer and Mn^{2+}) were adjusted. 30 pg/well of ProtA-NCAM were adsorbed to a 96 well microtiter plate and incubated with 0.2 µg of zST8SiaII?N86 in reaction buffer containing 1 mM CMP-Neu5Ac for 4 h at 27°C. *A.* Influence of buffer and divalent cation on zST8SiaII?N86 activity. *B.* Optimization of Mg^{2+} concentration at two different pH values.

1.3.9. Ligand binding analyses of zST8SiaII by STD-NMR spectroscopy

This method is based on saturation transfer from the target protein to ligands mediated by spin-diffusion and allows the determination of the binding epitope of the ligand. Ligand protons, which are close to the protein surface, exhibit high STD-NMR signal intensities and are more likely to be involved in substrate binding (Mayer and Meyer, 2000).

Binding properties of the substrate CMP-Neu5Ac towards zST8SiaIIΔN86 were analyzed by STD-NMR spectroscopy using 100 μg purified enzyme in the presence of a 100fold molar excess of the activated sugar (fig. 14 a/b). Likewise, isolated nucleotide moiety CMP (c/d) and the sugar moiety Neu5Ac (e/f) were tested. In parallel, ^{1}H-NMR-spectra were acquired for each ligand to allow assignment of all ligand specific peaks in the respective STD-NMR spectra. Comparison of the STD-NMR (upper panel) with the corresponding ^{1}H-NMR spectrum (lower panel) revealed that all protons of CMP-Neu5Ac were detectable in both experiments (fig. 14 a/b). Therefore, all protons of CMP-Neu5Ac are assumed to be in close contact to zST8SiaII?N86. The same observation was made for the nucleotide moiety CMP (fig. 14 c/d). Interestingly, no saturation transfer from zST8SiaII?N86 to protons of the sugar moiety Neu5Ac was detectable. Peaks that are visible in the STD-NMR spectrum of zST8SiaII?N86 in the presence of Neu5Ac are not in phase (fig. 14 e/f).
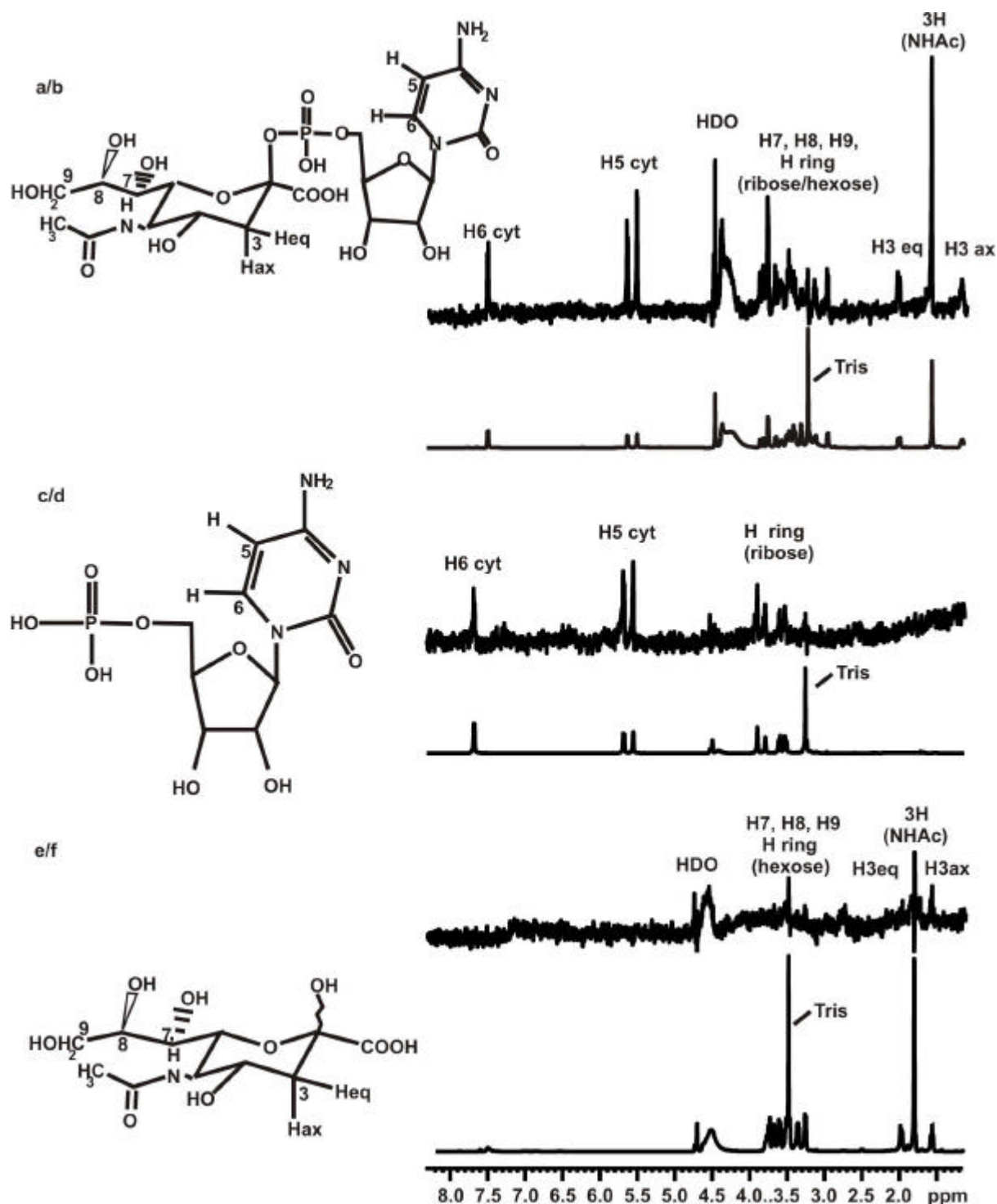
Figure 14: Binding properties of the activated sugar CMP-Neu5Ac. Spectra are shown for Neu5Ac (a/b), CMP (c/d) and CMP-Neu5Ac (e/f). 100 µg of purified zST8SiaII?N86 were incubated in deuterated reaction buffer (10 mM Tris$_{d5}$/DCl, 1 mM MgCl$_2$, pH 6.8) containing a 100fold molar excess of the substrate at 10°C. To assign STD signals, corresponding ^{1}H-NMR spectra are depicted below the respective STD spectra.

Taken together, STD-NMR experiments of zST8SiaII?N86 suggest that the complete CMP-Neu5Ac molecule is bound to the enzyme, whereby the nucleotide moiety appears to be crucially involved in substrate binding.

Next, we were interested to study the binding properties of the acceptor substrates. Therefore, 100 µg ST8SiaII?N86 were incubated with a 100fold molar excess of a2,3-sialyllactose which mimics the natural Neu5Aca2$\rightarrow$3Galß1$\rightarrow$R acceptor site used by ST8SiaII *in vivo* and sialic acid oligomers (degree of polymerization (Dp) Dp2-Dp6).

In this STD-NMR-study saturation transfer was observed for a2,3-sialyllactose predominantly found for H 3eq (2,3 ppm) and NHAc (1,75 ppm) of the Neu5Ac moiety, indicating that the recognition site of this acceptor seems to be the Neu5Ac moiety (fig. 15 a/b).

Saturation transfer was found for all sugar moieties of the artificial acceptors Dp2 (fig. 15 c/d), Dp3 (e/f) and Dp6 (g/h). This is demonstrated by the respective signals obtained for the H3eq proton of Neu5Ac, which allows to discriminate external sugar moieties in α-configuration (a_{ex}), from internal residues in α-configuration (a_{in}) and external residues in β-configuration (ß_{ex}). The ratio of these peak areas demonstrates that zST8SiaIIΔN86 binds oligosialic acids from dimer to hexamer. This suggests that parts of the growing polySia chain stay in close contact to the enzyme.
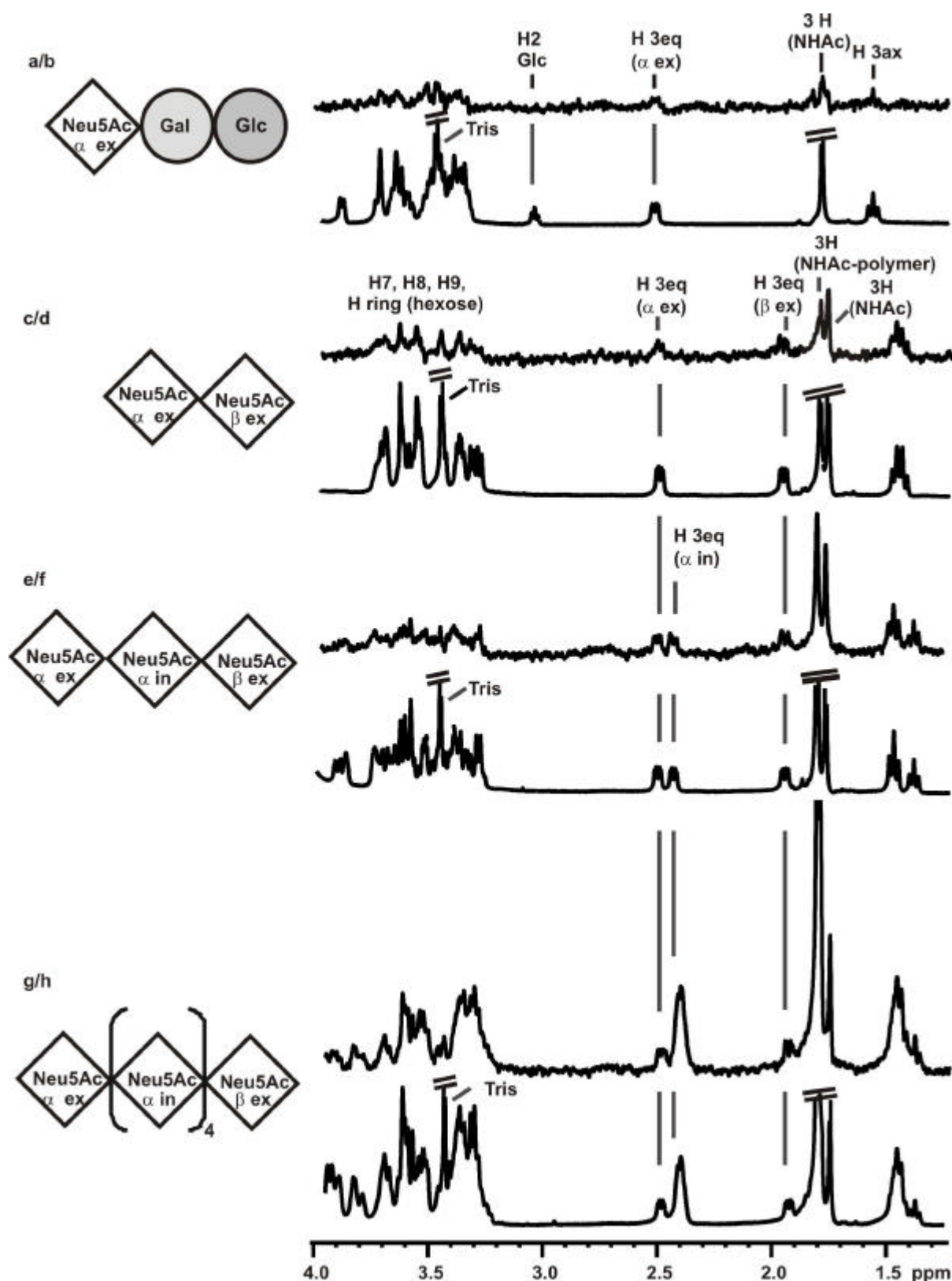
Figure 15: Binding properties of artificial acceptors analyzed by STD-NMR. Spectra are shown for a2,3-sialyllactose (a/b), Dp2 (c/d), Dp3 (e/f), and Dp6 (g/h). 100 µg of purified zST8SiaII?N86 were incubated in deuterated reaction buffer (10 mM Tris$_{d5}$/DCl, 1 mM MgCl$_2$, pH 6.8) containing a 100fold molar excess of the substrate at 10°C. To assign STD signals, the corresponding ^{1}H-NMR spectrum of the respective ligand is depicted below each STD-NMR spectrum.

Binding properties of the artificial acceptors (2,3-sialyllactose, Dp2, Dp3, Dp6) towards zST8SiaII?N86 did not alter in the presence of CMP-Neu5Ac (data not shown). Consequently, we assume that artificial acceptors and the donor substrate CMP-Neu5Ac bind independently to zST8SiaII?N86.

1.3.10. Activity studies for zST8SiaII?N86 by ^{1}H-NMR spectroscopy

Until now, only little is known about the minimal sugar-acceptor structure for polySTs. Accordingly, low levels of enzymatic activity were observed for oligosaccharides alone (Angata *et al.*, 2000; Angata, Suzuki, and Fukuda, 2002). Using STD-NMR spectroscopy, we could already demonstrate ligand binding of short oligosaccharides to zST8SiaII?N86 (1.3.9). Next, we established an NMR-based assay to determine the minimal acceptor structure for polyST activity. Therefore, 100 µg ST8SiaII?N86 were incubated with a 100fold molar excess of CMP-Neu5Ac and sialic acid oligomers. For this approach we used ^{1}H-NMR spectroscopy to monitor zST8SiaII?N86 activity towards different mono- and oligosaccharide acceptors continuously. The relative integrals for the enzymatic reaction of zST8SiaII?N86 with CMP-Neu5Ac and the artificial acceptor Dp6 are depicted in figure 16 *A*. The reduction of the H 3eq CMP-Neu5Ac signal (0.426) corresponds directly with an increase of the a_{in} H 3eq oligoSia signal (0.520), whereas the a_{ex} and $ß_{ex}$ H 3eq signals of oligoSia remain constant. The broadening of a_{in} H 3eq signals at 2.45 ppm strongly suggested the synthesis of a sialic acid polymer (>Dp6). The same results were obtained with the acceptor Dp3. The reduction of the H 3eq CMP-Neu5Ac signal (0.499) corresponds directly with an increase of the a_{in} H 3eq of polySia signal (0.312), whereas the a_{ex} and $ß_{ex}$ H 3eq signals of polySia remained constant (fig. 16 *B*). In the case of the acceptor α2,3-sialyllactose, product formation of Neu5Aca(2,8)-Neu5Aca(2,3)-Galactoseß(1,4)-Glucose, was monitored by the developing H3eq signal of the internal aNeu5Ac (Neu5Ac a in) at 2.45 ppm (fig. 16 *C*).
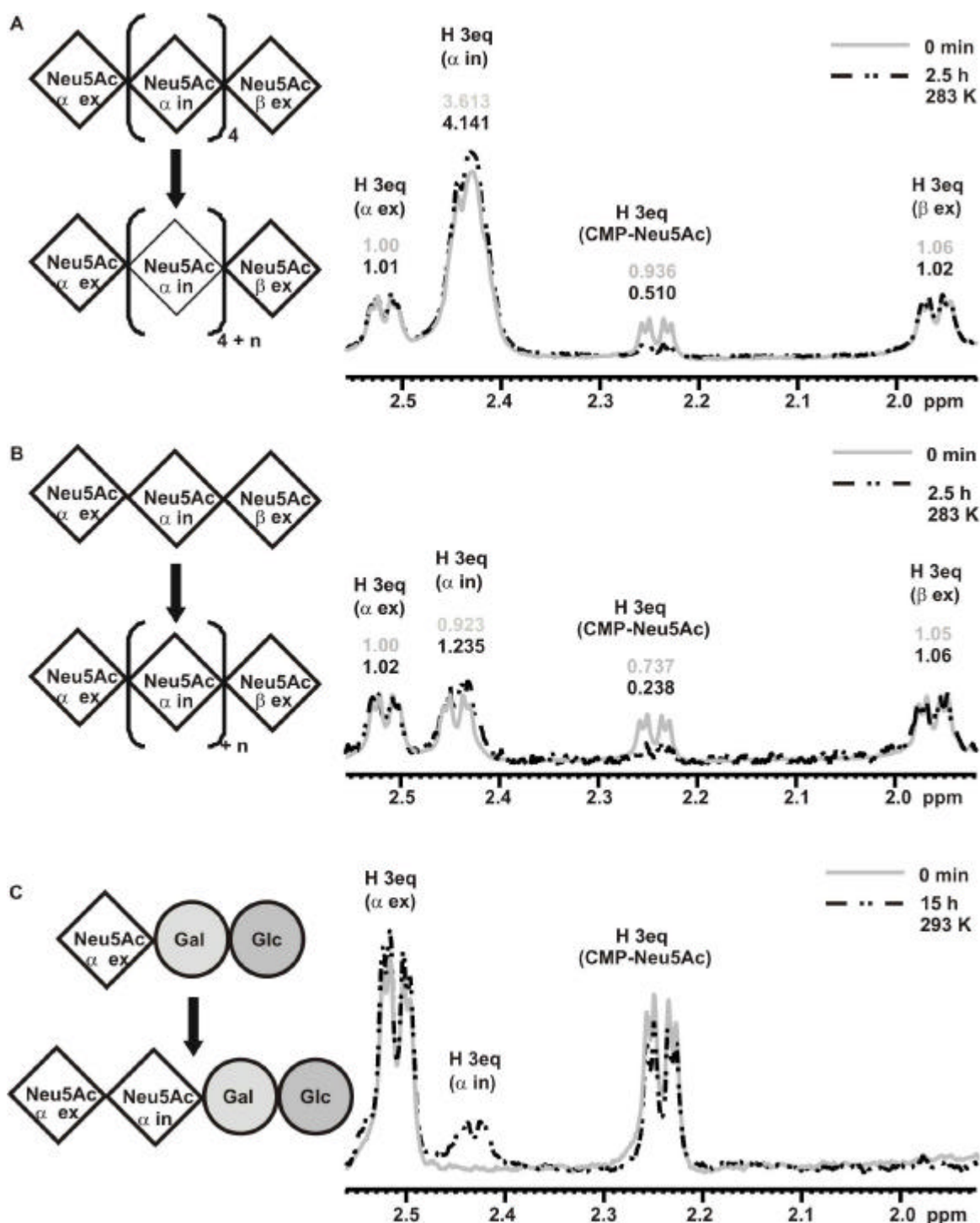
Figure 16: Acceptor studies for zST8SiaII?N86 by ^1H-NMR spectroscopy. ^1H-NMR-spectra are shown for zST8SiaII?N86 activity with oligoSia hexamer (*A*), trimer (*B*) and a2,3-sialyllactose (C). 100 µg of purified zST8SiaII?N86 were incubated in deuterated reaction buffer (10 mM $Tris_{d5}$/DCl, 1 mM $MgCl_2$, pH 6.8) containing a 100fold molar excess of CMP-Neu5Ac and acceptor.

In *A*. the relative integrals for CMP-Neu5Ac and DP6 before (grey) and after (black) incubation with zST8SiaII?N86 are depicted. The reduction of the H3eq CMP-Neu5Ac signal (0.426) corresponds directly with an increase of the a_{in} H 3eq of polySia signals (0.520). Broadening of a_{in} H 3eq signals at 2.45 ppm strongly suggests the synthesis of a sialic acid polymer. In *B*. the reduction of the H 3eq CMP-Neu5Ac signal (0.499) corresponds directly with an increase of the a_{in} H 3eq of polySia signal (0.312), whereas the a_{ex} and $ß_{ex}$ H 3eq signals of polySia remained constant. In *C*. the spectra reveal the formation of Neu5Aca(2,8)-Neu5Aca(2,3)-Galactoseß(1,4)-Glucose from a2,3-sialyllactose and CMP-Neu5Ac by zST8SiaII?N86. The H 3eq signal of the rising internal aNeu5Ac (Neu5Ac a in) is visible at 2.45 ppm. NMR integration error: ±10-15 %.

All artificial acceptors tested by STD-NMR and ^{1}H-NMR spectroscopy were found to bind to zST8SiaII?N86 and shown to serve as acceptor substrates for chain elongation. The only exception was monomeric Neu5Ac.

The Sia monomer is mainly present in β-configuration (95%), whereas the oligomeric acceptors are in a-configuration at the non-reducing end. To analyze if a-configuration is essential for recognition by the enzyme, we tested a monomer with a fixed a-configuration (Neu5Aca2Me) as a putative acceptor for zST8SiaII?N86.

Interestingly, zST8SiaII?N86 was indeed capable to transfer sialic acid from the activated sugar CMP-Neu5Ac to the a-anomer of Neu5Aca2Me (fig. 17 *A*). Under the applied conditions, no polymer but exclusively the Neu5Aca(2,8)-Neu5Aca2Me dimer was formed due to the high molar excess of the α-anomer. As expected, incubation of zST8SiaII?N86 with the corresponding ß-anomer Neu5Acß2Me or free Neu5Ac (a : ß; 5%:95%) did not result in the formation of detectable amounts of dimer (fig. 17 *B*). Due to hydrolysis of unstable CMP-Neu5Ac (2.3 ppm) the formation of an additional peak for free Neu5Ac (free NHAc (1.83 ppm)) occurs over time (fig. 17 *B*).

For the first time we succeeded in demonstrating that a-configuration at the non-reducing end of the acceptor substrate is crucial for polyST activity. In addition, these findings indicate that the minimal acceptor length required for zST8SiaII?N86 activity is a monomer.
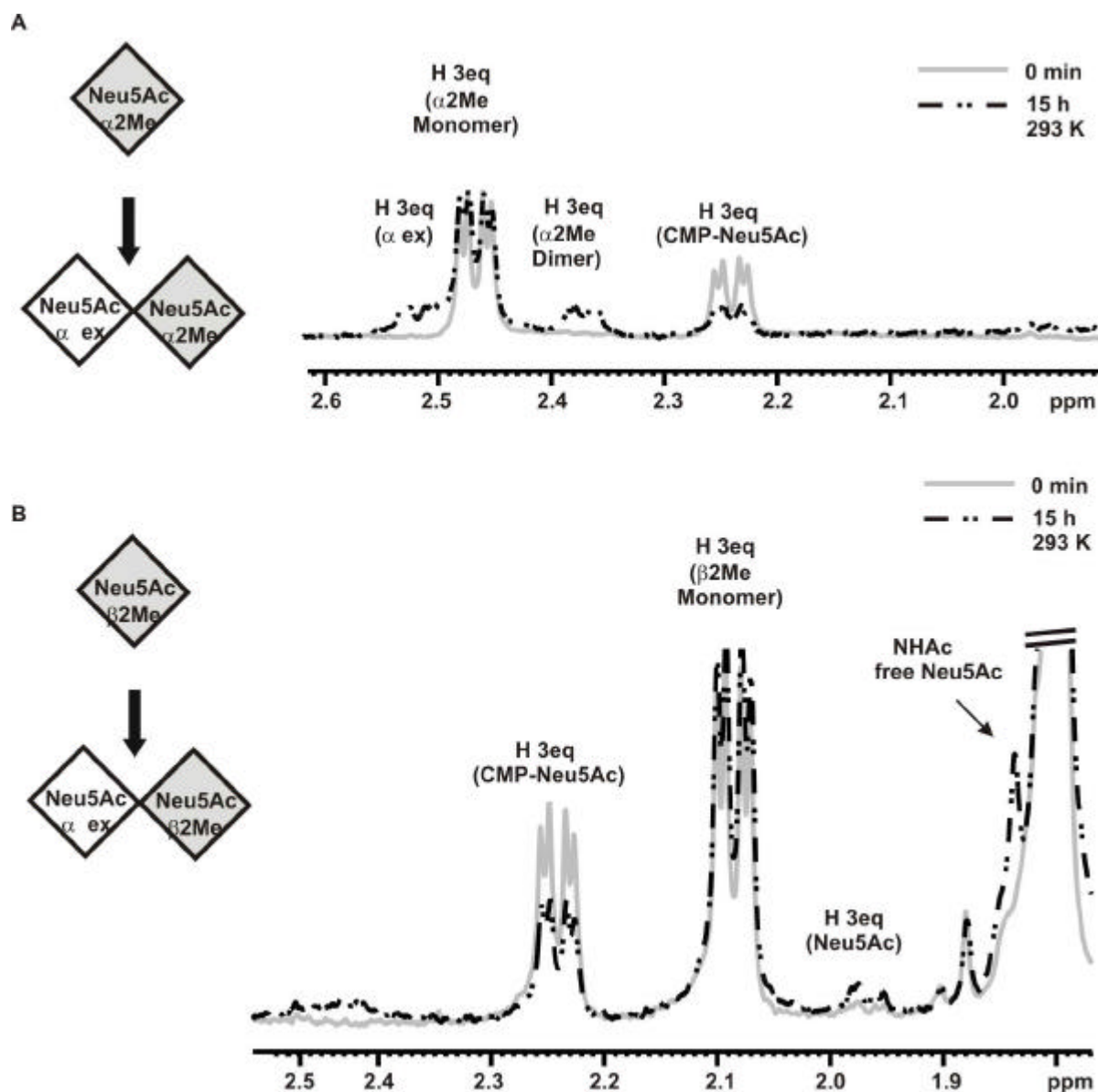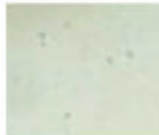
Figure 17: Minimal acceptor length required for zST8SiaII?N86 activity. ^{1}H-NMR-spectra of zST8SiaII reactions using an a- or ß- Sia anomer (Neu5Ac(a or ß)2Me) were acquired to define the minimal acceptor for zST8SiaII?N86 activity. 100 µg of purified zST8SiaII?N86 were incubated in deuterated reaction buffer (10 mM Tris$_{d5}$/DCl, 1mM MgCl$_2$, pH 6.8) containing a 100fold molar excess of CMP-Neu5Ac and a- or ß- Sia anomer for 15 h at 20°C.

In *A*. the zST8SiaII?N86 activity on Neu5Aca2Me is depicted. The signals at 2.38 ppm and 2.55 ppm suggest the synthesis of a Neu5Aca(2,8)-Neu5Aca2Me dimer. For the corresponding Neu5Acß2Me no product peak was observed. Non-enzymatic hydrolyses of unstable CMP-Neu5Ac is indicated by the appearance of a peak at 1.83 ppm for the NHAc of free Neu5Ac.

1.3.11. Crystallization attempts of zST8SiaII?N86

Currently, no information is available on the 3D-structure of polysialyltransferases. None of the prokaryotic or eukaryotic polySTs have been crystallized so far. Also, structure prediction software did not allow similarity building of any 3D-model for members of the α2,8-sialyltransferase family. For the first time we succeeded in purifying a eukaryotic polyST to homogeneity in high yields, enabling us to start a comprehensive crystallization approach. Therefore the pure His-tagged zST8SiaII?N86 variant was used for crystal screening in the presence or absence of the donor analogue CMP-Neu5Ac3F (Mueller-Dieckmann, 2006). As a first result, we obtained two initial conditions containing precrystals as depicted in figure 18. An extensive approach is required to optimize crystallization conditions and to solve the 3D-structure, which is far beyond the scope of the present study.

Crystallization experiments	5.7 mg/ml zST8SiaIIΔN86 10 mM Tris/HCl pH 7.5 10 mM MnCl$_2$
day 19 day 25	2 mM CMP-Neu5Ac-3F 2 M (NH$_4$)$_2$ SO$_4$ 0.1 M Phosphate-citrate-buffer pH 4.2 EMBL-Hamburg

day 53
 	
day 137
	1.26 M Sodium phosphate
	     monobasic monohydrate
	0.14 M Potassium phosphate
	     dibasic
	pH 5.6

Figure 18: Crystallization experiments for zST8SiaII?N86. Pictures of precrystals at different timepoints (left panel) and the corresponding crystallization conditions (right panel) are depicted.

1.4. Discussion

Poly-a2,8-sialic acid (polySia) is a posttranslational modification of the neural cell adhesion molecule (NCAM) and an important regulator of NCAM-mediated cellular plasticity. The two enzymes involved in polySia biosynthesis in vertebrates are the polysialyltransferases (polyST), ST8SiaII and ST8SiaIV (Eckhardt *et al.*, 1995; Nakayama *et al.*, 1995; Scheidegger *et al.*, 1995; Kojima *et al.*, 1995). During development, polySia biosynthesis is mainly mediated by ST8SiaII whereas ST8SiaIV is the predominant enzyme in adults (Oltmann-Norden *et al.*, 2008). In addition to its essential role in neural development, polySia represents an oncodevelopmental antigen that is re-expressed on several malignant tumors. Expression of polySia in the tumors facilitates detachment of cells from the primary tumor and thus promotes the first step in metastasis (Roth *et al.*, 1988; Fukuda, 1996; Zuber *et al.*, 2005; Scheidegger *et al.*, 1994; Tanaka *et al.*, 2001; Glüer *et al.*, 1998b; Glüer *et al.*, 1998a; Hildebrandt *et al.*, 1998; Seidenfaden *et al.*, 2003). Enzymes involved in polySia biosynthesis, therefore, represent attractive targets for anti-cancer therapy. Although the mammalian polySTs have been cloned back in 1995 (Eckhardt *et al.*, 1995; Nakayama *et al.*, 1995; Scheidegger *et al.*, 1995; Kojima *et al.*, 1995) there is still little known about the catalytic mechanism and structural features of these important enzymes.

Detailed analyses of structure-function relationships in polySTs are mainly hampered by the lack of expression systems capable to supply sufficient amounts of active enzymes. The tertiary organization of these type-II-transmembrane glycoproteins that involve two essential disulfide bonds and up to six partly polysialylated *N*-glycans impedes the development of straight forward approaches for the purification of polyST. The integrity of the *N*-glycan attachment sites N89 (3) and N219 (5) of the mammalian enzymes is crucial for ST8SiaII activity (Mühlenhoff *et al.*, 2001; Close *et al.*, 2001). Interestingly, however, the homologous enzyme from the lower vertebrate zebrafish (zST8SiaII) lacks one out of these two crucial *N*-glycosylation sites whereupon a functional enzyme is maintained (Marx *et al.*, 2007). Therefore, we speculated that a single *N*-glycan in zST8SiaII might be sufficient to obtain a stable and active enzyme variant. Based on this assumption zST8SiaII was selected as a suitable candidate for an extensive protein engineering and purification approach.

To determine the minimal active enzyme variant of zST8SiaII we analyzed a set of N-terminally truncated variants with regard to activity and expression levels. As shown in figure 7, zST8SiaII could be truncated by up to 86 amino acids without significant loss of enzymatic activity. This experiment shows that the first two *N*-glycosylation attachment sites

(N51 and N86) are of minor importance as the truncated, but fully active enzyme, zST8SiaIIΔN86 lacks both sites.

To investigate the impact of the remaining three *N*-glycosylation sites of zST8SiaII, a comprehensive site-directed mutagenesis approach was performed based on the construct zST8SiaII?N86. Only *N*-glycosylation site N95 (#3) was found crucial for enzymatic activity (fig. 8) consistent with the data published for the corresponding *N*-glycan attachment site of the mouse homologue (Mühlenhoff *et al.*, 2001), emphasizing the importance of this highly conserved site in vertebrate ST8SiaIIs. In addition, *N*-glycosylation site N140 (#4) is highly conserved in vertebrates although no significant effect on polyST activity is known so far (Mühlenhoff *et al.*, 2001; Close *et al.*, 2001).

A unique feature of zST8SiaII among the eukaryotic polySTs is the positioning of *N*-glycosylation attachment site N174 (#5) which is surprisingly located in the conserved L-motif. Single amino acid substitution zST8SiaIIΔN86-N174Q lacking this *N*-glycosylation site, revealed a shift in molecular mass compared to the corresponding enzyme variant harboring the site, when analyzed by SDS-PAGE (fig. 8). This finding highlights the accessibility of *N*-glycosylation site N174 located within the L-motif, supporting the assumption that the L-motif is part of the outer surface as described previously (Angata *et al.*, 2001). Interestingly, no effect on neither enzymatic activity nor expression efficiency was detectable in the zST8SiaII variant lacking *N*-glycosylation site N174 (#5) (fig. 8).

The relevance of *N*-glycosylation sites #3, #4 and #5 of zST8SiaII was investigated based on the truncated enzyme variant that lacks the first 86 amino acids. To exclude artificial effects resulting from the loss of the transmembrane domain and parts of the stem region, the study was repeated by expressing full-length enzymes in polySia-free CHO cells. Using this additional assay system we could unequivocally confirm that zST8SiaII activity crucially depends on the presence of *N*-glycan N95 (#3), whereas the mammalian homologues require at least a second *N*-glycan (Mühlenhoff *et al.*, 2001). Consequently we assumed zST8SiaII to be a suitable candidate for successful high yield purification.

Subsequently, we were interested to determine the system suitable for high-level expression of active zST8SiaII. Because folding of polyST depends on two disulfide bonds and the presence of an *N*-glycan, the bacterial expression systems were mostly inapplicable. Hitherto, mammalian expression systems allowed only low-level expression of functional polySTs that are not sufficient for a detailed biochemical characterization.

We chose insect cell expression, which is well established for high yield expression of recombinant proteins and that guarantees basic glycosylation structures and correct formation

of disulfide bonds. As shown in figure 10 the baculovirus system generated high amounts of recombinant N-terminally truncated zST8SiaII variants. Best expression efficiency was observed for N-terminally truncated zST8SiaII variants lacking 26 and 86 amino acids, respectively. Unfortunately, drastically reduced expression was detected with the enzyme variant harboring only one *N*-glycosylation site (fig. 10). This effect is consistent with our observations in the mammalian system. Using an ELISA to estimated protein concentration of *N*-glycosylation depletion variants of ProtA-ST8SiaII?86 we could demonstrate an up to fourfold decrease in expression levels for the ProtA-ST8SiaII?86?3?4?5 variant (data not shown). Based on these results the variants zST8SiaIIΔN26 and zST8SiaIIΔN86 were chosen for purification of the secreted His-tagged enzymes from *Sf*9 cells (fig. 11). To our surprise we found that zST8SiaII?N26 was N-terminally degraded while zST8SiaII?N86 remained stable after purification. Therefore, we used zST8SiaII?N86 for large-scale production of recombinant enzyme from insect cell supernatants, resulting in a final yield of up to 2 mg/L.

The quaternary state of zST8SiaII?N86 was determined by size-exclusion chromatography, indicating the monomer as the functional active unit (fig. 12). This result is consistent with the data published on human ST8SiaIV. In the presence or absence of reducing agents, this polyST was found as a monomer when analyzed by SDS-PAGE (Angata *et al.*, 2001).

Purification of functional zST8SiaII?N86 in high yield enabled us to start new approaches to analyze the biochemical properties of polySTs. Binding properties of substrates towards zST8SiaIIΔN86 were investigated by Saturation-Transfer-Difference (STD)-NMR spectroscopy. Interaction of the donor substrate CMP-Neu5Ac with zST8SiaII?N86 is predominantly mediated by the nucleotide moiety, as highest saturation transfer was observed for this part of the molecule. Similar observations were recently described for ß-galactoside a2,6-sialyltransferase (ST6GalI), another member of the α2,8-sialyltransferase family (Liu, and Prestegard, 2007). In addition no binding of Neu5Ac alone was detectable (fig. 14), arguing for that the nucleotide moiety of CMP-Neu5Ac has a major impact on first binding contacts and guidance of the substrate to the active site. Binding studies of the acceptor substrate polySia towards zST8SiaII?N86 were carried out using defined sialic acid oligomers such as dimers, trimers and hexamers. Interestingly, the dimer received decreased amounts of saturation transfer compared to the longer chain oligomers, indicating that more than two Sia residues might be in close contact to the active site.

Furthermore, enzymes acting on polymeric substrates can possess additional (secondary) substrate binding sites that are not necessarily located in close proximity to the active site as

recently shown for the polySia degrading enzyme endoneuraminidase F (Stummeyer *et al.*, 2005). The highly conserved PSTD motif restricted to polysialyltransferases of the α2,8-sialyltransferase protein family, might constitute an additional polySia binding site. The PSTD is a structurally unique polybasic motif (pI~12) and was postulated previously to tether nascent polySia chains, facilitating the processive addition of new Neu5Ac residues to the non-reducing end of the growing chain (Nakata, Zhang, and Troy, 2006).

For a2,3-sialyllactose which mimics an acceptor site used by ST8SiaII *in vivo,* saturation transfer was predominantly found for the Neu5Ac moiety, suggesting that ST8SiaII interacts rather with sialic acid residues than with the entire *N*-glycan structure. Although it has to be taken into account that these results were obtained for artificial, protein-free acceptor substrates, using a soluble truncated polyST *in vitro*. Using STD-NMR spectroscopy, we succeeded for the first time in demonstrating interaction of zST8SiaII?N86 with defined short-chain oligoSia *in vitro*, although enzymatic activity of polyST towards a mixture of oligoSia and monosialyl-oligosaccharids was reported previously (Angata *et al.*, 2000). Using ^{1}H-NMR-spectroscopy to observe zST8SiaII?N86 reaction on sialic acid hexamers, trimers, and 2,3-monosialyl trisaccharids, we could confirm enzymatic activity for zST8SiaII?N86.

Moreover, STD-NMR studies revealed that a sialic acid dimer is bound to zST8SiaII?N86 whereas Neu5Ac alone showed no significant interaction. Comparison of these two molecules displays that nearly 95 % of Neu5Ac are present in the ß-configuration, whereas the non-reducing end of a dimer is fixed in a-configuration. As chain elongation of polySia mediated by polySTs takes place at the non-reducing end, the configuration of this sialic acid residue might be significant for binding and zST8SiaII?N86 activity. To verify the hypothesis that an a-configuration of Neu5Ac at the non-reducing end is required for chain initiation and elongation we analyzed sialic acid derivatives fixed in the α- or β-configuration (Neu5Aca2ME and Neu5Acβ2ME) as well as free Neu5Ac by ^{1}H-NMR spectroscopy. As expected, only Neu5Ac in α-configuration could initiate chain elongation demonstrating that an a-configuration at the non-reducing end is a prerequisite for zST8SiaII?N86 activity. These results indicate that even a monomer might be sufficient to prime polyST mediated chain elongation.

To gain further insight into the catalytic mechanism of polySTs with regard to chain initiation, elongation and termination, the accessibility to structural data would be a valuable source. But so far, no 3D structural data for polySTs are available and prediction software does not allow similarity building of 3D models for any of the members of the α2,8-

sialyltransferase family. For the first time we succeeded in purifying a eukaryotic polyST to homogeneity and generated high yields which enabled us to start crystallization trials. Initial promising precrystals (fig. 18) were obtained for zST8SiaII?N86 that have to be optimized in further studies.

In conclusion, we succeeded to purify zST8SiaIIΔN86 to homogeneity in high yield that enabled us to start a comprehensive biochemical characterization of the eukaryotic enzyme. STD-NMR spectroscopy studies of zST8SiaII?N86 allowed a first insight into substrate binding properties and provide a basis for further studies aiming at understanding the catalytic mechanism of eukaryotic polySTs.

Chapter 2:

Engineering of murine ST8SiaII to a non *N*-glycosylated polysialyltransferase

2.1. Introduction

Polysialic acid (polySia) is a linear homopolymer comprised of up to 90 N-acetylneuraminic acid residues in an a2,8-linkage (Brisson *et al.*, 1992; Galuska *et al.*, 2008). In vertebrates, polySia is predominantly found as posttranslational modification of the neural cell adhesion molecule (NCAM) (Rothbard *et al.*, 1982; Hildebrandt, Mühlenhoff, and Gerardy-Schahn, 2008), although three other polySia carriers have been identified, the a subunit of the voltage dependent sodium channel (Zuber *et al.*, 1992), the scavenger receptor CD36, identified as soluble protein in human breast milk (Yabe *et al.*, 2003) and, as shown in a most recent study, neuropilin-2 expressed on matured dendritic cells (Curreli *et al.*, 2007). PolySia can be added to *N*-glycans and *O*-glycans of the respective acceptor structures. Concerning NCAM, only *N*-glycans have been reported to be polysialylated *in vivo* whereas recent cell-culture experiments using the full-length enzyme as well as several domain deletion variants of NCAM pointed out that *O*-glycans can be used as alternative acceptor sites (Close *et al.*, 2003; Colley, 2008). For CD36 and neuropilin-2, polySia is reported on *O*-glycans, exclusively (Yabe *et al.*, 2003; Curreli *et al.*, 2007). PolySia transferred onto the synthesizing enzymes, the polySTs, by contrast, is *N*-glycosidically linked (Mühlenhoff *et al.*, 2001).

The biosynthesis of polySia in vertebrates is mediated by two polySTs, ST8SiaII and ST8SiaIV and both enzymes have been cloned and characterized from mammals (Eckhardt *et al.*, 1995; Nakayama *et al.*, 1995; Scheidegger *et al.*, 1995; Kojima *et al.*, 1995). Simultaneous depletion of these genes generated a polySia-negative phenotype and thus proved that no other polyST exists in the mammalian system (Weinhold *et al.*, 2005).

Eukaryotic polySTs share four highly conserved motifs and two disulfide bonds that are essential for enzymatic activity (Datta and Paulson, 1995; Datta, Sinha, and Paulson, 1998; Kitazume-Kawaguchi, Kabata, and Arita, 2001; Nakata, Zhang, and Troy, 2006; Angata *et al.*, 2001). Furthermore, six and five *N*-glycan attachment sites have been identified in mammalian ST8SiaII and ST8SiaIV, respectively. For the murine ST8SiaII (mST8SiaII) *N*-glycans in positions N89 and N219 are critical for enzymatic activity whereas mST8SiaIV crucially depends on the presence of *N*-glycosylation site N74 (Mühlenhoff *et al.*, 2001;

Close *et al.*, 2001). Interestingly, specific *N*-glycosylation sites in polySTs are polysialylated in a self-modification reaction called autopolysialylation (Mühlenhoff *et al.*, 2001).

To gain further insight into the catalytic mechanism of polyST mediated polySia assembly, detailed *in vitro* studies are necessary that require large quantities of recombinant polyST.

However, the production of functional recombinant enzymes requires *N*-glycosylation competent expression systems that also support the formation of disulfide bonds (Mühlenhoff *et al.*, 2001; Angata *et al.*, 2001). Therefore, bacterial expression systems that allow low-cost and time-saving large-scale production of recombinant enzymes have, with a single exception, so far failed to generate the functionally active enzymes. The exception is the monosialyltransferase ST3Gal-V, which has been obtained as functional recombinant enzyme after bacterial expression, even though the enzyme was previously demonstrated to depend on the presence of three *N*-glycans (Uemura *et al.*, 2006).

A surprising observation was that *N*-glycosylation sites even though defined as functionally important, are not necessarily conserved in homologous enzymes among species. A recent publication demonstrated that *N*-glycan functions can be replaced by a specific stretch of amino acids present at the equivalent position in homologous enzymes resulting in a non-glycosylated but functional interspecies variant (Uemura *et al.*, 2006). Uemura and coworkers who identified this phenomenon recently, made use of it to generate an *N*-glycan free form of the α2,3-sialyltransferase ST3Gal-V. In their study, the authors replaced the non-conserved *N*-glycan by the identified SUNGA (for <u>su</u>bstitution of <u>N</u>-glycan functions in glycosyltransferases by specific <u>a</u>mino acids) sequence and generated a non-glycosylated but functional enzyme that could be expressed in bacteria (Uemura *et al.*, 2006). Beside the applicability of cost-effective, large-scale production of recombinant enzymes in bacteria, engineered non-glycosylated enzyme variants would provide further advantages. For instance increased protein homogeneity should improve the suitability of the enzyme fraction for protein crystallization.

Therefore, the second goal of my PhD study was to generate a polyST variant with no- or a minimal number of *N*-glycans by use of the SUNGA technique. As shown in this part, I succeeded in generating *N*-glycan free mST8SiaII variants that maintained enzymatic activity and allowed soluble expression using a bacterial system.

2.2. Experimental Procedures

2.2.1. Materials

Endoneuraminidase NF (endoNF) was purified from *Escherichia coli K1* bacteriophage as described previously (Gerardy-Schahn *et al.*, 1995). Recombinant soluble proteinA NCAM was expressed in CHO 2A10 cells and purified as described in Mühlenhoff *et al.* (1996).

The plasmids pFlagST8SiaII, pFlagST8SiaII Q^3N^5, pFlagST8SiaII Q^3Q^5, pProtA-ST8SiaII, pProtA-ST8SiaII Q^3N^5, and pProtA-ST8SiaII Q^3Q^5 were kindly provided from Dr. Mühlenhoff from our laboratory (Mühlenhoff *et al.*, 2001). The plasmid pSecTagST8SiaII?N31 was kindly provided by Dr. Stummeyer from our laboratory.

2.2.2. Sequence analyses of polySTs

Multiple sequence alignment was generated with *MultAlin* (Corpet, 1988) using the following accession numbers:

mouse: NP_033207

chicken: NP_001001604 XP_413877

african clawed frog: AB007468.1

zebrafish: NP_705948

pufferfish: CAG29377

2.2.3. Site-directed mutagenesis of mST8SiaII

N-glycosylation site deficient mST8SiaII variants were generated by PCR using the QuikChange site-directed mutagenesis kit (Stratagene) following the manufactures guidelines. *N*-glycosylation sites were disrupted by substituting the asparagine (N) in the **N**-X-S/T motifs by serine (S) or methionine (M). For site directed mutagenesis the plasmids pFlagST8SiaII Q^3Q^5 or pFlagST8SiaII Q^3N^5 were used as template. The primer pairs used are listed below (point mutations are in bold):

N89Ss:CATCCAAATGGAGACAC**TCA**CAGA CGCTCTCTCTGAG

N89Sas:CTCAGAGAGAGCGTCTG**TGA**GTGTCTCCATTTGGATG

N219Ss:GAGGACCTTGTG**TCG**GCCACGTGGCGGG

N219Sas:CCCGCCACGTGGC**CGA**CACAAGGTCCTC

VNAT(218-221)ASEEs:GGCCTTTGAGGACCTT**GCGAGCGAGGAG**TGGCGGGAGAAGCTGCTG

VNAT(218-221)ASEEas:CAGCAGCTTCTCCCGCCACTC**CTCGCTCGC**AAGGTCCTC

AAAGGCC

VNAT(218-221)AMEEs:GGCCTTTGAGGACCTT**GCGATGGAGGAG**TGGCGGGAGA
AGCTGCTG

VNAT(218-221)AMEEas:CAGCAGCTTCTCCCGCCACTC**CTCTATCGC**AAGGTCCTC
AAAGGCC

PCR products were subcloned into *Eco*RI sites of pFlagST8SiaII Q^{3}Q^5 or pFlagST8SiaII Q^{3}N^5 and the identity of all constructs was confirmed by sequencing. To obtain the corresponding ProtA-fusion proteins, the *Eco*RI digested PCR product was subcloned into *Eco*RI sites of pProtAST8SiaII Q^{3}Q^5 or pProtAST8SiaII Q^{3}N^5. For immunofluorescence staining soluble expressed ST8SiaII S^{3}AS^{5}EE variant was generated by subcloning of the *Eco*RI digested PCR product into *Eco*RI sites of pSecTag-ST8SiaII?N31. The vector pSecTag (Invitrogen) encodes the sequence of Ig?-chain leader and a C-terminal myc epitope followed by a hexa histidine tag (His). The plasmid pSecTag-ST8SiaII?N31 drives the expression of secreted C-terminal Myc-His-tagged ST8SiaII?N31.

2.2.4. Expression plasmids

To construct N-terminally truncated and tagged mST8SiaII Q^{3}AS^{5}EE variants for expression in bacteria, mST8SiaII Q^{3}AS^{5}EE was amplified from the plasmid pFlagST8SiaII Q^{3}AS^{5}EE using the following primer pair (restriction sites are in bold):

AG47s: GCG**AAGCTT**TGATCGGGAATTCTGGAGGC

AG48as: GC**CTCGAG**TTACGTAGCCCCATCACAC

PCR products were digested with *Hind*III and *Xho*I, gel purified (Qiagen) and ligated into the corresponding restriction sites of pET43-Strep, a modified pET43 vector (Novagen) containing the sequence encoding an N-terminal NusA fusion protein and Strep-tag II followed by a thrombin cleavage site. The resulting plasmid pET43-Strep-ST8SiaII Q^{3}AS^{5}EE drives the expression of N-terminally NusA-StrepII-fusion proteins. The insert was further subcloned into *Hind*III and *Xho*I sites of a modified pET43 expression vector containing the sequences encoding a N-terminal MBP fusion protein, FactorXa cleavage site, Strep-tagII and a thrombin cleavage site. The resulting plasmid pET43-MBP-ST8SiaII Q^{3}AS^{5}EE drives the expression of N-terminally MBP-StrepII-fusion protein. As described above the plasmid encoding N-terminal Strep-II tagged mST8SiaII Q^{3}AS^{5}EE was generated using a modified vector pET22 (Novagen).

To construct N-terminally truncated mST8SiaII Q^{3}AS^{5}EE variant containing a C-terminal tag for expression in bacteria, mST8SiaII Q^{3}AS^{5}EE was amplified from the plasmid pFlagST8SiaII Q^{3}AS^{5}EE using the following primer pair (restriction sites are in bold) :

MM39s: CATG**CCATGG**AAATCGGGAATTCTGGA

AG50as: CG**CTCGAG**CGTAGCCCCATCACACTG

The resulting PCR product was digested with *Nco*I and *Xho*I and after gel purification (Qiagen) ligated into the corresponding restriction sites of pET23 (Novagen). The resulting plasmid pET23-ST8SiaII Q^{3}AS^{5}EE-His drives the expression of C-terminally His-tagged protein.

To construct N-terminally truncated mST8SiaII S^{3}AS^{5}EE for expression in insect cells, the plasmid pFlag-ST8SiaII S^{3}AS^{5}EE was digested with *Eco*RI. After gel purification (Qiagen) the obtained DNA-fragment was subcloned into *Eco*RI sites of pFastBac-HBM-mST8SiaII?31, a modified pFastbac1 vector (Invitrogen) containing a honeybee melitin (HBM) secretion signal and a N-terminal His-tag. The plasmid mST8SiaII?31 was kindly provided by Dr. Stummeyer from our laboratory. The identity of all constructs was confirmed by sequencing.

2.2.5. Cultivation of LMTK⁻ and CHO cells

Mouse fibroblast cells (LMTK⁻) and *Chinese hamster ovary* (CHO)-2A10 cells were kept in a humidified incubator at 37°C and 5% CO_2. Cells were cultured in DMEM/HAM's F12 medium (Biochrom) supplemented with 5 % fetal calf serum (biochrom) and 1 mM sodium pyruvate (Gibco BRL). Confluent cell layers were treated with PBS/EDTA to detach the cells from culture vessels and diluted 1:20 in fresh medium.

For long term storage in liquid nitrogen, cells were pelleted by centrifugation (5 min, 200xg, RT) and resuspended in culture medium containing 20 % fetal calf serum and 10 % DMSO at a concentration of 1×10^7 cells/ml. Aliquots of 1 ml were filled in cryo vials, stored overnight at -80°C and then transferred to liquid nitrogen.

To recover frozen cell pellets, they were kept on dry ice for 5 min, thawed in a water bath at 37°C and diluted by drop wise addition of culture medium containing 10 % fetal calf serum. After centrifugation (5 min, 200xg, RT) the cell pellet was resuspended in culture medium containing 10 % fetal calf serum and transferred to culture vessels.

2.2.6. Cultivation of *Sf9* cells

Suspension cultures of *Spodoptera frugiperda (SF9)* cells were cultivated at 27°C and 90 rpm in protein free Insect XPress-medium (BioWhittaker). Cell density was maintained between 0.5×10^6 and 5×10^6 cells per millilitre by diluting dense cultures in fresh medium.

For long term storage in liquid nitrogen, cells were pelleted by centrifugation (5 min, 200xg, RT) and resuspended in the conditioned culture medium containing 10 % DMSO at a

concentration of 2×10^7 cells/ml. Aliquots of 1 ml were filled in cyro vials and cooled down by subsequent incubations at 4°C and -20°C for 1 h each. Cells were stored overnight at -80°C and then transferred to liquid nitrogen.

To recover frozen cell pellets, they were kept on dry ice for 5 min, thawed in a water bath at 37°C and directly added to 30 ml culture medium in a culture vessel.

2.2.7. Transfection of LMTK⁻ and CHO cells

For immunofluorescence staining 0.9×10^5 cells were seeded per well of a six well tissue culture plate, containing coverslips. Cells were cultivated overnight as described in 2.2.5. For transient transfection a transfection mix was prepared by diluting 1 µg DNA and 6 µl Lipofectamin in 100 µl OptiMEM each. Both dilutions were combined and incubated for 30 min at RT. The LMTK⁻ cell layer (70-80 % confluent) was washed two times in PBS and incubated with freshly prepared transfection mix diluted in 1 ml OptiMEM for 5 h. The transfection was stopped by replacement of the transfection mix with 2 ml culture medium. Cells were cultivated for an additional 48 h.

For the in vitro assay (2.2.15) 1.9×10^6 CHO-2A10 cells were seeded per 100 mm culture vessels and cultivated in a humidified incubator at 37°C and 5% CO_2. Transfection was performed as described above using the four fold among.

2.2.8. Immunofluorescence of ST8SiaII variants in LMTK⁻ cells

48 h after transfection (see 2.2.7) cells were washed with PBS, fixed in 4 % paraformaldehyde for 20 min, and washed twice with PBS. Coverslips were blocked in 20 % horse serum in PBS for 30 min. Subsequently, polySia staining was performed with 5 µg/ml of primary monoclonal antibody 735 (Behring Werke Marburg) in 20 % horse serum. After washing three times with PBS, the cells were incubated for 30 min at RT with sheep anti-mouse IgG-Cy3 (1:300, Sigma) in 20 % horse serum. The cells were washed thrice with PBS, and coverslips were mounted in vectashield (Vectashield) and analyzed under an Axiovert 200 M fluorescence microscope (Zeiss).

2.2.9. Recombinant expression of ST8SiaII Q^3AS^5EE in bacteria

<u>Transformation of bacteria</u>

50-100 µl of competent *E .coli* AD494(DE3) or Origami(DE3) were thawed on ice and 10 ng of plasmid DNA were added. The mix was placed for 10 min on ice. After a heat shock for 40 sec at 42 °C, samples were incubated for another 10 min on ice. Subsequently, 300 µl of

LB medium were added and the bacterial culture was incubated at 37 °C. After 20-40 min the bacterial culture was plated on selective LB-agar plates containing the appropriate antibiotics.

<u>Expression of recombinant proteins in *E. coli*</u>

For bacterial expression of recombinant proteins the pET-vector system (Novagen) was used. 30-500 ml cultures of *E. coli* strains Origami(DE3) or Ad494(DE3) transformed with the respective expression plasmids were grown in LB or power broth (PB) medium containing selective antibiotics at appropriate temperature and 300 rpm to an optical density of $OD_{600nm}=$ 0.6 for LB or $OD_{600nm}=1.2$ for PB medium. Subsequently, the expression of the recombinant protein was induced with 0.1 mM or 1 mM isopropyl-1-thio-ß-D-galactopyranoside (IPTG) for 3 h at 30°C or 24 h at 15 °C. Cells were harvested by centrifugation (15 min, 6,000xg, 4°C). The bacterial pellet was stored at -20°C.

<u>Preparation of soluble and insoluble *E. coli* fractions:</u>

For analytical preparation bacterial pellets obtained from 1 ml of expression culture were resuspended in 100 µl TE buffer (10 mM Tris-HCl, pH 8.0; 1 mM EDTA) containing 10 µg of lysozyme and the samples were incubated for 15 min at 37°C. After sonication in a beaker resonator (Branson, 100 % duty cycle, output control 5) for 2 min at 4°C the soluble (supernatant) and insoluble fractions (pellet) were separated by centrifugation (15 min, 11,000xg, 4°C). Soluble and insoluble fractions were analyzed by 10 % SDS-PAGE followed by western blot analysis and coomassie staining (2.2.16/17).

For large scale preparation, the bacterial pellet obtained from 500 ml expression culture was resuspended in 5 ml buffer A (MBP-ST8SiaII Q^3AS^5EE: 20 mM Tris/HCl pH 7.5; 25 mM NaCl or NusA-Strep-ST8SiaII Q^3AS^5EE: 100 mM Tris/HCl pH8.0; 150 mM NaCl) and supplemented with protease inhibitors (40 µg/ml Bestatin; 1 mM PMSF; 0.5 µg/ml Leupeptin; 1 µg/ml Pepstatin). Bacteria were lysed by sonication with a microtip (Branson Sonifier, 50 % duty cycle, output control 5, 4°C) using eight pulses of 30 s intermitted by breaks of 30 s. Cell debris were removed by centrifugation (15 min, 20,000xg, 4°C).

Resulting supernatant containing MBP-ST8SiaII Q^3AS^5EE was directly coupled to the equilibrated amylose resin (NewEnglandBiolabs), whereas the supernatant containing NusA-Strep-ST8SiaII Q^3AS^5EE was additionally supplemented with 20 µg/ml avidin (IBA) and incubated for 30 min at 4°C. After centrifugation (15 min, 12,000xg, 4°C) supernatant was filtered (0.8 µm cellulose acetate filter; Sartorius) and applied on equilibrated strep-tactin matrix (IBA).

2.2.10. NusA-Strep-purification of ST8SiaII Q^{3}AS^{5}EE

Supernatant obtained as described in 2.2.9. was applied on 250 µl strep-tactin matrix (IBA). Subsequently, the matrix was washed with 30 column volumes (CV) of buffer A (100 mM Tris/HCl pH 8.0; 150 mM NaCl). The protein was eluted with 5 CV of buffer E (buffer A containing 2.5 mM desthiobiotin). Protein containing fractions were analyzed by SDS-PAGE followed by western blot analysis and coomassie staining (2.2.16/17). PolyST containing fractions were concentrated in a vivaspin concentrator (10,000 MVCO PES; Vivascience), quick-frozen in liquid nitrogen and stored at -80°C.

2.2.11. Maltose-Binding-Protein (MBP)-purification of ST8SiaII Q^{3}AS^{5}EE

Supernatant obtained as described in 2.2.9. was incubated with 1 ml of amylose resin (NewEnglandBiolabs) for 1 h at 4 °C and for further washing packed into a column. The column was washed with 15 column volumes of buffer A (20 mM Tris/HCl pH 7.5; 25 mM NaCl) with a flow rate of 0.5 ml/min and protein eluted with buffer B (buffer A containing 10 mM maltose). 1 ml fractions were collected and protein containing fractions were analyzed by SDS-PAGE followed by western blot analysis and coomassie staining (2.2.16/17). PolyST containing fractions were concentrated in a vivaspin concentrator (10,000 MVCO PES; Vivascience), quick-frozen in liquid nitrogen, and stored at -80°C or further analyzed by size-exclusion chromatography.

2.2.12. Size-exclusion chromatography

A Superdex 200 HR 10/30 column (Amersham Biosciences) was equilibrated in degassed and 0.22 µm sterile filtrated buffer T (MBP-ST8SiaII Q^{3}AS^{5}EE: 50 mM Tris/HCl pH 7.5; 300 mM NaCl) using the Äkta FPLC system (GE Healthcare). Purified protein was applied and eluted in 0.5 ml fractions at a flow rate of 0.5 ml/min. Polysialyltransferase containing fractions were concentrated in a vivaspin concentrator (10,000 MVCO PES; Vivascience) and stored at -80°C after quick-freezing in liquid nitrogen.

2.2.13. mST8SiaII S^{3}AS^{5}EE expression and purification from insect cells

Recombinant baculoviruses were generated based on transposon-mediated recombination in *E. coli* DH10Bac cells using the Bac-to-Bac Baculovirus Expression System (Invitrogen).
<u>Preparation of recombinant bacmid DNA:</u>
100 µl of competent *E. coli* DH10Bac were thawed on ice and incubated for 30 min with 20 ng of the respective pFastBac vector construct. The transformation mix was subjected to a heat shock at 42°C for 45 sec and incubated on ice for 2 min. 900 µl of SOC-medium were

added, the cell suspension was incubated at 37°C for 4 h before plated on selective LB-agar plates containing 50 µg/ml kanamycin, 7 µg/ml gentamicin, 10 µg/ml tetracycline and 40 µg/ml IPTG. For blue-white screening 30 µl of X-Gal solution (20 mg/ml in DMSO) were spread on the plates prior to plating. Positive transformants were identified after 48 h incubation at 37°C as pure white colonies and re-streaked on fresh plates to confirm the phenotype. 5 ml LB-medium containing 50 µg/ml kanamycin, 7 µg/ml gentamicin and 10 µg/ml tetracycline were inoculated with a positive colony and incubated overnight at 37°C and 300 rpm. Bacmid DNA was isolated using the "Concert High Purity Plasmid Purification System" (GibcoBRL) according to the manufactures instructions. 3 ml of bacterial culture were pelleted (1 min, 12,000xg, RT), resuspended in 400 µl buffer E1 and lysed for 5 min at RT after addition of 400 µl buffer E2. 400 µl neutralization buffer E3 was added, the samples were centrifuged (10 min, 12,000xg, RT) and the supernatant was applied to the concert HP columns, equilibrated in buffer E4. After washing two times with 2.5 ml buffer E5, bound bacmid DNA was eluted in 900 µl buffer E6. 630 µl of 2-propanol were added to the eluent and the DNA was pelleted (30 min, 20,000xg, 4°C). The pellet was washed with 1 ml of 70% ethanol and centrifugated (15 min, 20000xg, 4°C). The bacmid DNA was air-dried for 30 min and resolved in 50 µl of 5 mM Tris/HCl pH 8 for 2 h at RT and stored at 4°C.

<u>Production of recombinant baculoviruses and high-titer stocks:</u>

Baculoviruses were produced by transfecting the prepared recombinant bacmid DNA into *Sf9* cells. For transient transfection $1x10^6$ cells were seeded per well of a six well tissue culture plate. Transfection mix was prepared from 5 µl of bacmid DNA and 6 µl Cellfectin (Invitrogen) in 100 µl of culture media each. Both dilutions were combined and incubated for 30 min at RT. The medium was aspirated from adherend *Sf9* cells and replaced with transfection mix diluted in 1 ml culture medium. The transfection mix was removed after 14 h and replaced with 2 ml culture medium. The transfected cells were incubated at 27°C for 4-7 days until signs of viral infection like enlarged cell diameters and a granular appearance of the cells were clearly visible.

The supernatant (low-titer P1-stock) was harvested and stored at -80°C. For virus amplification 40 µl P1-stock were added to 4 ml *Sf9* cells ($0.5x10^6$ cells/ml) in a 25 cm^2 cell culture bottle (Sarsted) and incubated for 3-4 days (P2-stock). Further amplification of the baculovirus stock was performed by infecting 50 ml suspension culture ($2x10^6$ cells/ml) with 50 µl of P2-stock. After three days, the cells were pelleted by centrifugation (5 min, 300xg, RT) and the supernatant was sterile filtered (0.2 µm cellulose acetate filter; Sartorius) and stored at 4°C (P3-stock).

<u>Baculoviral expression of ST8SiaII variants in *Sf9* cells:</u>

For baculoviral expression of recombinant mST8SiaIIS^{3}ASEE^5 log-phase *Sf9* cells at a density of 1.5-2x10^6 cells/ml were infected with different concentrations of P3-stock and cultivated for time response at 27 °C and 90 rpm. Culture supernatants were assayed for protein expression by SDS-PAGE followed by western blot analysis (2.2.16). The dose of baculovirus required for optimal expression of recombinant protein was used for subsequent large scale expressions cultures.

<u>Purification of baculoviral expressed zST8SiaII variants from *Sf9* cells:</u>

4 L-expression cultures were infected with the optimal baculovirus concentration and harvested at the time point determined previously. To harvest the expressed recombinant protein, cells were pelleted (10 min, 300xg, 4°C) and the supernatant was adjusted with NaOH to pH 7.5 and re-centrifugated (20 min, 7,000xg, 4°C). Subsequently, the supernatant was filtered (0.22 µM Millipore-1L-device) and concentrated to 200 ml (Ultrasette 10,000 MWCO) at 4°C. To remove low molecular weight inhibitors the concentrate was diluted 1:5 with buffer DT (50 mM Tris/HCl; 100 mM NaCl; pH 7.5) and concentrated to 80 ml. Protein containing solution was filtered (0.22 µM) and 10 % glycerol was added. Coupling to Ni^{2+}chelating matrix (Probond-resin; Invitrogen) was performed overnight at 4°C. For all following steps Äkta FPLC (GE Healthcare) was used with a flow rate of 1 ml/min. The protein was eluted stepwise starting with 25 mM imidazole in precooled buffer A (50 mM Tris/HCl pH 7.5; 150 mM NaCl; 10 % glycerol) followed by 80 mM imidazole and 400 mM imidazole in buffer A, respectively. 1 ml fractions were collected and protein containing fractions were analyzed with SDS-PAGE followed by western blot analysis and silver staining (2.2.11/12). Polysialyltransferase containing fractions were concentrated in a vivaspin concentrator (10,000 MVCO PES; Vivascience), quick-frozen in liquid nitrogen and stored at -80°C.

2.2.14. Enzyme linked immunosorbent assay for polyST activity

To monitor polyST activity in a non radioactive test system an enzyme-linked immunosorbent assay (ELISA) had previously been established by Dr. Stummeyer from our laboratory. Therefore, a 96 well microtiter plate (Greiner) was coated with 25 µl/well of 10 µg/ml mouse IgG (Pierce) in PBS for 3 h at RT. After washing thrice with PBS plastic surface was blocked with 1 % BSA in PBS (Sigma) overnight at 4°C. For NCAM-polysialylation 25 µl of 30 ng/ml polySia free proteinA-NCAM fusion protein was adsorbed for 1 h at RT. After washing three timeswith PBS and once with reaction buffer (10 mM MES, 10 mM MnCl$_2$) 0.2 µg-1 µg polyST were directly incubated in reaction buffer,

containing 1 mM CMP-Neu5Ac and 3.3 % humans serum for 3 h at 27°C or overnight at RT. The plates were washed two times with PBS and subsequently incubated with 25 µl/well of biotinylated fab-fragments of mAb 735 (Davids Biotechnologie) diluted 1:500 in 1% BSA (Sigma) for 1 h at RT. Afterwards, plates were washed three times with PBS. The bound biotinylated antibody was detected with streptavidin-horseradish peroxidase conjugate (Roche) using 20 µl of a 1:20,000 dilution per well. After 30 min at 37°C plates were washed three times with PBS and developed with 50 µl of substrate solution containing 5 µg 3,3',5,5'-tetramethylbenzidine (TMB), 100 mM sodium acetate, 100 mM citric acid, and 0.0045 % H_2O_2. Reactions were stopped after 20 min by adding 25 µl 2 N H_2SO_4, and the optical density at 450 nm was measured in PowerWave 340 microtiter plate spectrophotometer (BioTek).

2.2.15. *In vitro* assay for NCAM polysialylation

For the *in vitro* NCAM-polysialylation assay polySia negative CHO-2A10 cells, defective in the ST8SiaIV gene (Gerardy-Schahn *et al.*, 1995) were transfected as described in 2.2.7. To standardize the concentration of ProtA-ST8SiaII variants for the polysialylation assay, an enzyme-linked immunosorbent assay (ELISA) was used as described by Mühlenhoff *et al.* (2001).

Round-bottom microtiter plates (Greiner) were coated overnight with 0.2 µg murine IgG (Pierce) at 4°C and blocked with bovine serum albumin (1 % in PBS) (Sigma) for 2 h at RT. Plates were washed with PBS prior to addition of 20 µl/well cell supernatant that contained ProtA-ST8SiaII variants. Plates were incubated for 1 h at RT to allow binding of ProtA-polyST fusion-variants to IgG. In parallel, serial dilutions (1 - 0.05 ng/ml) of the recombinant IgG-binding fragment of ProteinA (Sigma) were included to generate a standard curve. After the adsorption step, plates were washed three times with PBS, before adding 20 µl/well of biotinylated anti-ProteinA antibody in an 1:80,000 dilution (Sigma). The plates were incubated for 1 h at 37°C and washed three times with PBS. The bound biotinylated antibody was detected with streptavidin-horseradish peroxidase conjugate (Roche) using 20 µl/well of an 1:20,000 dilution. After 30 min at 37°C plates were washed three times with PBS and developed with 50 µl/well of substrate solution containing 5 µg 3,3',5,5'-tetramethylbenzidine (TMB), 100 mM sodium acetate, 100 mM citric acid, and 0.0045 % H_2O_2. The staining reaction was stopped after 20 min by adding 25 µl/well 2 N H_2SO_4, and the optical density at 450 nm was determined using a PowerWave 340 microtiter plate spectrophotometer (BioTek). All samples were measured in serial dilutions, and triple values were analyzed for each dilution.

PolyST activity was assayed by incorporation of [^{14}C]-labeled sialic acid residues into a growing polySia chain and monitored by SDS-PAGE followed by autoradiography. 30 ng of recombinant polySia-free ProtA-NCAM was incubated with 20 µl of IgG-coated sepharose beads (Pierce) for 1 h at 4°C. After washing with PBS 1 µg of enzyme variants was added and incubated for 1 h at 4°C. Afterwards beads were washed three times with 1 ml PBS and two time with 1 ml reaction buffer (10 mM MES buffer pH 6.7; 10 mM MnCl$_2$) and resuspended in 40 µl reaction buffer containing 0.12 mM (21 Bq/µl) [^{14}C]-CMP-Neu5Ac (GE Healthcare). Samples were incubated at 37°C and 1300 rpm to allow enzyme reaction. After 4 h, the reactions were terminated by washing (two times with 1 ml PBS). As an assay control, one out of two parallel samples was treated with 20 µg/ml of the polySia-degrading enzyme EndoNF in a final volume of 50 µl PBS for 30 min at 37°C. After two additional washing steps with 1 ml PBS each, residual buffer was removed and 20 µl of 2xLaemmli loading buffer containing 2 % ß-mercaptoethanol were added. Samples were heated for 10 min at 60°C and analyzed by SDS-PAGE followed by autoradiography (Mühlenhoff *et al.*, 2001).

2.2.16. SDS-PAGE analysis and immunoblotting

For protein separation a SDS-PAGE was performed according to Laemmli (Laemmli, Beguin, and Gujer-Kellenberger, 1970). SDS-PAGEs were composed of a 3 % stacking gel [125 mM Tris/HCl pH 6.8; 0.1 % SDS; 3% polyacrylamide(40 % 4 K-Mix, AppliChem)] and a separating gel in a range of 7-14 % polyacrylamide [375 mM Tris/HCl pH 8.8; 0.1 % SDS; 7-14 % Acrylamide (40 % 4 K-Mix, AppliChem)]. After mixing all components polymerization was initiated by adding 0.1 % TEMED and 1 % ammonium persulphate.

For sample preparation, the samples were diluted 1:1 with Laemmli buffer containing 2 % ß-mercaptoethanol and boiled for 5 min or heated to 60°C for 10 min, if they contained heat-sensitive polySia.

Electrophoresis was performed in SDS-electrophoresis buffer (50 mM Tris; 350 mM glycine; 0.1 % SDS) at 60 V for the stacking gel and at 140 V for the separating gel.

After SDS-PAGE, separated proteins were transferred onto a nitrocellulose membrane (Schleicher & Schüll), using a semidry blotting chamber (Biometra) at 2 mA/cm^2 for 45 min. Gel and membrane were placed between two layers of filter paper (Whatman) soaked in blotting buffer (48 mM Tris, 39 mM glycine). Western blots were developed using the recommended primary antibody concentration, followed by anti-mouse alkaline phosphatase conjugate (Dianova). Nitro blue tetrazolium (NBT) and 5-bromo-4-chloro-3-inodyl phosphate (BCIP) were used as substrates for alkaline phosphatase staining reaction.

2.2.17. Silver staining /coomassie staining

Silver staining:

After SDS-PAGE, protein bands were visualized by silver staining. Initially, the SDS-gel was incubated in fixation solution (10 % acetic acid; 30 % ethanol; 1.85 % formaldehyde) for 20 min. After washing three times with 50 % ethanol for 20 min the gel was incubated for exactly 1 min in thiosulphate solution (20 mg thiosulphate in 20 ml H_2O) and washed in deionised water for 40 seconds. Subsequently the gel was incubated in silver staining solution (0.2 % $AgNO_3$; 2.8 % formaldehyde) for 20 min. After washing with deionised water the gel was incubated in developing solution (6 % $NaCO_3$; 2 % (v/v) thiosulphate solution; 1.85 % formaldehyde) until the bands appeared. Staining was stopped by washing with water and stop solution (10 % acetic acid; 30 % ethanol). Before drying, the gel was incubated in 30 % ethanol for 30 min and subsequently in drying solution (10 % glycerol; 20 % ethanol) for 20 min. Gels were dried in cellophane foil overnight at 50 °C.

Coomassie staining:

After SDS-PAGE, protein bands were stained by colloidal solution of Roti[®]-blue (Roth). In according to the manufactures instructions a staining solution was prepared in 20 % methanol. SDS-gels were incubated in staining solution overnight at RT and destained in 25 % methanol.

After incubation in drying buffer (10 % glycerol; 20 % ethanol) for 20 min at RT. Gels were dried in cellophane foil overnight at 50 °C.

2.3. Results

2.3.1. Phylogenetic display of the *N*-glycosylation patterns in the polysialyltransferase ST8SiaII

The eukaryotic polysialyltransferase (polyST) ST8SiaII is a member of the a2,8-sialyltransferase protein family and therefore comprises all three conserved sialyl-motifs (S-motif, L-motif and VS-motif). ST8SiaII contains six *N*-glycan attachment sites conserved over a wide range of species such as mouse, chicken and African clawed frog, (fig. 19 *A*).

Mutational studies carried out with the murine enzyme (mST8SiaII) have demonstrated that enzymatic activity crucially depends on the presence of two out of six *N*-glycan attachment sites, N89 (#3) and N219 (#5) (Close *et al.*, 2001; Mühlenhoff *et al.*, 2001).

Interestingly, the functional ST8SiaII isolated from zebrafish lacks the *N*-glycosylation site corresponding to N219 (#5) in mouse (Marx *et al.*, 2007). A multiple sequence alignment carried out with *MultAlin* (Corpet, 1988) revealed that the bonefishes -zebrafish and pufferfish- comprise the conserved sequence SEE instead of the *N*-glycan attachment site (fig. 19 *A)*. This offers the possibility to apply a method called SUNGA (substitution of *N*-glycan functions in glycosyltransferases by specific amino acids) with the aim to substitute the *N*-glycan function (#5) in mST8SiaII by the bonefish sequence (Uemura *et al.*, 2006). For ST8SiaII the method SUNGA is restricted to the *N*-glycosylation attachment site N219 (#5) as site N89 (#3) is conserved among all known polySTs.

This study aims at generating a minimally or even non-glycosylated mST8SiaII variant by a directed engineering approach.
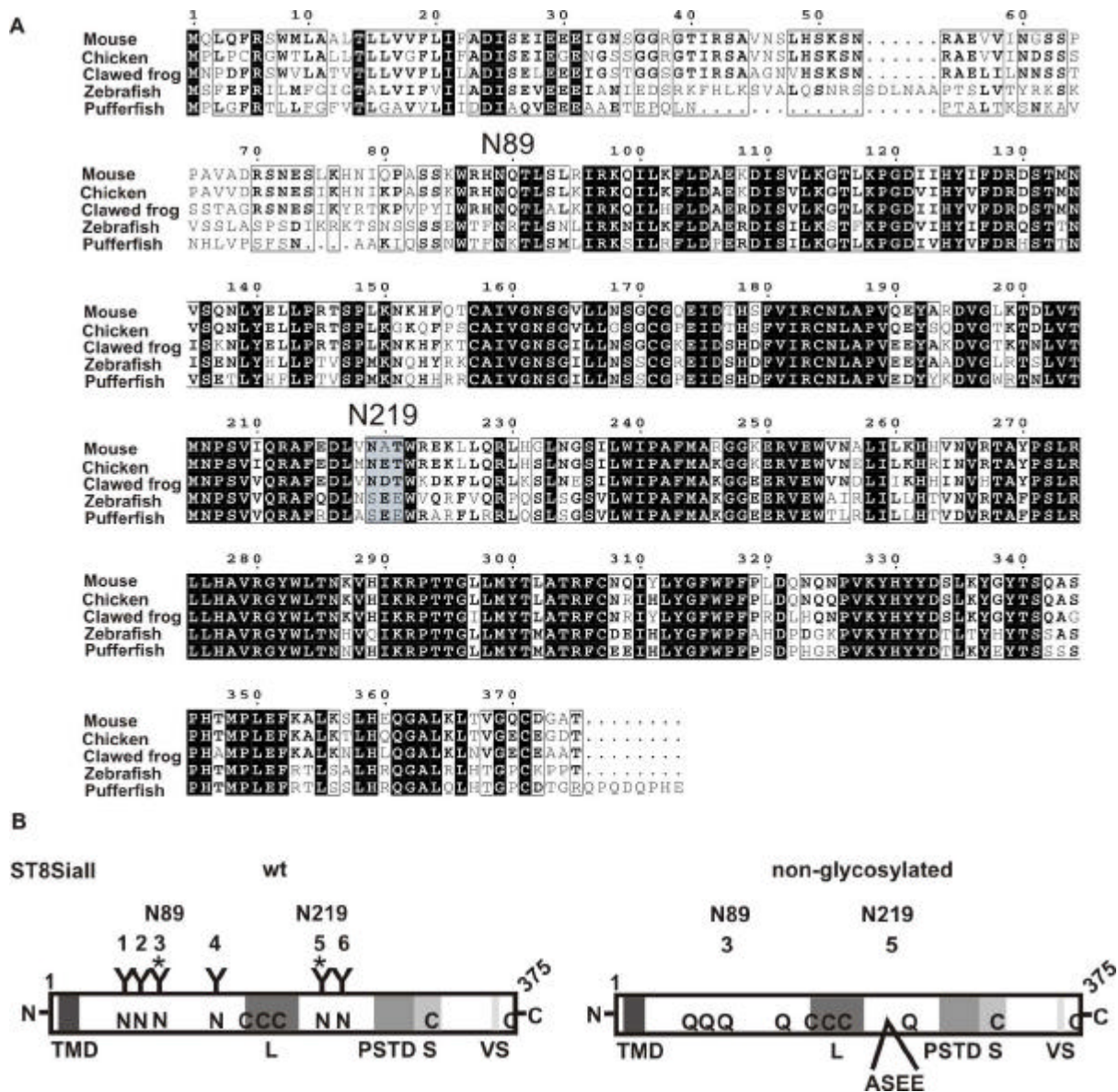
Figure 19: Multiple sequence alignment and scheme of murine ST8SiaII. *A.* Multiple sequence alignment of different ST8SiaIIs was generated with *MultAlin* (Corpet, 1988). Sequence identity is highlighted in dark boxes and important *N*-glycosylation attachment sites N89 and N219 are indicated. *B.* Schematic representation of the murine polysialyltransferase ST8SiaII. Positioning of *N*-glycosylation sites are given by the respective asparagine residues (N) whereupon sites required for polyST activity are marked by an asterisk. Sialyl-motifs (L, S and VS), polyST domain (PSTD) and conserved cysteine residues (C) are indicated The *N*-glycosylation pattern of wild-type ST8SiaII is depicted in the left panel, whereas a non-glycosylated variant is shown in the right panel. In the non-glycosylated variant *N*-glycosylation sites 1,2,3,4 and 6 were removed by substitution of the respective asparagine residues by glutamine (N→Q) within the **N**-X-S/T consensus motifs. SUNGA was introduced on *N*-glycosylation site N219 (5) by exchanging the sequence V**N**AT found in the murine enzyme by the bonefish sequence ASEE.

2.3.2. Engineering of minimally glycosylated mST8SiaII

In the following, a set of *N*-glycosylation depletion variants of mST8SiaII was generated with the final aim to obtain an active *N*-glycosylation free enzyme. Based on already existing data, the study could be started with a mST8SiaII variant, containing only two out of six *N*-glycan sites, the sites N89 (#3) and N219 (#5), known to be required for activity (Close *et al.*, 2001; Mühlenhoff *et al.*, 2001). *N*-glycosylation sites naturally occurring in the positions N60, N72, N134 and N234 were replaced by glutamine ((Q60 (#1), Q72 (#2), Q134 (#4) and Q234 (#6)) as shown in figure 19 *B*.

In a first trial to create a non-glycosylated variant of mST8SiaII we started from a mST8SiaII variant in which all *N*-glycan sequons had been replaced by exchange of asparagine to glutamine (N/Q). This construct termed mST8SiaII Q^3Q^5 was already existing in the laboratory as mST8SiaII?1-6 (Mühlenhoff *et al.*, 2001). To apply the SUNGA strategy in the mST8SiaII Q^3Q^5 the sequence of the former *N*-gycan #5 (VQ^5AT) was substituted by either the conserved bonefish sequence AS^5EE, resulting in the variant mST8SiaII Q^3AS^5EE or modified by single substitution of Q^5 to S^5 (mST8SiaII Q^3S^5). Glycosylation variants were transiently transfected in polySia-free LMTK$^-$ cells expressing NCAM and enzymatic activity was detected by polySia surface staining with polySia specific mab 735. Although reduced if compared to the wild type control, polySia staining could be clearly observed on cells transfected with mST8SiaII Q^3AS^5EE, indicating residual activity in the non-glycosylated variant (fig. 20 *A*).

To our surprise we also found marginal polysialylation activity for mST8SiaII Q^3S^5. This variant carries only the exchange to serine whereas the neighboring amino acids were not modified to match the bonefish sequence (fig. 20 *A* and fig. 19 *A*). Additionally, comparison of two previous *N*-glycosylation depletion studies of ST8SiaII (Mühlenhoff *et al.*, 2001; Close *et al.*, 2001) suggested, that generally, substitution of the respective **N**-X-S/T asparagine residues to serine appears to be more favorable for enzyme activity than substitutions to glutamine. Therefore we analyzed enzyme variants mST8SiaII Q^3N^5 and mST8SiaII S^3N^5 as depicted in figure 20 *A*. This direct comparison revealed that the serine variant is indeed more active. Therefore we hypothesized that enzymatic activity of the *N*-glycan-free polyST-variants ST8SiaII Q^3AS^5EE and ST8SiaII Q^3S^5 might be enhanced, if a serine-residue is introduced instead of a glutamine at *N*-glycosylation site N89 (#3). As shown in figure 20 this hypothesis proved to be correct because slightly enhanced intensities of polySia surface staining was found for mST8SiaII S^3AS^5EE and mST8SiaII S^3S^5. A single

serine substitution at *N*-glycosylation site 3 (mST8SiaII S^3Q^5) was, however, not enough to restore activity (fig. 20 *A*).
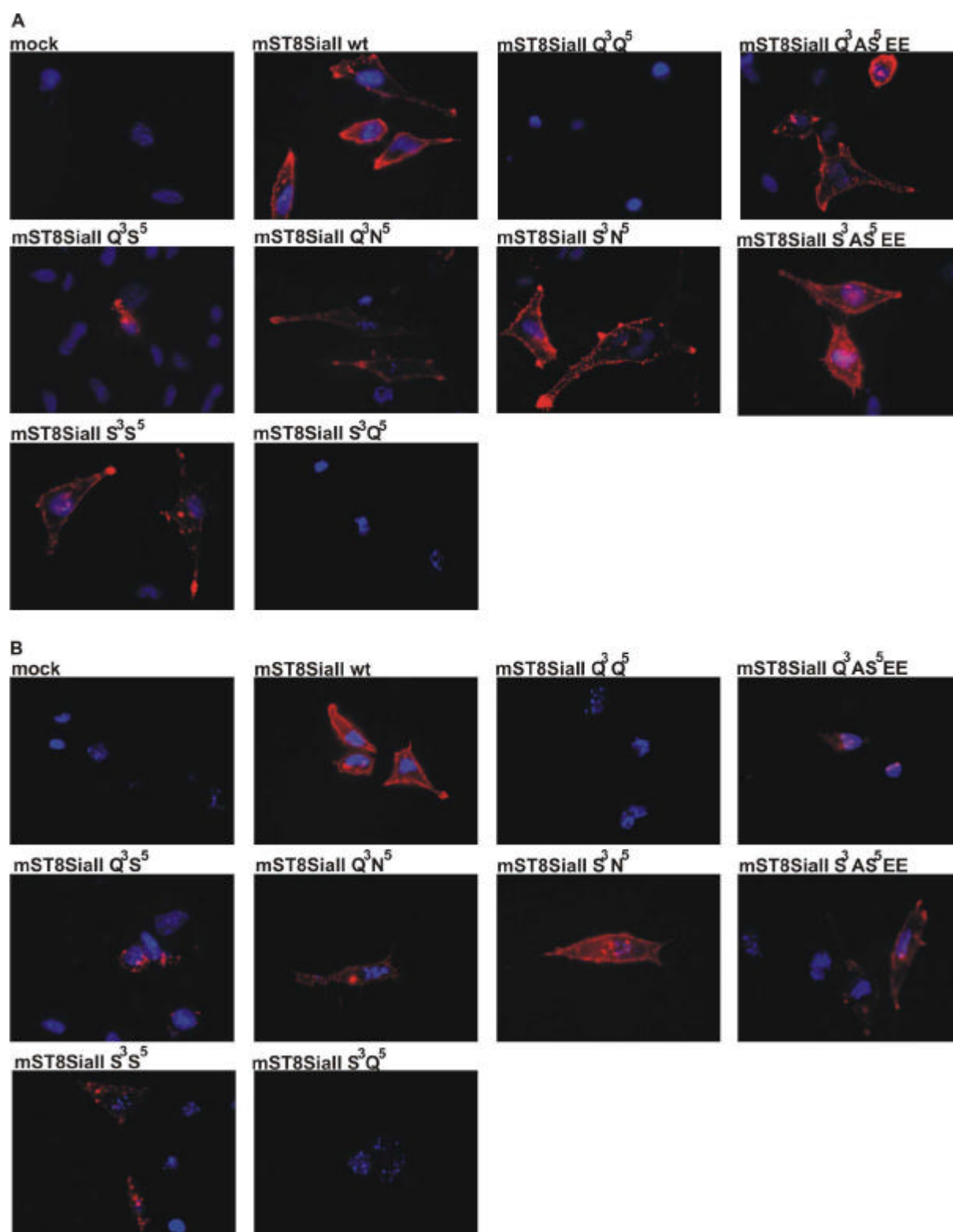
Figure 20: Polysialylation activity of *N*-glycosylation variants of full-length mST8SiaII. N-terminally Flag-tagged wild-type and *N*-glycosylation variants of mST8SiaII were transiently expressed in the presence or absence of NCAM in polySia free LMTK⁻ cells. 48 h post transfection, cells were fixed with paraformaldehyde and polySia surface was stained using mAb 735. Cell staining was visualized at 630-fold magnification. *A*. PolySia staining in the presence of stable transfected NCAM. *B*. PolySia staining in the absence of NCAM.

Transient transfection in polySia-free LMTK⁻ cells was repeated for all mST8SiaII variants described above, but in the absence of the polySia-acceptor NCAM (fig. 20 *B*). This study was carried out to detect autopolysialylation, whereupon no polySia staining was expected for all *N*-glycan-free mST8SiaII variants due to the lack of acceptor sites. Fully unexpected, faint polySia staining occurred in the absence of NCAM with all *N*-glycan-free mST8SiaII variants that were shown to be competent in NCAM-polysialylation before (fig. 20 *A+B*). Although at this point the presence of a second endogenous polySia acceptor in LMTK⁻ cells cannot be excluded, a second possibility to explain this effect might be that polySia is artificially attached to *O*-glycosylation sites in the active enzyme if there are no *N*-glycan acceptors present. Of particular importance is the fact, that potential *O*-glycan attachment sites were inserted in all active *N*-glycan-free mST8SiaII variants by the introduction of serine residues. To exclude the latter possibility, we analyzed the additional *N*-glycan-free variant mST8SiaII Q^3AM^5EE lacking artificial serine residues. The variant was shown to be functionally active in LMTK⁻ cells in the presence of NCAM (fig. 21 *A*). By contrast, no polysialylation activity was detectable with mST8SiaII Q^3AM^5EE in the absence of the polySia acceptor NCAM (fig. 21 *B*). This result indicates that artificial *O*-glycans attached to S^5 serve as polySia acceptor and simultaneously argues against the presence of an additional endogenous polySia acceptor in LMTK⁻ cells. Moreover, clone ST8SiaII Q^3AM^5EE also evidences that NCAM-polysialylation competence in polySTs is not essentially dependent on the glycosylation (*N*- or *O*-glycans) of the protein.
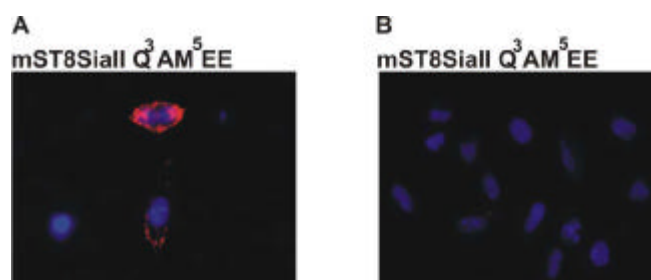
Figure 21: Polysialylation activity of a non-glycosylated variant of full-length mST8SiaII. N-terminally Flag-tagged non-glycosylated variant of mST8SiaII was transiently expressed in the presence or absence of NCAM in polySia free LMTK⁻ cells. 48 h post transfection, cells were fixed with paraformaldehyde and polySia surface was stained using mAb 735. Cell staining was visualized at 630-fold magnification. *A*. PolySia staining in the presence of NCAM. *B*. PolySia staining in LMTK⁻ cells transfected with the polyST variants in the absence of NCAM.

To control if functionality of mST8SiaII variants as described above can be preserved also in soluble protein forms, we exemplarily analyzed the construct mST8SiaIIΔN31-S^3AS^5EE in LMTK⁻ cells as described above. Due to the use of the Igκ leader sequence for secretion, this

protein should be released to the culture medium. To facilitate protein detection and enrichment, a C-terminal Myc/His-tag was added. As depicted in figure 22, NCAM-polysialylation capacity was preserved also in the soluble enzyme variant.
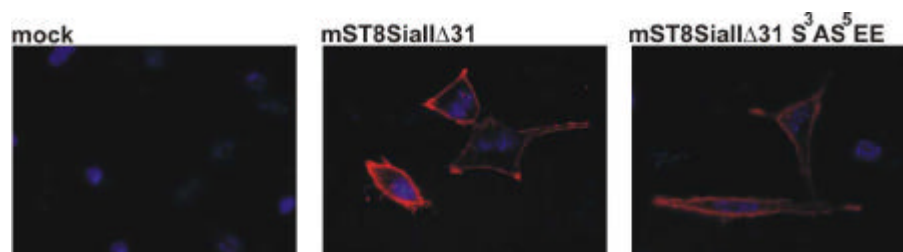
Figure 22: Polysialylation activity of a non-glycosylated variant of secreted mST8SiaII?31. N-terminally truncated and C-terminally Myc-His tagged mST8SiaII variants were transiently expressed in the presence of NCAM in polySia free LMTK⁻ cells. 48 h post transfection, cells were fixed with paraformaldehyde and polySia surface was stained using mAb 735. Cell staining was visualized at 630-fold magnification.

Taken together, the SUNGA allowed us for the first time the generation of a non-glycosylated but active mST8SiaII variant. Because the protein was found to be active in the full-length and N-terminally truncated form, the clone with highest activity mST8SiaII-Q^3AS^5EE was chosen for soluble expression in bacteria.

2.3.3. Recombinant expression of mST8SiaII Q^3AS^5EE in bacteria

Based on our finding that various *N*-glycan-free mST8SiaII variants maintained enzymatic activity, we chose one of them for recombinant expression in bacteria. It has to be taken into account that polySTs comprise two essential disulfide bonds that are usually not formed in bacteria. Fortunately, there are some engineered bacterial strains such as *E. coli* Ad494(DE3) and Origami(DE3) available that promote disulfide bond formation. The construct mST8SiaII Q^3AS^5EE was cloned in various bacterial vectors harboring different tags or fusion proteins for purification. Recombinant expression of these ST8SiaII Q^3AS^5EE variants was tested in *E. coli* Ad494(DE3) and origami(DE3) under different conditions. The best conditions for the four tested constructs are shown in figure 23 *A*. Pellets of expression cultures were lysed by sonication and the insoluble (I) as well as the soluble (S) fractions were analyzed by 10 % SDS-PAGE followed by western blot analysis and coomassie staining (fig. 23 *B*). All mST8SiaII Q^3AS^5EE variants were mainly found in the insoluble fraction, nonetheless significant amounts of soluble protein were achievable with enzyme variants that

contain an N-terminal fusion protein (NusA or maltose binding protein (MBP)). By contrast, only a marginal quantity was produced of the N-terminally Strep-tagged mST8SiaII Q^{3}AS^{5}EE and soluble C-terminally His-tagged enzyme was not detectable (fig. 23 *B*).
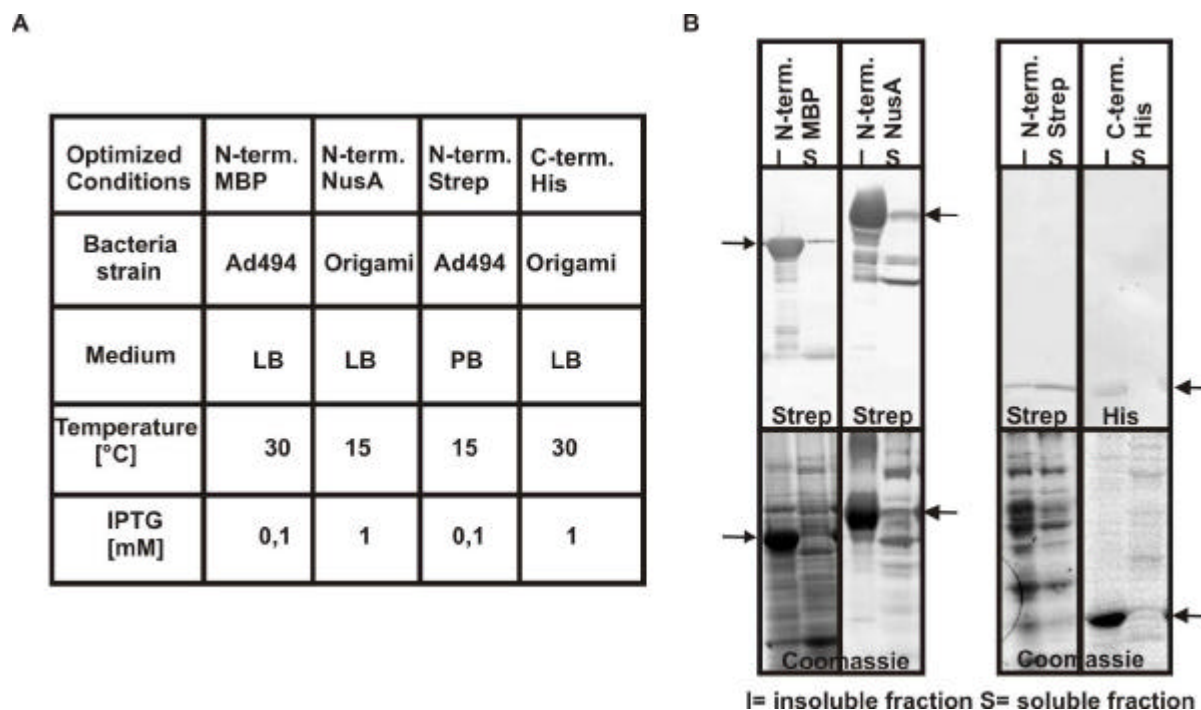

Figure 23: Expression of mST8SiaII Q^{3}AS^{5}EE in bacteria. All variants were expressed in the bacterial *E. coli* strains Ad494 and Origami assisting development of disulfide bonds. *A*. Optimized condition for all four different mST8SiaII Q^{3}AS^{5}EE variants are listed. LB: lysogeny broth-medium, PB: PowerBroth-medium. *B*. Insolube (I) and solube (S) fractions were prepared and analyzed by SDS-PAGE followed by western blot analysis and coomassie staining. For western blotting antibodies directed against the respective tags were used. mST8SiaII variants are marked with arrows.

2.3.4. Purification of ST8SiaII Q^{3}AS^{5}EE fusion proteins from bacteria

As soluble expression of NusA- and MBP-fusion proteins of mST8SiaII Q^{3}AS^{5}EE was detectable, we hypothesized that parts of the protein are properly folded enzyme variants. Consequently, a trial was undertaken to purify NusA-ST8SiaII Q^{3}AS^{5}EE and MBP-ST8SiaII Q^{3}AS^{5}EE from 500 ml bacterial culture. The NusA-ST8SiaII Q^{3}AS^{5}EE variant was enriched via the added Strep-tag II using strepTactin sepharose and MBP-ST8SiaII Q^{3}AS^{5}EE was purified by the amylose-resin system. Isolated enzymes were analyzed by 10 % SDS-PAGE followed by coomassie staining (fig. 24, lower panel) and western blot analysis (fig. 24, upper panel). Significant expression of the NusA-fused enzyme variant was detectable in the crude lysate (Apply) but binding to StrepTactin sepharose was barely

detectable. The protein thus remained in the flow through (fig. 24 *A*). By contrast, large quantities of the MBP-fused mST8SiaII Q^{3}AS^{5}EE variant could be enriched using the amylose-resin system, although several C-terminal degradation products are visible in the coomassie staining as well as in the western blot (fig. 24 *B*). Enzymatic activity of the two mST8SiaII Q^{3}AS^{5}EE variants enriched from bacterial expression cultures was analyzed in an ELISA based activity assay. Therefore purified enzymes were incubated in the presence of 30 pg of ProtA-NCAM adsorbed to a well of a 96 microtiter plate and reaction buffer containing 1 or 5 mM CMP-Neu5Ac. As a positive control we used the *N*-glycosylated form of mST8SiaII?N31 that was purified from *Sf*9 insect cells. As indicated in the Table added to figure 24, no activity was detectable for MBP-ST8SiaII Q^{3}AS^{5}EE and NusA-ST8SiaII Q^{3}AS^{5}EE fusion protein.
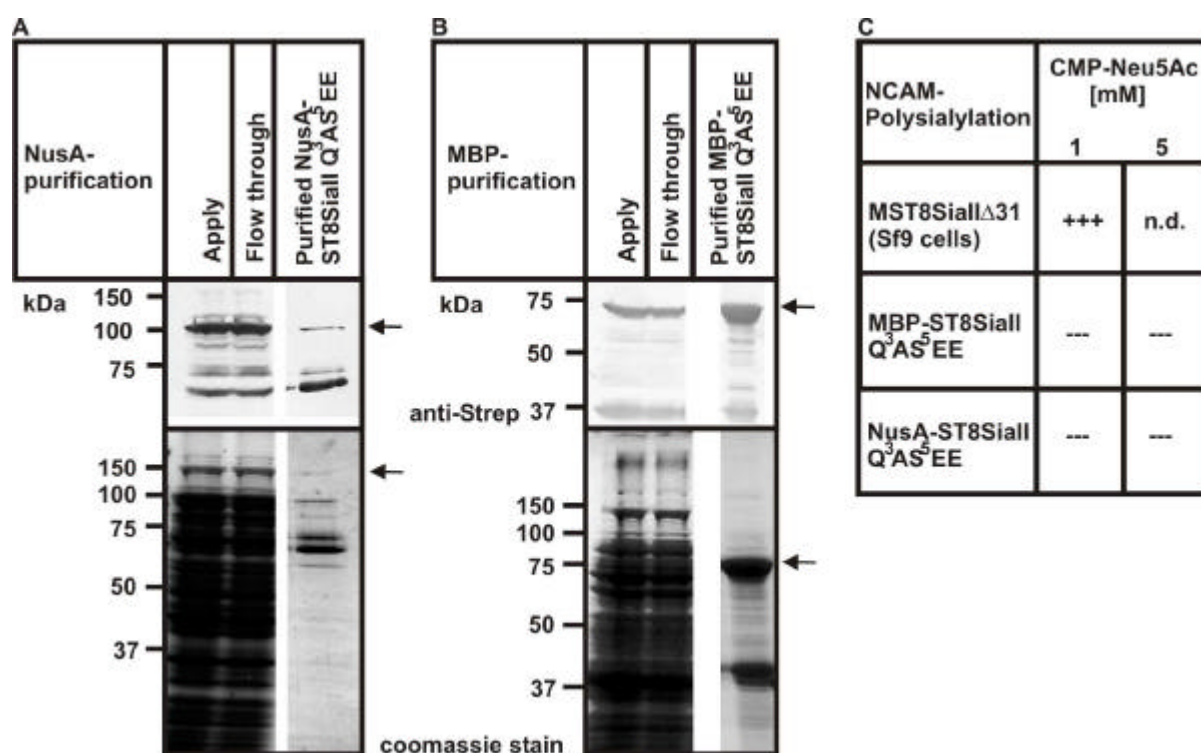
Figure 24: Purification of mST8SiaII Q^{3}AS^{5}EE variants from 500 ml bacteria culture. Bacteria were lysed by sonication and coupled for 2 h to the corresponding matrix for purification. Protein was eluted stepwise and peak fractions were analyzed with 10 % SDS-PAGE followed by western blot analysis and coomassie staining. PolyST containing fractions were incubated with reaction buffer (10 mM sodium cacodylate buffer pH 6.7; 10 mM MnCl$_2$) containing 1or 5 mM CMP-Neu5Ac and 30 pg NCAM adsorbed to an IgG-coated microtiter plate overnight at RT. *A*. Purification of NusA-Strep-ST8SiaII Q^{3}AS^{5}EE *B*. Purification of MBP-ST8SiaII Q^{3}AS^{5}EE. *C*. ELISA based activity assay for NCAM-polysialylation.

Taken together, we could enrich MBP-ST8SiaII Q^{3}AS^{5}EE from bacterial expression cultures with a final yield of up to 0.6 mg/L, however, activity was not detectable for the purified enzyme.

2.3.5. Size-exclusion chromatography of bacterial expressed MBP-ST8SiaII Q^{3}AS^{5}EE

To trace the molecular reasons for the loss of activity in bacterial expressed MBP-ST8SiaII Q^{3}AS^{5}EE the quaternary organization of the isolated enzyme was analyzed by size-exclusion chromatography using a superdex 200 column. The elution profile is shown in figure 25 *A*. Protein containing peak fractions were analyzed by SDS-PAGE followed by silver staining and western blot analysis using StrepTactin-AP to prove the presence of MBP-ST8SiaII Q^{3}AS^{5}EE (fig. 25 *B*). This experiment clearly revealed that MBP-ST8SiaII Q^{3}AS^{5}EE is eluted in the void volume and thus indicates the formation of high-molecular weight oligomers or aggregates that may prevent functionality.
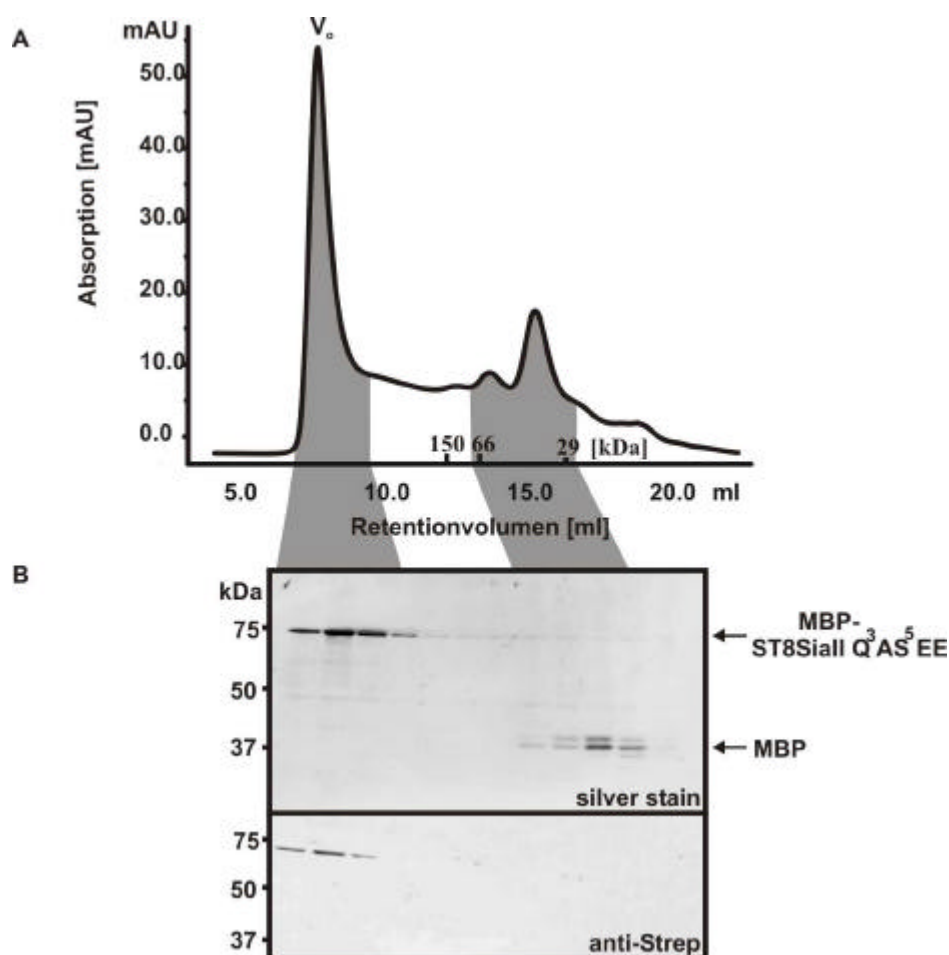
Figure 25: Size-exclusion chromatography of MBP-ST8SiaII Q^{3}AS^{5}EE. The purified MBP-ST8SiaII Q^{3}AS^{5}EE was analyzed by size-exclusion chromatography using a Superdex 200 column. *A*. Elution profile of MBP-ST8SiaII Q^{3}AS^{5}EE. Void volume (V$_0$) and retention volumes of standard proteins are indicated. Peak fractions are shaded in grey. *B*. Peak fractions were analyzed by 10 % SDS-PAGE followed by silver staining or western blotting using an anti-StrepTactin-AP antibody.

2.3.6. Recombinant Expression of *N*-glycan free mST8SiaII S^{3}AS^{5}EE in *Sf9* cells

In an alternative approach to obtain sufficient amounts of an *N*-glycan free polyST, the enzyme variant mST8SiaII S^{3}AS^{5}EE was investigated for expression in insect cells. A baculoviral based insect cell expression system (Gibco BRL) was established for the N-terminally His-tagged construct lacking the first 31 amino acids. Due to an N-terminally located honey bee melittin signal the His-tagged mST8SiaII S^{3}AS^{5}EE variant was secreted into the cell culture medium. Supernatants of infected *Sf*9 cells were collected at different time points post infection, concentrated by trichloric acetic acid precipitation and analyzed by SDS-PAGE and western blotting. The time course of mST8SiaII S^{3}AS^{5}EE secretion is shown in figure 26 and demonstrates that the amount of expressed recombinant mST8SiaII S^{3}AS^{5}EE is barely detectable.
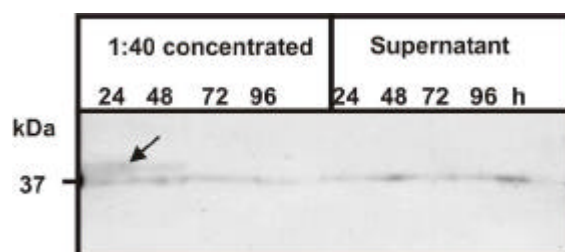
Figure 26: Baculoviral expression of secreted mST8SiaII S^{3}AS^{5}EE variant in *Sf*9 cells. Analysis of time response data after baculoviral expression of mST8SiaII S^{3}AS^{5}EE in *Sf*9 cells. After 24, 48, 72 and 96 h cell culture supernatants of infected *Sf*9-cells were analyzed by 10 % SDS-PAGE - directly (supernatant) and after trichloric acetic acid precipitation (1:40 concentrated) - followed by western blot analysis using an anti-penta-His antibody. mST8SiaII S^{3}AS^{5}EE variant is marked with an arrow (upper band).

2.3.7. Purification of histidine tagged mST8SiaII S^{3}AS^{5}EE expressed in *Sf9* cells

Despite of the extremely low expression yield, a 4 L culture of *Sf*9 cells was infected and a trial was undertaken to purify the N-terminally His-tagged mST8SiaII S^{3}AS^{5}EE from the supernatant, harvested 48 h post baculoviral infection. After volume reduction to 100 ml the recombinant protein was purified by Ni^{2+}-NTA-beads. Eluted fractions were analyzed by 10 % SDS-PAGE followed by silver staining and western blot analysis (fig. 27 *A*). Although, the enzyme variant mST8SiaII S^{3}AS^{5}EE was detectable by western blotting the respective silver stain revealed mainly impurities (fig. 27 *A*). Nevertheless a testing for enzymatic activity was undertaken using the ELISA based polysialylation assay. Therefore, 36 pg/well of ProtA-NCAM were coupled to an IgG coated 96 well microtiter plate. Thereafter, 0.5 µg or 1.0 µg of purified His-ST8SiaII S^{3}AS^{5}EE were incubated in reaction buffer (10 mM

sodium cacodylate buffer pH 6.7; 10 mM MnCl$_2$) containing 1 mM or 10 mM CMP-Neu5Ac overnight at room temperature. While activity observed for the positive control demonstrated integrity of the test system, the non-glycosylated enzyme variant was completely inactive.


A.

| *Sf*9 cell purification | Apply * | Flow through* | Purified His-ST8 SiaII S^{3}AS^{5}EE |

B.

NCAM-polysialylation	1 mM CMP-Neu5Ac	10 mM CMP-Neu5Ac
His-ST8SiaIIΔ31 (0.3 µg)	+++	n.d.
His-ST8SiaII S^{3}AS^{5}EE (0.5 µg)	---	---
His-ST8SiaII S^{3}AS^{5}EE (1 µg)	---	---

* TCA precipitated
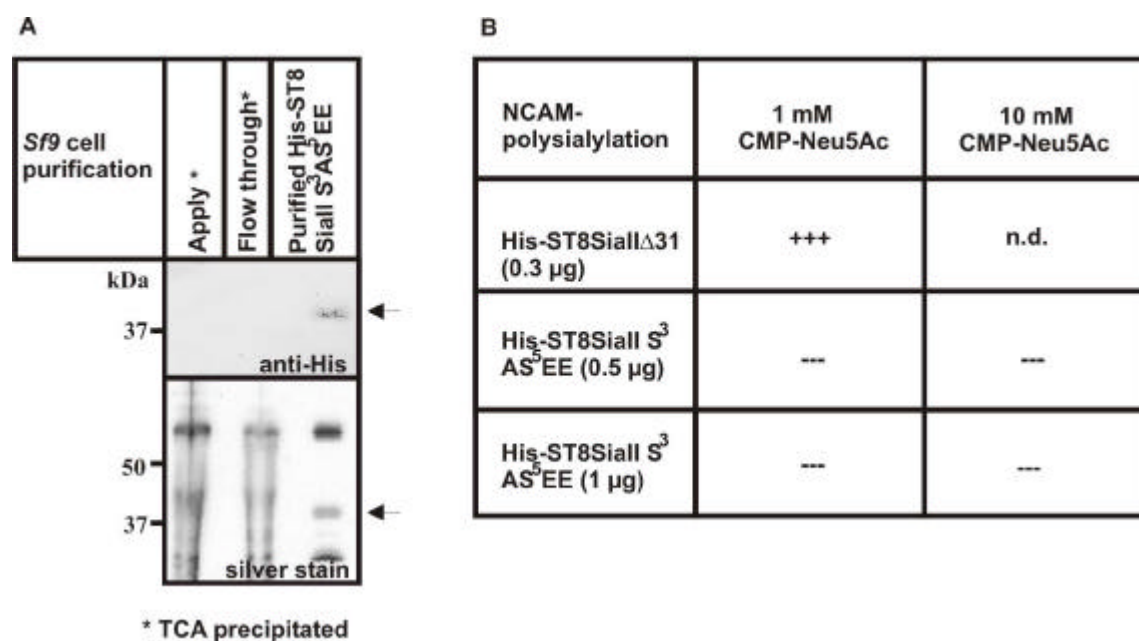
Figure 27: Purification of mST8SiaII S^{3}AS^{5}EE from *Sf*9 cells. *A.* N-terminally His-tagged mST8SiaII S^{3}AS^{5}EE variant was baculoviral expressed in *Sf*9 cells. 48 h post infection, secreted protein was harvested by concentrating cell culture supernatant and incubated overnight with Ni^{2+}-NTA-beads. Protein was eluted stepwise with imidazole and peak fractions were analyzed by 10 % SDS-PAGE followed by silver staining and western blot analysis using anti-penta-His antibody. *B.* For NCAM-polysialylation an ELISA based approach was performed. ProtA-NCAM was coupled to an IgG coated 96-well plate and 0.3 µg of His-mST8SiaII?31 or 0.5 µg/1.0 µg of ST8SiaII S^{3}AS^{5}EE were incubated in reaction buffer (10 mM sodium cacodylate buffer pH 6.7; 10 mM MnCl$_2$) containing 1 mM or 10 mM CMP-Neu5Ac overnight at RT.

2.3.8. PolySia staining of glycosylation depleted mST8SiaII?31 variants *in vitro*

This low yield in the expression of recombinant mST8SiaII S^{3}AS^{5}EE in *Sf*9 cells prompted us to switch back to the mammalian cell system. Therefore, a set of *N*-glycosylation variants based on the construct mST8SiaII?31 was generated as N-terminal proteinA fusion variants and transiently expressed in CHO-2A10 cells, which, due to a mutation in the endogenous polyST gene are polySia negative. After 72 h, 1 µg of each enzyme was immobilized on IgG-sepharose beads and incubated with 0.12 mM CMP-[^{14}C]Neu5Ac in the presence of 30 ng ProtA-NCAM for 4 h at 37°C. Samples were separated by 7 % SDS-PAGE before and after treatment with the polySia-degrading enzyme endoneuraminidaseF (endoNF) and reaction products were visualized by autoradiography. Polysialylation activity is indicated by a broad radioactive smear that can be removed by endoNF treatment. Due to the fact that endoNF

does not degrade the last three sialic acid residues of a polySia chain, protein acceptors are visible due to the remaining $[^{14}C]$-labeled sialic acids. Using this assay system we could investigate NCAM-polysialylation competence of the ProtA-ST8SiaII glycosylation variants, but again only the fully *N*-glycosylated ProtA-ST8SiaII generated detectable levels of NCAM polysialylation *in vitro* and *in vivo* (fig. 28 *A*; fig. 20 *A*). By contrast, while clearly active *in vivo*, no activity was found with the *N*-glycan free enzymes mST8SiaII Q^3N^5 and ST8SiaII Q^3AS^5EE *in vitro* (fig. 28 *A*; fig. 20 *A*). These findings were confirmed by analyzing all variants in the ELISA-based assay system described above (fig. 28 *C*, 2.3.7). Expression of all variants was analyzed by SDS-PAGE followed by western blot analysis using an antibody directed against the ProtA fusion part. Although semi-quantitative, the western blot clearly demonstrated drastically reduced expression levels for the *N*-glycan variants. The observed shift in molecular mass that is visible in the western blot is due to a decreased molecular weight of nearly 5 kDa per absent *N*-glycosylation site (fig. 28 *B*).
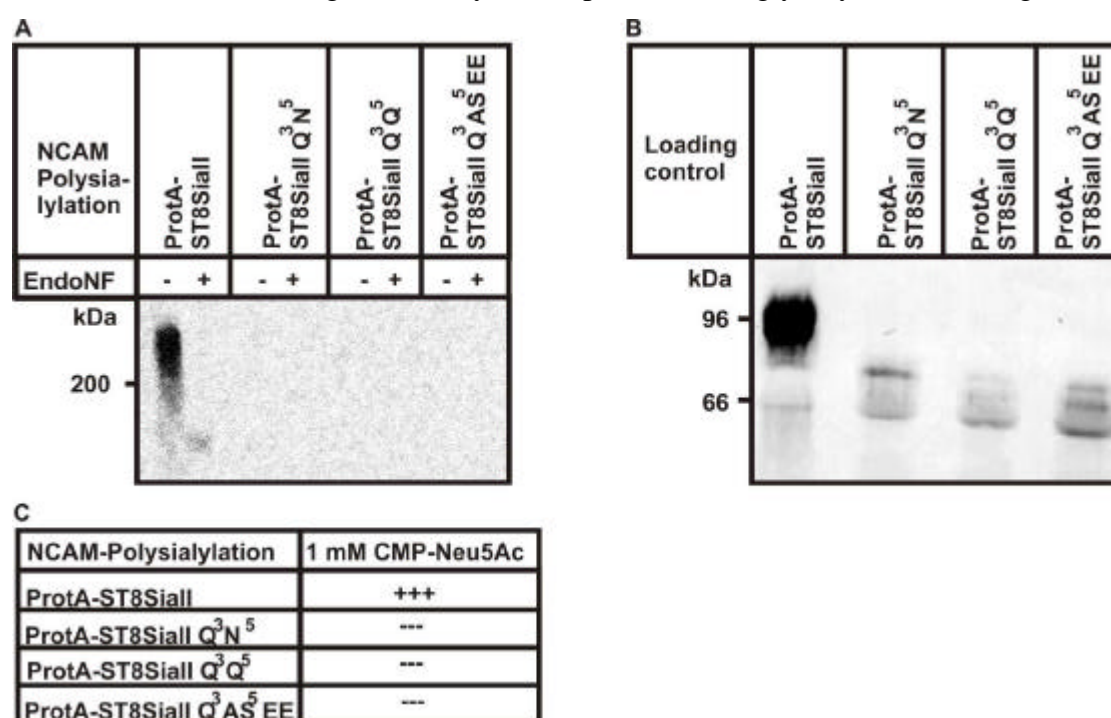
Figure 28: *In vitro* activity of *N*-glycosylation site depleted variants of mST8SiaII. *N*-glycosylation variants of N-terminally truncated mST8SiaII?N31 were transiently expressed as proteinA fusion constructs in CHO-2A10 cells. *A*. 36 ng of ProtA-NCAM were adsorbed to IgG-Sepharose-beads containing 1 µg of proteinA-ST8SiaII variants. Reaction was performed in reaction buffer (10 mM sodium cacodylate buffer pH 6.7; 10 mM MnCl₂) containing 0.25 mM CMP-$[^{14}C]$-Neu5Ac for 4h at 37°C. Samples were separated by 10 % SDS-PAGE before (-) and after (+) treatment with EndoneuraminidaseF (EndoNF) and visualized by autoradiography. *B*. Loading control: Western blot analysis of 1 µg Sepharose immobilized proteinA-ST8SiaII variants. Samples were analyzed by 10 % SDS-PAGE followed by western blotting using an antibody directed against the proteinA part. *C*. In an ELISA based approach 36 pg protA-NCAM were coupled to IgG antibody to a 96-well plate and 0.1 µg of ProtA-ST8SiaII or 0.2 µg of ST8SiaII variants were incubated in reaction buffer (10 mM sodium cacodylate buffer pH 6.7; 10 mM MnCl₂) containing 1 mM or 10 mM CMP-Neu5Ac overnight at RT.

The results shown above demonstrate that expression of *N*-glycan depleted polySTs is a major hurdle in eukaryotic cells. A reason for this may be misfolding of the protein in the absence of *N*-glycans which are major elements in the ER-quality control system. Further engineering steps are needed to increase solubility and to obtain more efficiently expressed protein.

2.4. Discussion

In vertebrates, the unique linear homopolymer polysialic acid (polySia) is composed of α2,8-linked *N*-acetylneuraminic acid (Troy, 1992). Biosynthesis of this carbohydrate is catalyzed by the polysialyltransferases (polySTs) ST8SiaII and ST8SiaIV, exclusively, as simultaneous deletion of both genes resulted in polySia-negative mice (Weinhold *et al.*, 2005). Up to now, polysialylation was identified as posttranslational modification of only five proteins, whereupon the neural cell adhesion molecule (NCAM) is by far the most prevalent (Rothbard *et al.*, 1982; Hildebrandt, Mühlenhoff, and Gerardy-Schahn, 2008). Additional acceptors are neuropilin-2 (Curreli *et al.*, 2007), the scavenger receptor, CD36 found in human breast milk (Yabe *et al.*, 2003) and the a-subunit of the voltage dependent sodium channel (Zuber *et al.*, 1992). Furthermore, modification of polySTs by polySia has been referred to as autopolysialylation (Mühlenhoff *et al.*, 1996; Mühlenhoff *et al.*, 2001). The rarity of this modification suggests the presence of specific protein-protein interactions between polySTs and their acceptor proteins, as recently rationalized by the identification of a polyST recognition site on NCAM (Close *et al.*, 2003; Mendiratta *et al.*, 2005; Mendiratta *et al.*, 2006; Colley, 2008). Although polysialylation is limited to a few specific protein carriers, this modification was identified on *N*-glycans as well as *O*-glycans.

Detailed *in vitro* analyses are required to further investigate structure-function relationships in eukaryotic polySTs. Unfortunately, the complex tertiary organization of these type-II-transmembrane glycoproteins that involve two essential disulfide bonds and up to six partly polysialylated *N*-glycans impedes the development of straight forward approaches for the purification of polyST. This is particularly true, because integrity of the *N*-glycan attachment sites N89 (#3) and N219 (#5) of the mammalian enzymes is important for ST8SiaII activity (Mühlenhoff *et al.*, 2001; Close *et al.*, 2001). Nonetheless, a new method called SUNGA (substitution of *N*-glycan functions in glycosyltransferases by specific amino acids) recently

allowed engineering of a functional, non-glycosylated monosialyltransferase ST3Gal-V, although this enzyme is usually dependent on the presence of three N-glycans (Uemura *et al.*, 2006). Based on this result, we were interested in engineering a non-glycosylated polyST, as an N-glycan free enzyme harbors significant advantages. For instance, the lack of N-glycans would circumvent the necessity of a cost-intensive and time-consuming N-glycosylation competent expression system and allow recombinant expression using the more convenient bacterial system. Moreover, purification of the more homogeneous non-glycosylated polyST variant should be more suitable for protein crystallization than a heavily glycosylated enzyme.

To engineer a non-glycosylated murine ST8SiaII (mST8SiaII), we generated several enzyme variants that differ exclusively in the constitution of N-glycosylation sites N89 (#3) and N219 (#5) as indicated. All these mST8SiaII variants lack in addition the N-glycosylation sites #1, #2, #4 and #6 as they were found to be of minor importance with regard to activity (Mühlenhoff *et al.*, 2001; Close *et al.*, 2001). The respective asparagine residues in the **N-X-S/T** consensus motifs are substituted by glutamine. So far, the attempt to generate a non-glycosylated mST8SiaII variant failed, as deletion of all six N-glycosylation sites by substitution of the respective asparagine residues by glutamine, resulted in the inactive enzyme mST8SiaII Q^3Q^5 (Mühlenhoff *et al.*, 2001). In the present study, multiple sequence alignment of various ST8SiaII homologues revealed that one out of the two essential N-glycosylation attachment sites in the mST8SiaII is suitable to implement SUNGA. Consequently, we exchanged the sequence of N-glycosylation site N219 (#5) of mST8SiaII (VN^5AT) by the conserved sequence AS^5EE, found at the equivalent position in bonefish homologues (fig. 19). The resulting variant mST8SiaII Q^3AS^5EE maintained enzymatic activity as demonstrated by polySia surface immunofluorescence staining of transiently transfected LMTK⁻ (polySia⁻/NCAM⁺) cells (fig. 20 *A*). Although polysialylation activity of mST8SiaII Q^3AS^5EE is drastically reduced compared to the fully glycosylated wild-type enzyme. Nevertheless, this is the first demonstration that an N-glycan free mST8SiaII exhibits functional activity. Because the SUNGA substitution was not possible on N-glycosylation site N89 (#3) - this site is conserved among all known polySTs - the trial to substitute this site was based on an earlier report showing that substitution of the asparagine residue in N-glycosylation sites by serine maintains higher levels of residual activity in polySTs (Mühlenhoff *et al.*, 2001; Close *et al.*, 2001). Indeed, this measure applied to site #3 by generating the N-glycan free variant mST8SiaII S^3AS^5EE (fig. 20 *A*) considerably improved enzymatic activity. Because also SUNGA applied at position #5 introduced a serine

residue, we investigated further if the serine residue contained in the bonefish sequence AS^{5}EE is the major cause for preserved enzymatic activity. Therefore, the enzyme variants mST8SiaII Q^{3}S^5 and mST8SiaII S^{3}S^5 were produced and analyzed. Both variants revealed, however, significantly reduced activity if compared to the SUNGA clone with the substitution AS^{5}EE. This finding clearly highlighted the positive effect achieved by the SUNGA method. Nonetheless, our studies also confirm that serine substitutions cause less harm in the polyST than glutamine substitutions in the **N-**X-S/T sequon.

Because enzymatic activity of *N*-glycan free variants in the first part of this study was analyzed in the presence of the polySia acceptor NCAM, it was a surprise that faint polySia surface staining was observed in the absence of NCAM (fig. 20 *B*). Two theories are conceivable to explain polysialylation activity of *N*-glycan free mST8SiaII variants in the absence of NCAM. On the one hand the presence of an endogenous and so far unknown polySia acceptor in the used LMTK$^-$ cells would perfectly explain residual polySia surface staining of cells transfected with non-glycosylated mST8SiaII variants. On the other hand, serine residues were inserted in all active *N*-glycan free mST8SiaII variants that might have resulted in artificial *O*-glycans serving as alternative polySia acceptors. Polysialylation has already been proven to occur on *O*-glycans of neuropilin-2 and the scavenger receptor CD36 (Curreli *et al.*, 2007; Yabe *et al.*, 2003). To distinguish between the two theories, we analyzed the *N*-glycan free variant mST8SiaII Q^{3}AM^{5}EE which lacks artificial serine residues. Transient transfection of mST8SiaII Q^{3}AM^{5}EE in polySia-free LMTK$^-$ cells resulted in significant polySia surface staining in the presence of NCAM, demonstrating that this enzyme variant is active (fig. 21 *A*). By contrast, no polysialylation activity was detectable for ST8SiaII Q^{3}AM^{5}EE in the absence of NCAM, arguing for *O*-glycosylation due to the presence of serine rather than for an additional endogenous acceptor molecule in LMTK$^-$ cells (fig. 21 *B*). Nonetheless, the occurrence of *O*-glycans has to be investigated by e.g. mass spectrometry to unequivocally confirm this finding.

To obtain sufficient amount of recombinant polyST for further studies, a mST8SiaII variant that allows soluble and homogenous expression would be advantageous. Therefore, we exemplarily truncated an *N*-glycan free mST8SiaII variant by the transmembrane domain (first 31 amino acids) and subcloned the construct into pSecTag vector, to express it as a secretory protein. Subsequent analysis of this mST8SiaII variant in LMTK$^-$ cells revealed that the enzyme maintained activity (fig. 22). In conclusion, engineering of an *N*-glycan free mST8SiaII variant that was proven functional in mammalian cell culture forms the basis for soluble expression of polyST in bacteria.

As mST8SiaII requires two essential disulfide bonds, we chose the engineered bacterial *E. coli* strains Ad494(DE3) and Origami(DE3) that promote disulfide bond formation and therefore allow efficient expression of eukaryotic enzymes harboring crucial disulfide bridges. To optimize bacterial expression of mST8SiaII Q^3AS^5EE we tested four constructs differing in their N-terminal tags or fusion protein parts with regard to expression strains, temperature, medium and concentration of the expression inducing reagent IPTG. Best expression efficiency was obtained for mST8SiaII Q^3AS^5EE variants harboring an N-terminal NusA- or MBP-fusion protein, whereas marginal or no soluble expression was achieved with His- or Strep-tagged enzyme variants (fig. 23 *B*). Large N-terminal solubility-enhancing fusion parts presumably assist folding of mST8SiaII Q^3AS^5EE and prevent immediate aggregation of the native proteins. Successful soluble expression of non-glycosylated mST8SiaII Q^3AS^5EE variants in bacteria enabled us to start purification of the eukaryotic polyST. A final yield of up to 0.6 mg/L purified MBP-mST8SiaII Q^3AS^5EE was obtained, whereas purification attempts of the NusA-variant failed (fig. 24). However, unfortunately, no enzymatic activity was detectable for the purified MBP-mST8SiaII Q^3AS^5EE in the ELISA-based assay system (fig. 24 *C*). To trace back the loss of activity in the purified MBP-ST8SiaII Q^3S^5EE, we first investigated the oligomerization state of the enzyme. Size-exclusion chromatography was used and MBP-ST8SiaII Q^3AS^5EE was eluted in the void volume, clearly demonstrating the formation of high-molecular weight oligomers or aggregates. Because the zebrafish ST8SiaII was shown in Chapter 1 (fig. 12) to be a monomeric enzyme we assume that formation of aggregates may prevent functionality. A possible reason for aggregate formation could be an insufficient competence of the used bacteria to allow formation of the two essential disulfide bonds.

To investigate whether the lack of enzymatic activity originates from misfolded aggregates due to insufficient disulfide bond formation, we analyzed an *N*-glycan free mST8SiaII variant in a eukaryotic expression system. As the non-glycosylated enzyme variant mST8SiaII S^3AS^5EE maintained highest activity, this variant was chosen for expression in *Sf*9 insect cells. Initial experiments displayed minor expression efficiency resulting in a marginal yield of 100 µg/L purified enzyme (fig. 27 *A*). Nonetheless, NCAM-polysialylation competence of the purified enzyme was tested in the ELISA-based assay system, but no enzyme activity was detectable, although substrate concentrations were increased to compensate for a possibly increased Km value of the non-glycosylated enzyme variant (fig. 27 *B*).

Finally we tried to verify NCAM-polysialylation activity of the non-glycosylated mST8SiaII variants *in vitro* and therefore generated ProtA-ST8SiaII variants for soluble expression in polySia deficient CHO-2A10 cells. Polysialylation ability of the ProtA-fusion constructs was analyzed in an *in vitro* assay as described previously (Mühlenhoff *et al.*, 2001). No enzymatic activity was detectable for the engineered ProtA-ST8SiaII Q^3AS^5EE variant. Remarkably, no enzymatic activity was detectable as well for the ProtA-ST8SiaII Q^3N^5 and ProtA-ST8SiaII Q^3Q^5 variants *in vitro*, which is consistent with the previous observations made by Dr. Mühlenhoff (Mühlenhoff *et al.*, 2001). The same results were obtained for ProtA-ST8SiaII variants when tested in the ELISA based assay.

In this study we succeeded for the first time in engineering a functional non-glycosylated murine ST8SiaII variant by implementing the SUNGA method. This progress facilitated soluble expression of recombinant polyST in the cost-effective bacterial system. Although enzymatic activity of non-glycosylated ST8SiaII variants could be demonstrated in cell-culture experiments, activity could not be confirmed *in vitro*. In summary it can be stated, that the first soluble expression of a mammalian polyST in a glycan free form using bacterial and eukaryotic system can be regarded as success. However, additional effort is needed to establish conditions that allow expression and testing of the functional enzyme.

General Discussion

The Polysialyltransferases (polySTs), ST8SiaII and ST8SiaIV, synthesize the homopolymer polysialic acid (polySia), a posttranslational modification of some *O*-and *N*-linked glycans in vertebrates. The knock-out of both polySTs in mice demonstrates the crucial impact of polySia on life and survival. The absence of ST8SiaII in mice caused morphological changes in brain structures and altered fear conditioning (Angata *et al.*, 2004), whereas the loss of ST8SiaIV resulted in reduced learning and memory in adult mice (Eckhardt *et al.*, 2000). The knock-out of both polySTs led to a complete loss of polySia and caused drastic growth retardation in the early postnatal phase. More than 80 % of these mice died during the first four weeks after birth (Weinhold *et al.*, 2005; Angata *et al.*, 2007).

In adults, the external addition of polySia in nerve deletion sites promotes nerve regeneration (El Maarouf and Rutishauser, 2008) by contrast the re-expression of polySTs in tumors (mainly ST8SiaII), enhances metastasis and impairs the actuarial survival rate of patients (Tanaka *et al.*, 2001). Therefore, the controlled expression or inhibition of the polySia synthesizing polySTs is of emerging importance.

Although the mammalian polySTs were cloned 13 years ago, there is still little known about the biochemical properties and the structure-function relationships of these important enzymes.

The detailed analysis of structure-function relationships in polySTs is mainly hampered by the lack of expression systems capable to supply sufficient amounts of active enzymes. The two polySTs - ST8SiaII and ST8SiaIV - are transmembrane type II glycoproteins containing six and five *N*-glycan attachment sites, respectively. The integrity of the *N*-glycan attachment sites N89 and N219 for ST8SiaII as well as N74 for ST8SiaIV is important for enzymatic activity (Mühlenhoff *et al.*, 2001; Close *et al.*, 2001). Furthermore, the polySTs comprise two essential disulfide bonds posing an additional challenge on recombinant expression and purification of these enzymes. Thus, expression of the eukaryotic polySTs is restricted to *N*-glycan competent expression systems that ensure the formation of disulfide bonds. Although, mammalian and insect cell expression systems fulfill these requirements, they bear the problem of low yields of recombinant protein.

Here, we were interested in establishing high yield expression systems to obtain sufficient amounts of recombinant enzyme for ligand binding studies and crystallization approaches to gain information about the catalytic mechanism of eukaryotic polySTs. In the present study we followed two different strategies to establish high yield expression systems of

recombinant active ST8SiaII. The aim of the first part of this work was to express and analyze ST8SiaII from the lower vertebrate zebrafish that lacks one out of the two *N*-glycosylation sites that are important for polyST activity (Marx *et al.*, 2007; Mühlenhoff *et al.*, 2001; Close *et al.*, 2001). In the second part, we started to engineer the murine ST8SiaII (mST8SiaII) to a non-glycosylated ST8SiaII variant for expression in the cost-efficient and timesaving bacterial expression systems.

In this study we were focused on the *N*-glycan functions and their influence on ST8SiaII activity and expression. The mST8SiaII variant lacking the 3rd *N*-glycosylation site were already found to exhibit decreased activity as well as decreased expression levels and increased degradation in comparison to the fully glycosylated wild-type enzyme or variants lacking another *N*-glycan function (Dr. Mühlenhoff, personal communication). In the present study we could confirm these findings for zST8SiaII variants lacking the 3rd *N*-glycan attachment site (1.3.3).

Interestingly, only for ST8SiaII from higher vertebrates another conserved *N*-glycosylation attachment site (N219) was reported to be important for enzymatic activity (Mühlenhoff *et al.*, 2001; Close *et al.*, 2001). Remarkably, the lower vertebrates zebrafish and pufferfish, do not comprise a corresponding 5th *N*-glycosylation attachment site, whereupon enzymatic activity is maintained (Marx *et al.*, 2007). Therefore we suggest that the 5th *N*-glycosylation site of higher vertebrates might have gained an additional and so far unknown function in the course of evolution. That would explain the dramatic loss of enzymatic activity whenever this *N*-glycan attachment site is affected by amino acid substitutions. For instance, the *N*-glycan free mST8SiaII variant, obtained by substituting all respective asparagine residues located in a N-X-S/T consensus motifs by glutamine (mST8SiaII Q^3Q^5), was found to be devoid of activity (fig. 20; Mühlenhoff *et al.*, 2001). Remarkably, we could engineer an *N*-glycan free mST8SiaII variant that maintained residual activity by substitution of the 5th *N*-glycosylation site by conserved amino acids located at the equivalent position of the pufferfish ST8SiaII homologue. This method is called SUNGA and enables the investigation of evolutionary effects of *N*-glycan functions (Uemura *et al.*, 2006). Therefore, we generated a set of *N*-glycosylation depletion variants to further analyze the impact of the 5th *N*-glycosylation site of mST8SiaII with regard to enzymatic activity and expression efficiency of recombinant enzyme. The resulting non-glycosylated mST8SiaII variants ST8SiaII Q/S^3S^5, ST8SiaII Q/S^3AS^5EE and ST8SiaII Q/S^3AM^5EE, but not the ST8SiaII Q/S^3Q^5 variants catalyzed NCAM-polysialylation in LMTK$^-$ (polySia$^-$/NCAM$^+$) cells as visualized by polySia surface staining. Unexpectedly, the serine-containing *N*-glycan free enzyme variants

(ST8SiaII Q/S^{3}S^5, ST8SiaII Q/S^{3}AS^{5}EE) maintained polySia surface staining in the absence of the polySia acceptor NCAM. A suitable explanation for polySia surface staining in the absence of NCAM would be the presence of a so far unknown endogenous polySia acceptor in LMTK$^-$ cells. Although we can not exclude that the inserted serine residues might have resulted in artificial *O*-glycans serving as alternative polySia acceptors. Taken together, we could confirm the major impact of the 5th *N*-glycosylation site on mST8SiaII activity, although we could not discover the function of this site in mammalian polySTs (Mühlenhoff *et al.*, 2001; Close *et al.*, 2001).

The major goal of the present study was to produce high amounts of homogenous and functional recombinant ST8SiaII to facilitate analyses of structure-function relationships and crystallization approaches. Two different strategies were adapted for this demand.

On the one hand we succeeded in generating the functional *N*-glycan free enzyme variant mST8SiaII Q/S^{3}AS^{5}EE, that enabled us for the first time to achieve soluble expression in a bacterial expression system and subsequent purification of the recombinant enzyme. However, so far we could not demonstrate enzymatic activity of the purified mST8SiaII variant, what might be explicable with the formation of aggregates as found by size-exclusion chromatography. Further studies are required to obtain functional mST8SiaII using the bacterial expression systems. Possible starting points might be co-expression of mST8SiaII with chaperones (Uemura *et al.*, 2006) or renaturation of purified enzyme in vitro (Saribas *et al.*, 2007).

In addition we could demonstrate that ST8SiaII from zebrafish (zST8SiaII) - in contrast to all homologous enzymes from higher vertebrates - lacks one out of the two *N*-glycosylation sites that are important for polyST activity, whereupon the zebrafish enzyme maintains activity (Marx *et al.*, 2007). Using zST8SiaII we succeeded in expression and purification of recombinant enzyme from insect cells in high yields. This progress enabled us for the first time to start a detailed biochemical characterization of a eukaryotic ST8SiaII. Interestingly, zST8SiaII was found as a monomer by size-exclusion chromatography, suggesting a monomer as the catalytically active unit. By contrast, the prokaryotic polySTs were shown to assemble into high-order oligomers (Freiberger *et al.*, 2007). Remarkably, eukaryotic and prokaryotic polySTs reveal no sequence similarities neither on DNA- nor on amino acid level.

Furthermore, we established a STD-NMR spectroscopy based ligand epitope mapping for the zST8SiaII?N86. For the first time we could demonstrate that binding of the activated sugar CMP-Neu5Ac towards the enzyme is mainly mediated by the nucleotide moiety CMP.

Moreover, by analyzing binding properties of sialic acid oligomers towards zST8SiaII we could show that at least six α2,8-linked sialic residues of polySia are in close proximity to the enzyme's surface. Furthermore, by monitoring the enzymatic reaction of zST8SiaII?N86 using ^{1}H-NMR-spectroscopy, we could detect product formation in the presence of the artificial acceptor Neu5Ac2Me, a sialic acid monomer in a fixed a-configuration. This finding suggests a monomer as the minimal acceptor for polyST chain initiation and elongation.

Moreover, this assay system (STD-NMR-spectroscopy in combination with activity assays based on ^{1}H-NMR-spectroscopy) provides the vantage point for future studies to analyze the binding site in detail and to design inhibitors for polySTs (von Itzstein, 2007). The selective inhibition of ST8SiaII represents a promising target for cancer therapy. Although ST8SiaII and ST8SiaIV are highly homologous and catalyze the equivalent reaction on the same acceptors, only ST8SiaII showed reduced NCAM-polysialylation competence, if the unnatural sialic acid precursor N-butanoylmannosamine (ManNBut) was supplemented in cell culture (Bork *et al.*, 2007). A specifically designed inhibitor against ST8SiaII, re-expressed in tumors, might therefore have less adverse effects in therapy, since ST8SiaIV is the prominent polyST in adults.

To gain more information about the catalytically active unit and the catalytic mechanism of ST8SiaII, we were interested to solve the three-dimensional structure by protein crystallization. For protein crystallization, a homogeneously expressed protein increases the prospect of success. The zST8SiaII?N86 could be purified in high quality from insect cells and initial precrystalls were obtained, however the remaining *N*-glycosylation sites might have interfered with the crystallization process and consequently impeded the formation of high quality crystals. Therefore, future studies to optimize bacterial expression and subsequent purification of the *N*-glycan-free mST8SiaII Q^{3}AS^{5}EE enzyme variant would be promising.

References

Amores,A., Force,A., Yan,Y.L., Joly,L., Amemiya,C., Fritz,A., Ho,R.K., Langeland,J., Prince,V., Wang,Y.L., Westerfield,M., Ekker,M., and Postlethwait,J.H. (1998) Zebrafish hox clusters and vertebrate genome evolution *Science* **282**: 1711-1714.

Angata,K., Huckaby,V., Ranscht,B., Terskikh,A., Marth,J.D., and Fukuda,M. (2007) Polysialic acid-directed migration and differentiation of neural precursors are essential for mouse brain development *Mol.Cell Biol.* **27**: 6659-6668.

Angata,K., Long,J.M., Bukalo,O., Lee,W., Dityatev,A., Wynshaw-Boris,A., Schachner,M., Fukuda,M., and Marth,J.D. (2004) Sialyltransferase ST8Sia-II assembles a subset of polysialic acid that directs hippocampal axonal targeting and promotes fear behavior *J Biol.Chem.* **279**: 32603-32613.

Angata,K., Suzuki,M., and Fukuda,M. (1998) Differential and cooperative polysialylation of the neural cell adhesion molecule by two polysialyltransferases, PST and STX *J Biol.Chem.* **273**: 28524-28532.

Angata,K., Suzuki,M., and Fukuda,M. (2002) ST8Sia II and ST8Sia IV polysialyltransferases exhibit marked differences in utilizing various acceptors containing oligosialic acid and short polysialic acid. The basis for cooperative polysialylation by two enzymes *J Biol.Chem.* **277**: 36808-36817.

Angata,K., Suzuki,M., McAuliffe,J., Ding,Y., Hindsgaul,O., and Fukuda,M. (2000) Differential biosynthesis of polysialic acid on neural cell adhesion molecule (NCAM) and oligosaccharide acceptors by three distinct alpha 2,8-sialyltransferases, ST8Sia IV (PST), ST8Sia II (STX), and ST8Sia III *J Biol.Chem.* **275**: 18594-18601.

Angata,K., Yen,T.Y., El Battari,A., Macher,B.A., and Fukuda,M. (2001) Unique disulfide bond structures found in ST8Sia IV polysialyltransferase are required for its activity *J Biol.Chem.* **276**: 15369-15377.

Angata,T., Varki,A. (2002) Chemical diversity in the sialic acids and related alpha-keto acids: an evolutionary perspective *Chem.Rev.* **102**: 439-469.

Batchelor,P.E., Howells,D.W. (2003) CNS regeneration: clinical possibility or basic science fantasy? *J Clin.Neurosci.* **10**: 523-534.

Bitter-Suermann,D., Roth,J. (1987) Monoclonal antibodies to polysialic acid reveal epitope sharing between invasive pathogenic bacteria, differentiating cells and tumor cells *Immunol.Res.* **6**: 225-237.

Bork,K., Gagiannis,D., Orthmann,A., Weidemann,W., Kontou,M., Reutter,W., and Horstkorte,R. (2007) Experimental approaches to interfere with the polysialylation of the neural cell adhesion molecule in vitro and in vivo *J Neurochem.* **103 Suppl 1**: 65-71.

Brisson,J.R., Baumann,H., Imberty,A., Perez,S., and Jennings,H.J. (1992) Helical epitope of the group B meningococcal alpha(2-8)-linked sialic acid polysaccharide *Biochemistry* **31**: 4996-5004.

Close,B.E., Colley,K.J. (1998) In vivo autopolysialylation and localization of the polysialyltransferases PST and STX *J Biol.Chem.* **273**: 34586-34593.

Close,B.E., Mendiratta,S.S., Geiger,K.M., Broom,L.J., Ho,L.L., and Colley,K.J. (2003) The minimal structural domains required for neural cell adhesion molecule polysialylation by PST/ST8Sia IV and STX/ST8Sia II *J Biol.Chem.* **278**: 30796-30805.

Close,B.E., Tao,K., and Colley,K.J. (2000) Polysialyltransferase-1 autopolysialylation is not requisite for polysialylation of neural cell adhesion molecule *J Biol.Chem.* **275**: 4484-4491.

Close,B.E., Wilkinson,J.M., Bohrer,T.J., Goodwin,C.P., Broom,L.J., and Colley,K.J. (2001) The polysialyltransferase ST8Sia II/STX: posttranslational processing and role of autopolysialylation in the polysialylation of neural cell adhesion molecule *Glycobiology* **11**: 997-1008.

Colley,K.J. (2008) Structural Basis for the Polysialylation of the Neural Cell Adhesion Molecule *Neurochem.Res.*

Corpet,F. (1988) Multiple sequence alignment with hierarchical clustering *Nucleic Acids Res.* **16**: 10881-10890.

Cunningham,B.A., Hemperly,J.J., Murray,B.A., Prediger,E.A., Brackenbury,R., and Edelman,G.M. (1987) Neural cell adhesion molecule: structure, immunoglobulin-like domains, cell surface modulation, and alternative RNA splicing *Science* **236**: 799-806.

Curreli,S., Arany,Z., Gerardy-Schahn,R., Mann,D., and Stamatos,N.M. (2007) Polysialylated neuropilin-2 is expressed on the surface of human dendritic cells and modulates dendritic cell-T lymphocyte interactions *J Biol.Chem.* **282**: 30346-30356.

Daniel,L., Durbec,P., Gautherot,E., Rouvier,E., Rougon,G., and Figarella-Branger,D. (2001) A nude mice model of human rhabdomyosarcoma lung metastases for evaluating the role of polysialic acids in the metastatic process *Oncogene* **20**: 997-1004.

Datta,A.K., Paulson,J.C. (1995) The sialyltransferase "sialylmotif" participates in binding the donor substrate CMP-NeuAc *J Biol.Chem.* **270**: 1497-1500.

Datta,A.K., Sinha,A., and Paulson,J.C. (1998) Mutation of the sialyltransferase S-sialylmotif alters the kinetics of the donor and acceptor substrates *J Biol.Chem.* **273**: 9608-9614.

David,S., Aguayo,A.J. (1981) Axonal elongation into peripheral nervous system "bridges" after central nervous system injury in adult rats *Science* **214**: 931-933.

Drickamer,K. (1993) A conserved disulphide bond in sialyltransferases *Glycobiology* **3**: 2-3.

Eckhardt,M., Bukalo,O., Chazal,G., Wang,L., Goridis,C., Schachner,M., Gerardy-Schahn,R., Cremer,H., and Dityatev,A. (2000) Mice deficient in the polysialyltransferase ST8SiaIV/PST-1 allow discrimination of the roles of neural cell adhesion molecule protein and polysialic acid in neural development and synaptic plasticity *J Neurosci.* **20**: 5234-5244.

Eckhardt,M., Gotza,B., and Gerardy-Schahn,R. (1998) Mutants of the CMP-sialic acid transporter causing the Lec2 phenotype *J Biol.Chem.* **273**: 20189-20195.

Eckhardt,M., Mühlenhoff,M., Bethe,A., Koopman,J., Frosch,M., and Gerardy-Schahn,R. (1995) Molecular characterization of eukaryotic polysialyltransferase-1 *Nature* **373**: 715-718.

El Maarouf,A., Petridis,A.K., and Rutishauser,U. (2006) Use of polysialic acid in repair of the central nervous system *Proc.Natl.Acad.Sci.U.S.A* **103**: 16989-16994.

El Maarouf,A., Rutishauser,U. (2008) Use of PSA-NCAM in Repair of the Central Nervous System *Neurochem.Res.*

Endo,T. (2007) Dystroglycan glycosylation and its role in alpha-dystroglycanopathies *Acta Myol.* **26**: 165-170.

Fawcett,J.W., Asher,R.A. (1999) The glial scar and central nervous system repair *Brain Res.Bull.* **49**: 377-391.

Freiberger,F., Claus,H., Gunzel,A., Oltmann-Norden,I., Vionnet,J., Mühlenhoff,M., Vogel,U., Vann,W.F., Gerardy-Schahn,R., and Stummeyer,K. (2007) Biochemical characterization of a Neisseria meningitidis polysialyltransferase reveals novel functional motifs in bacterial sialyltransferases *Mol.Microbiol.* **65**: 1258-1275.

Fukuda,M. (1996) Possible roles of tumor-associated carbohydrate antigens *Cancer Res.* **56**: 2237-2244.

Galuska,S.P., Geyer,R., Gerardy-Schahn,R., Mühlenhoff,M., and Geyer,H. (2008) Enzyme-dependent variations in the polysialylation of the neural cell adhesion molecule (NCAM) in vivo *J Biol.Chem.* **283**: 17-28.

Gerardy-Schahn,R., Bethe,A., Brennecke,T., Mühlenhoff,M., Eckhardt,M., Ziesing,S., Lottspeich,F., and Frosch,M. (1995) Molecular cloning and functional expression of bacteriophage PK1E-encoded endoneuraminidase Endo NE *Mol.Microbiol.* **16**: 441-450.

Glüer,S., Schelp,C., Madry,N., von Schweinitz,D., Eckhardt,M., and Gerardy-Schahn,R. (1998a) Serum polysialylated neural cell adhesion molecule in childhood neuroblastoma *Br.J Cancer* **78**: 106-110.

Glüer,S., Schelp,C., von Schweinitz,D., and Gerardy-Schahn,R. (1998b) Polysialylated neural cell adhesion molecule in childhood rhabdomyosarcoma *Pediatr.Res.* **43**: 145-147.

Haile,Y., Berski,S., Drager,G., Nobre,A., Stummeyer,K., Gerardy-Schahn,R., and Grothe,C. (2008) The effect of modified polysialic acid based hydrogels on the adhesion and viability of primary neurons and glial cells *Biomaterials* **29**: 1880-1891.

Harduin-Lepers,A., Mollicone,R., Delannoy,P., and Oriol,R. (2005) The animal sialyltransferases and sialyltransferase-related genes: a phylogenetic approach *Glycobiology* **15**: 805-817.

Harduin-Lepers,A., Vallejo-Ruiz,V., Krzewinski-Recchi,M.A., Samyn-Petit,B., Julien,S., and Delannoy,P. (2001) The human sialyltransferase family *Biochimie* **83**: 727-737.

Hildebrandt,H., Becker,C., Glüer,S., Rosner,H., Gerardy-Schahn,R., and Rahmann,H. (1998) Polysialic acid on the neural cell adhesion molecule correlates with expression of polysialyltransferases and promotes neuroblastoma cell growth *Cancer Res.* **58**: 779-784.

Hildebrandt,H., Mühlenhoff,M., and Gerardy-Schahn,R. (2008) Polysialylation of NCAM *Neurochem.Res.*

Hildebrandt,H., Mühlenhoff,M., Weinhold,B., and Gerardy-Schahn,R. (2007) Dissecting polysialic acid and NCAM functions in brain development *J Neurochem.* **103 Suppl 1**: 56-64.

Hinsby,A.M., Berezin,V., and Bock,E. (2004) Molecular mechanisms of NCAM function *Front Biosci.* **9**: 2227-2244.

Hu,H., Tomasiewicz,H., Magnuson,T., and Rutishauser,U. (1996) The role of polysialic acid in migration of olfactory bulb interneuron precursors in the subventricular zone *Neuron* **16**: 735-743.

Johnson,C.P., Fujimoto,I., Rutishauser,U., and Leckband,D.E. (2005) Direct evidence that neural cell adhesion molecule (NCAM) polysialylation increases intermembrane repulsion and abrogates adhesion *J Biol.Chem.* **280**: 137-145.

Kean,E.L., Munster-Kuhnel,A.K., and Gerardy-Schahn,R. (2004) CMP-sialic acid synthetase of the nucleus *Biochim.Biophys.Acta* **1673**: 56-65.

Kitazume-Kawaguchi,S., Kabata,S., and Arita,M. (2001) Differential biosynthesis of polysialic or disialic acid Structure by ST8Sia II and ST8Sia IV *J Biol.Chem.* **276**: 15696-15703.

Kojima,N., Yoshida,Y., Kurosawa,N., Lee,Y.C., and Tsuji,S. (1995) Enzymatic activity of a developmentally regulated member of the sialyltransferase family (STX): evidence for alpha 2,8-sialyltransferase activity toward N-linked oligosaccharides *FEBS Lett.* **360**: 1-4.

Kolkova,K. (2008) Biosynthesis of NCAM *Neurochem.Res.*

Kudo,M., Takayama,E., Tashiro,K., Fukamachi,H., Nakata,T., Tadakuma,T., Kitajima,K., Inoue,Y., and Shiokawa,K. (1998) Cloning and expression of an alpha-2,8-polysialyltransferase (STX) from Xenopus laevis *Glycobiology* **8**: 771-777.

Kurosawa,N., Yoshida,Y., Kojima,N., and Tsuji,S. (1997) Polysialic acid synthase (ST8Sia II/STX) mRNA expression in the developing mouse central nervous system *J Neurochem.* **69**: 494-503.

Laemmli,U.K., Beguin,F., and Gujer-Kellenberger,G. (1970) A factor preventing the major head protein of bacteriophage T4 from random aggregation *J Mol.Biol.* **47**: 69-85.

Liedtke,S., Geyer,H., Wuhrer,M., Geyer,R., Frank,G., Gerardy-Schahn,R., Zahringer,U., and Schachner,M. (2001) Characterization of N-glycans from mouse brain neural cell adhesion molecule *Glycobiology* **11**: 373-384.

Liu,S., and Prestegard,J. (2007) Characterizing the Binding site of the Sialyltransferase ST6Gal I Using NMR of Bound Sugar Nucleotide Analogs Abstract Boston Meeting Nov.

Marx,M., Rivera-Milla,E., Stummeyer,K., Gerardy-Schahn,R., and Bastmeyer,M. (2007) Divergent evolution of the vertebrate polysialyltransferase Stx and Pst genes revealed by fish-to-mammal comparison *Dev.Biol.* **306**: 560-571.

Mayer,M., Meyer,B. (2000) Mapping the active site of angiotensin-converting enzyme by transferred NOE spectroscopy *J Med.Chem.* **43**: 2093-2099.

Mendiratta,S.S., Sekulic,N., Hernandez-Guzman,F.G., Close,B.E., Lavie,A., and Colley,K.J. (2006) A novel alpha-helix in the first fibronectin type III repeat of the neural cell adhesion molecule is critical for N-glycan polysialylation *J Biol.Chem.* **281**: 36052-36059.

Mendiratta,S.S., Sekulic,N., Lavie,A., and Colley,K.J. (2005) Specific amino acids in the first fibronectin type III repeat of the neural cell adhesion molecule play a role in its recognition and polysialylation by the polysialyltransferase ST8Sia IV/PST *J Biol.Chem.* **280**: 32340-32348.

Miragall,F., Kadmon,G., Faissner,A., Antonicek,H., and Schachner,M. (1990) Retention of J1/tenascin and the polysialylated form of the neural cell adhesion molecule (N-CAM) in the adult olfactory bulb *J Neurocytol.* **19**: 899-914.

Mueller-Dieckmann,J. (2006) The open-access high-throughput crystallization facility at EMBL Hamburg *Acta Crystallogr.D.Biol.Crystallogr.* **62**: 1446-1452.

Mühlenhoff,M., Eckhardt,M., Bethe,A., Frosch,M., and Gerardy-Schahn,R. (1996) Autocatalytic polysialylation of polysialyltransferase-1 *EMBO J* **15**: 6943-6950.

Mühlenhoff,M., Eckhardt,M., and Gerardy-Schahn,R. (1998) Polysialic acid: three-dimensional structure, biosynthesis and function *Curr.Opin.Struct.Biol.* **8**: 558-564.

Mühlenhoff,M., Manegold,A., Windfuhr,M., Gotza,B., and Gerardy-Schahn,R. (2001) The impact of N-glycosylation on the functions of polysialyltransferases *J Biol.Chem.* **276**: 34066-34073.

Muller,D., Djebbara-Hannas,Z., Jourdain,P., Vutskits,L., Durbec,P., Rougon,G., and Kiss,J.Z. (2000) Brain-derived neurotrophic factor restores long-term potentiation in polysialic acid-neural cell adhesion molecule-deficient hippocampus *Proc.Natl.Acad.Sci.U.S.A* **97**: 4315-4320.

Nakata,D., Zhang,L., and Troy,F.A. (2006) Molecular basis for polysialylation: a novel polybasic polysialyltransferase domain (PSTD) of 32 amino acids unique to the alpha 2,8-polysialyltransferases is essential for polysialylation *Glycoconj.J* **23**: 423-436.

Nakayama,J., Fukuda,M.N., Fredette,B., Ranscht,B., and Fukuda,M. (1995) Expression cloning of a human polysialyltransferase that forms the polysialylated neural cell adhesion molecule present in embryonic brain *Proc.Natl.Acad.Sci.U.S.A* **92**: 7031-7035.

Nelson,R.W., Bates,P.A., and Rutishauser,U. (1995) Protein determinants for specific polysialylation of the neural cell adhesion molecule *J Biol.Chem.* **270**: 17171-17179.

Oltmann-Norden,I., Galuska,S.P., Hildebrandt,H., Geyer,R., Gerardy-Schahn,R., Geyer,H., and Mühlenhoff,M. (2008) Impact of the polysialyltransferases ST8SiaII and ST8SiaIV on polysialic acid synthesis during postnatal mouse brain development *J Biol.Chem.* **283**: 1463-1471.

Paratcha,G., Ledda,F., and Ibanez,C.F. (2003) The neural cell adhesion molecule NCAM is an alternative signaling receptor for GDNF family ligands *Cell* **113**: 867-879.

Petridis,A.K., El Maarouf,A., and Rutishauser,U. (2004) Polysialic acid regulates cell contact-dependent neuronal differentiation of progenitor cells from the subventricular zone *Dev.Dyn.* **230**: 675-684.

Probstmeier,R., Bilz,A., and Schneider-Schaulies,J. (1994) Expression of the neural cell adhesion molecule and polysialic acid during early mouse embryogenesis *J Neurosci.Res.* **37**: 324-335.

Rockle,I., Seidenfaden,R., Weinhold,B., Mühlenhoff,M., Gerardy-Schahn,R., and Hildebrandt,H. (2008) Polysialic acid controls NCAM-induced differentiation of neuronal precursors into calretinin-positive olfactory bulb interneurons *Dev.Neurobiol.* **68**: 1170-1184.

Roth,J., Zuber,C., Wagner,P., Taatjes,D.J., Weisgerber,C., Heitz,P.U., Goridis,C., and Bitter-Suermann,D. (1988) Reexpression of poly(sialic acid) units of the neural cell adhesion molecule in Wilms tumor *Proc.Natl.Acad.Sci.U.S.A* **85**: 2999-3003.

Rothbard,J.B., Brackenbury,R., Cunningham,B.A., and Edelman,G.M. (1982) Differences in the carbohydrate structures of neural cell-adhesion molecules from adult and embryonic chicken brains *J Biol.Chem.* **257**: 11064-11069.

Rutishauser,U. (1998) Polysialic acid at the cell surface: biophysics in service of cell interactions and tissue plasticity *J Cell Biochem.* **70**: 304-312.

Rutishauser,U. (2008) Polysialic acid in the plasticity of the developing and adult vertebrate nervous system *Nat.Rev.Neurosci.* **9**: 26-35.

Rutishauser,U., Hoffman,S., and Edelman,G.M. (1982) Binding properties of a cell adhesion molecule from neural tissue *Proc.Natl.Acad.Sci.U.S.A* **79**: 685-689.

Saffell,J.L., Williams,E.J., Mason,I.J., Walsh,F.S., and Doherty,P. (1997) Expression of a dominant negative FGF receptor inhibits axonal growth and FGF receptor phosphorylation stimulated by CAMs *Neuron* **18**: 231-242.

Sanchez-Lopez,R., Nicholson,R., Gesnel,M.C., Matrisian,L.M., and Breathnach,R. (1988) Structure-function relationships in the collagenase family member transin *J Biol.Chem.* **263**: 11892-11899.

Saribas,A.S., Johnson,K., Liu,L., Bezila,D., and Hakes,D. (2007) Refolding of human beta-1-2 GlcNAc transferase (GnT1) and the role of its unpaired Cys 121 *Biochem.Biophys.Res.Commun.* **362**: 381-386.

Scheidegger,E.P., Lackie,P.M., Papay,J., and Roth,J. (1994) In vitro and in vivo growth of clonal sublines of human small cell lung carcinoma is modulated by polysialic acid of the neural cell adhesion molecule *Lab Invest* **70**: 95-106.

Scheidegger,E.P., Sternberg,L.R., Roth,J., and Lowe,J.B. (1995) A human STX cDNA confers polysialic acid expression in mammalian cells *J Biol.Chem.* **270**: 22685-22688.

Seidenfaden,R., Krauter,A., Schertzinger,F., Gerardy-Schahn,R., and Hildebrandt,H. (2003) Polysialic acid directs tumor cell growth by controlling heterophilic neural cell adhesion molecule interactions *Mol.Cell Biol.* **23**: 5908-5918.

Seki,T., Arai,Y. (1993) Distribution and possible roles of the highly polysialylated neural cell adhesion molecule (NCAM-H) in the developing and adult central nervous system *Neurosci.Res.* **17**: 265-290.

Sevigny,M.B., Ye,J., Kitazume-Kawaguchi,S., and Troy,F.A. (1998) Developmental expression and characterization of the alpha2,8-polysialyltransferase activity in embryonic chick brain *Glycobiology* **8**: 857-867.

Stummeyer,K., Dickmanns,A., Mühlenhoff,M., Gerardy-Schahn,R., and Ficner,R. (2005) Crystal structure of the polysialic acid-degrading endosialidase of bacteriophage K1F *Nat.Struct.Mol.Biol.* **12**: 90-96.

Tanaka,F., Otake,Y., Nakagawa,T., Kawano,Y., Miyahara,R., Li,M., Yanagihara,K., Inui,K., Oyanagi,H., Yamada,T., Nakayama,J., Fujimoto,I., Ikenaka,K., and Wada,H. (2001) Prognostic significance of polysialic acid expression in resected non-small cell lung cancer *Cancer Res.* **61**: 1666-1670.

Theodosis,D.T., Rougon,G., and Poulain,D.A. (1991) Retention of embryonic features by an adult neuronal system capable of plasticity: polysialylated neural cell adhesion molecule in the hypothalamo-neurohypophysial system *Proc.Natl.Acad.Sci.U.S.A* **88**: 5494-5498.

Toikka,J., Aalto,J., Hayrinen,J., Pelliniemi,L.J., and Finne,J. (1998) The polysialic acid units of the neural cell adhesion molecule N-CAM form filament bundle networks *J Biol.Chem.* **273**: 28557-28559.

Trombetta,E.S. (2003) The contribution of N-glycans and their processing in the endoplasmic reticulum to glycoprotein biosynthesis *Glycobiology* **13**: 77R-91R.

Troy,F.A. (1992) Polysialylation: from bacteria to brains *Glycobiology* **2**: 5-23.

Uemura,S., Kurose,T., Suzuki,T., Yoshida,S., Ito,M., Saito,M., Horiuchi,M., Inagaki,F., Igarashi,Y., and Inokuchi,J. (2006) Substitution of the N-glycan function in glycosyltransferases by specific amino acids: ST3Gal-V as a model enzyme *Glycobiology* **16**: 258-270.

Varki,N.M., Varki,A. (2007) Diversity in cell surface sialic acid presentations: implications for biology and disease *Lab Invest* **87**: 851-857.

von Itzstein,M. (2007) The war against influenza: discovery and development of sialidase inhibitors *Nat.Rev.Drug Discov.* **6**: 967-974.

Vutskits,L., Djebbara-Hannas,Z., Zhang,H., Paccaud,J.P., Durbec,P., Rougon,G., Muller,D., and Kiss,J.Z. (2001) PSA-NCAM modulates BDNF-dependent survival and differentiation of cortical neurons *Eur.J Neurosci.* **13**: 1391-1402.

Walsh,F.S., Parekh,R.B., Moore,S.E., Dickson,G., Barton,C.H., Gower,H.J., Dwek,R.A., and Rademacher,T.W. (1989) Tissue specific O-linked glycosylation of the neural cell adhesion molecule (N-CAM) *Development* **105**: 803-811.

Weinhold,B., Seidenfaden,R., Rockle,I., Mühlenhoff,M., Schertzinger,F., Conzelmann,S., Marth,J.D., Gerardy-Schahn,R., and Hildebrandt,H. (2005) Genetic ablation of polysialic acid causes severe neurodevelopmental defects rescued by deletion of the neural cell adhesion molecule *J Biol.Chem.* **280**: 42971-42977.

Yabe,U., Sato,C., Matsuda,T., and Kitajima,K. (2003) Polysialic acid in human milk. CD36 is a new member of mammalian polysialic acid-containing glycoprotein *J Biol.Chem.* **278**: 13875-13880.

Yang,P., Major,D., and Rutishauser,U. (1994) Role of charge and hydration in effects of polysialic acid on molecular interactions on and between cell membranes *J Biol.Chem.* **269**: 23039-23044.

Yang,P., Yin,X., and Rutishauser,U. (1992) Intercellular space is affected by the polysialic acid content of NCAM *J Cell Biol.* **116**: 1487-1496.

Zhao,Y.Y., Takahashi,M., Gu,J.G., Miyoshi,E., Matsumoto,A., Kitazume,S., and Taniguchi,N. (2008) Functional roles of N‑glycans in cell signaling and cell adhesion in cancer *Cancer Sci.* **99**: 1304-1310.

Zuber,C., Fan,J., Guhl,B., and Roth,J. (2005) Applications of immunogold labeling in ultrastructural pathology *Ultrastruct.Pathol.* **29**: 319-330.

Zuber,C., Lackie,P.M., Catterall,W.A., and Roth,J. (1992) Polysialic acid is associated with sodium channels and the neural cell adhesion molecule N-CAM in adult rat brain *J Biol.Chem.* **267**: 9965-9971.

Appendix 1 – Abbreviations

aa	Amino acid
AP	Alkaline phosphatase
BCIP	5-bromo-4-chloro-3-inodyl phosphate
BDNF	Brain-derived neurotrophic factor
BSA	Bovine serum albumin
C	Cysteine
CMP	Cytidine 5`-monophosphate
C-terminal	Carboxy-terminal
CTP	Cytidine 5`-triphosphate
DMEM	'Dulbecco`s Modified Eage`s medium'
?N	N-terminal truncation of x aa
DNA	Desoxyribonucleic acid
Dp	Degree of polymerization
ELISA	Enzyme linked immuno sorbant assay
EndoNF	Endoneuraminidase F
ER	endoplasmatic reticulum
FGFR	Fibroblast growth factor receptor
FN	Fibronectin
Gal	Galactose
GFRa	Glial-derived neurotrophic factor receptor a
kDa	kilo Dalton
K_M	Michaelis-Menten-Konstante
LTP	Long-term potentiation
IPTG	Isopropyl-beta-D-thiogalactopyranoside
mAB	monoclonal antibody
m	murine (mouse)
Me	beta-Mercaptoethanol
MBP	Maltose binding protein
MES	2-(N-morpholino)ethanesulfonic acid
N	Asparagine
NBT	Nitro blue tetrazolium
NCAM	Neural cell adhesion molecule
Neu5Ac	5-N-acetyl-neuraminic acid
NMR-Spectroscopy	Nuclear magnetic resonance spectroscopy
N-terminal	Amino-terminal
OD	Optical density
PAGE	Polyacrylamide gel electrophoresis
PBS	Phosphate buffered saline
PCR	Polymerase chain reaction
PMSF	Phenylmethansulfonylfluoride
PolySia	Polysialic acid
PolyST	Polysialyltransferase
PP_i	Pyrophosphate
ProtA	ProteinA
Q	Glutaminic acid
RT	Room temperature
S	Serine
SDS	Sodium dodecyl-sulphate

Sf9	*Spodoptera frugiperda*
Sia	Sialic acid
STD-NMR	Saturation transfer difference-NMR
SUNGA	<u>S</u>ubstitution of <u>N</u>-glycan functions in glycosyltransferases by specific <u>a</u>mino acids
SVZ	Subventricular zone
T	Threonine
TCA	Tri chloric acetic acid
TMB	3,3',5,5'-tetramethylbenzidine
U	Unit
V	Volume
W	Weight
wt	Wild-type
z	Zebrafish

Appendix 2 – curiculum vitae and publications

Almut Günzel

Privatanschrift	Liebigstr. 29
	30163 Hannover
	Deutschland
Email	guenzel.almut@mh-hannover.de
Geburtstag und Geburtsort	30.11.1979 in Gifhorn, Deutschland
Nationalität	Deutsch

Akademische Laufbahn

seit 01.02.2005	Promotion in der Arbeitsgruppe von Prof. Dr. Gerardy-Schahn, Abteilung Zelluläre Chemie (OE4330), Medizinische Hochschule Hannover
01.10.2004-31.12.2004	Wissenschaftliche Mitarbeiterin in der Arbeitsgruppe von Prof. Dr. Gerardy-Schahn, Abteilung Zelluläre Chemie (OE4330), Medizinische Hochschule Hannover
1.10.1999 – 19.08.2004	Biochemiestudium an der „Gottfried Wilhelm Leibniz" Universität Hannover (vormals Universität Hannover)
1999	Abitur
1986-1999	Schule

	Tätigkeitsfelder
	Forschungsarbeiten in der Arbeitsgruppe von Prof. Dr. Gerardy-Schahn, Abteilung Zelluläre Chemie (OE4330), Medizinische Hochschule Hannover
Promotionsarbeit	Vertebrate Polysialyltransferases: A Study of Structure-Function Relationships
Diplomarbeit	Struktur/Funktionsbeziehungen in eu- und prokaryontischen Polysialyltransferasen

Publikationsliste

Wissenschaftliche Publikationen:

Freiberger, F., Claus, H., Günzel, A., Oltmann-Norden, I., Vionnet, J., Mühlenhoff, M., Vogel, U., Vann, W.F., Gerardy-Schahn, R., and Stummeyer, K. (2007). Biochemical characterization of a *Neisseria meningitidis* polyST reveals novel functional motifs in bacterial sialyltransferases. *Mol. Microbiol.* **65(5)**, 1258-1275.

Hartlieb, S., Günzel, A., Gerardy-Schahn, R., Münster-Kühnel, A.K., Kirschning, A., and Dräger, G. (2008). Chemoenzymatic synthesis of CMP-N-acetyl-7-fluoro-7-deoxy-neuraminic acid. *Carbohydr Res.* 2008 Feb 10 [Epub ahead of print]

Posterbeiträge:

Günzel, A., Münster-Kühnel, A.-K., Lamerz, A.-C., Stummeyer, K., Bakker, H., Weinhold, B., Gerardy-Schahn, R., and Ritz-Sedlacek, V. (2005). Expression and functional analysis of the CMP-Neu5Ac-Synthetase from embryonic *Drosophila melanogaster*. GLYCO XVIII International Symposium on Glycoconjugates – Florenz, Italy.

Günzel, A., Münster-Kühnel, A.-K., Lamerz, A.-C., Stummeyer, K., Bakker, H., Weinhold, B., Gerardy-Schahn, R., and Ritz-Sedlacek, V. (2005). Functional analysis of the CMP-Neu5Ac-synthetase from embryonic *Drosophila melanogaster* . Joint Meeting – Hannover, Germany.

Günzel, A., Marx, M., Eggers, K., Bastmeyer, M., Stummeyer, K., and Gerardy-Schahn, R.(2007). Characterization of ST8SiaII from zebrafish. 3rd International meeting polySia – Bad Lauterberg, Germany.

Danksagung